UNIVERSIDADE DE LISBOA

Faculdade de Medicina de Lisboa

NLRP3 inflammasome as a target to reduce epileptiform activity in organotypic slices

Leonor Pedro Oliveira Ribeiro Rodrigues

Orientadora:
Doutora Cláudia Alexandra dos Santos Valente de Castro

Dissertação especialmente elaborada para obtenção do grau de Mestre em Neurociências

2018

UNIVERSIDADE DE LISBOA
Faculdade de Medicina de Lisboa

NLRP3 inflammasome as a target to reduce epileptiform activity in organotypic slices

Leonor Pedro Oliveira Ribeiro Rodrigues

Orientadora:
Doutora Cláudia Alexandra dos Santos Valente de Castro

Dissertação especialmente elaborada para obtenção do grau de Mestre em Neurociências

2018

A impressão desta dissertação foi aprovada pelo Conselho Científico da Faculdade de Medicina de Lisboa em reunião de 22 de Maio de 2018.

ACKNOWLEDGMENTS

Dois anos passaram desde que entrei no Laboratório da Professora Ana Sebastião - AsebLab pela primeira vez. Na altura, pela mão da Rita Ramalho a quem agradeço, comecei a tentar perceber o que era isto de ser cientista. Nada nos prepara previamente para esta vida que até então era desconhecida. Meses mais tarde, com a entrada neste projecto orientado pela investigadora Cláudia Valente, é que começo a entender um pouco do que teria de enfrentar dali em diante. Fazer investigação e compreender tudo o que isso implica não é fácil, especialmente no início. É preciso aprender a falhar e é preciso aprender a ser resiliente. A resiliência é mais importante neste trabalho do que a perfeição. A perfeição não existe. Hoje não estaria aqui se não fosse uma série de pessoas que me foram apoiando e levando, umas vezes ao colo, umas vezes de arrasto, sem nunca deixar que a desistência se apoderasse de mim.

À professora Ana Sebastião queria agradecer, não só por me ter recebido no seu laboratório, mas também por acreditar em mim. Ao longo do caminho, encorajou-me a ser uma formadora para miúdos que iam aparecendo à sua porta à procura de conhecimento. Desafiou-me pessoalmente a ensinar uma menina do 9º ano, obrigando-me a desconstruir a ciência de modo a simplificá-la para aqueles que nem sabem o que é pipetar. Desafiou-me também a ser mais do que uma mera aluna focada apenas e só no meu projecto. Ser investigador envolve também perceber tudo aquilo que um projecto e um laboratório implica. Compreender o processo das encomendas e as burocracias com elas relacionadas, saber gerir stocks, arranjar formas de arrumar os materiais de modo a ser mais funcional e pragmáticos a todos, entre outras coisas, fizeram de mim uma melhor cientista.

À Cláudia Valente agradeço a forma como me fez crescer enquanto cientista. À forma como me desafiou diversas vezes a fazer coisas que eu não sabia se estava ou não preparada. Como fazer pela primeira vez uma viagem sozinha para um país totalmente desconhecido para mim e onde teria de me desenrascar com o meu Inglês durante três semanas. Encorajou-me também a ir a diversos cursos do SynaNet e a começar a expor o meu trabalho em diversos encontros científicos. E tal como a professora Ana, também me desafiou a ensinar diversos estudantes de licenciatura e mestrado. Além disso, também queria agradecer ter-me feito perceber que nós nem sempre sabemos todas as respostas às nossas dúvidas e nem sempre compreendemos os resultados obtidos. Às vezes é preciso continuarmos em frente para percebermos aquilo que ficou para trás.

Ao Diogo Rombo agradeço a forma paciente como me ensinou electrofisiologia e tudo o que isso envolve, desde o setup até aos *softwares*. Obrigada por me ajudares a encontrar uma forma de analisar os registos electrofisiológicos, e sobretudo, obrigada por me fazeres perceber que às vezes há dias "não" em electro e que a culpa não é minha, simplesmente há dias em que os astros não estão alinhados.

À Joana Feire, um dos meus maiores apoios dentro do laboratório, obrigada por toda a amizade! Por me ouvires em todos os dias maus do laboratório (e na verdade fora dele) em que simplesmente só me apetecia chorar. Por toda a motivação que me davas quando não sabia se seria capaz de aguentar todas aquelas experiências falhadas e na verdade todo este trabalho de investigação. Por todos os dias que dizias "anda lanchar" e por todos os dias que ficámos à conversa, eu no banco e tu naquele *setup*. Fico sempre triste quando vou à tua sala e

tu já não estás lá… mas mesmo na Suíça não deixaste de acompanhar nesta fase final do meu mestrado.

Aos mizeses! O que era de mim sem vocês? Os meus maiores professores! João Gomes, Rita Belo, Sara Tanqueiro e Catarina Lourenço. Eu a vocês tenho mais do que agradecer. Adoptaram-me como uma de vocês e ajudaram-me em tudo aquilo que poderam. Ao João, obrigada toda a felicidade que trazes para o laboratório todos os dias. Obrigada por cuidares de mim e olhares por mim. Obrigada por me teres ajudado em tudo, mas especialmente obrigada por toda a amizade e carinho. Os dias seriam mais difíceis se não te tivéssemos lá para alegrar esta vida de cientista. À Rita, obrigada pela tua maneira dela ser. Fizeste por mim mais do que muita gente faria. Tiraste do teu tempo para me explicares várias coisas e para olhares comigo para os meus resultados. Fizeste de mim uma pessoa mais crítica sobre o meu trabalho e ensinaste-me a pensar quase como investigadora. À Sara e à Catarina, obrigada por todos os conselhos sobre Western blots e ELISAs, conselhos sobre o laboratório e muitos outros. Obrigada por toda a ajuda que me foram dando ao longo do caminho! Não poderia falar destes mizeses, sem falar na sua orientadora, Maria José Diógenes. A ela deixo apenas um grande obrigada do fundo do coração pela sua maneira de ser.

A todos os outros alunos do laboratório, especialmente à Sara Paulo, Tatiana Morais, Rui Rodrigues e Nádia Rei obrigada por terem feito parte deste percurso também. Aos meus instruendos: Ana Sofia Carmo, André Miranda, Caitlin Martins, Joana Mateus, Catarina Carvalhas, obrigada por me ensinarem a simplificar a ciência e por fazerem com que eu também aprendesse um pouco mais.

Mas não foram só pessoas do laboratório que me ajudaram durante todo este processo. Muitos foram aqueles que me ajudaram a desanuviar deste trabalho tão exigente. Obrigada a todos os meus amigos e um obrigada muito especial à Márcia Martins. Obrigada pelo apoio de todos os dias, obrigada por seres a minha pessoa. E ainda um grande obrigada por me teres desafiado a ir fazer um estágio de observação no INEM. Sabes bem que “pertencer” ao INEM por uns dias fez com que eu ganhasse a força necessária para acabar esta tese, depois de mais um embate na minha vida. Fez-me sentir feliz outra vez.

Para terminar queria agradecer à minha mãe pelo apoio incondicional. Obrigada por discutires comigo assuntos do laboratório. Obrigada por me fazeres o jantar, especialmente quando chego à noite a casa depois de um dia gigante no laboratório. Obrigada por perceberes que escrever a tese implica mesmo estar no quarto fechada sem ter tempo para distrações. Obrigada por me deixares fazer o que eu quiser, seja aqui, seja na Finlândia, em Roma ou em Lancaster. À minha irmã, queria agradecer ter-me ido buscar ao laboratório às 22h nos dias longos de electro. Ao Prof. Mamede agradeço ter cuidado da minha mãe.

E como não podia faltar, agradeço ao meu pai. Agradeço-lhe a minha maneira de ser. Agradeço ser igual a ti na minha relação aos outros. A tua frase “mais idade mais responsabilidade” há-de ecoar para sempre na minha cabeça. E sei que cada vez mais vou tendo mais responsabilidades neste “carreira” de investigação. Espero que estejas orgulhoso e que estejas aqui comigo.

Tenho a certeza que este caminho se tornou um pouco mais fácil com cada um de vocês.

No one is good alone

RESUMO

A epilepsia é uma doença do foro neurológico caracterizada pela predisposição duradoura para gerar crises epilépticas. Cada crise é uma perturbação transitória da atividade neuronal que se torna síncrona e excessiva, interrompendo, momentaneamente, a função normal do cérebro. Calcula-se que, em Portugal, 1 em cada 200 pessoas tenha esta disfunção do sistema neurológico. Não existe cura para a epilepsia, no entanto, existem fármacos antiepilépticos (FAEs) que previnem a ocorrência de crises epilépticas. Os FAEs são prescritos de acordo com o tipo de epilepsia e com os fatores individuais de cada pessoa. Por vezes são necessárias várias tentativas e/ou politerapia para encontrar a medicamentação adequada para controlar as crises. Contudo nem todas as pessoas reagem aos FAEs. Estima-se que 30-40% das pessoas em todo o mundo sofrem de epilepsia refratária, ou seja, não têm a doença controlada.

Uma vez que a epilepsia refratária pode ser incapacitante em algumas vertentes pessoais e profissionais e existe um elevado número de pessoas a sofrer desta doença, é necessário uma melhor compreensão da epilepsia e do processo de epileptogénese. Este processo é responsável por tornar um cérebro normal num cérebro com atividade neuronal anormal. Além disso, também é imprescindível testar novas terapias antiepileptogénicas que possibilitem uma melhor qualidade de vida a estes doentes.

A maioria dos FAEs modula os mecanismos excitatórios e inibitórios relacionados direta ou indiretamente com a neurotransmissão. No entanto, tem havido um crescente interesse no estudo de moléculas/ fármacos anti-inflamatórios como terapias antiepileptogénicas. Além dos neurónios, as células gliais, ou seja, os astrócitos e a microglia, têm um papel importante no processo de epileptogénese. Estas células gliais estão envolvidas no processo de neuroinflamação produzindo diversas citocinas e outras moléculas que irão potenciar a inflamação. Atualmente sabe-se que existe um circuito positivo entre a epilepsia e a inflamação. A atividade epiléptica promove a libertação de fatores inflamatórios e a inflamação, por sua vez, potencia a atividade epiléptica. Uma das citocinas pro-inflamatórias mais estudada no âmbito da epilepsia é a interleucina-1β (IL-1β). Estudos recentes demonstraram que a expressão desta molécula está aumentada em modelos animais de epilepsia, bem como em pacientes com esta patologia.

A IL-1β é produzida por um complexo multiproteico associado à imunidade inata denominado de inflamassoma NLRP3. Este complexo é ativado na presença de agentes patogénicos ou perigosos ao organismo, tais como os lipopolissacarídeos (LPS) e a adenosina trifosfato (ATP). Os LPS são moléculas que estão presentes na membrana exterior de bactérias gram-negativas, enquanto o ATP é uma molécula que transporta energia e é essencial às células. Ao ser ativado, o inflamassoma NLRP3 promove a clivagem da pro-IL-1β (forma inativa) em IL-1β, através da ativação da capase-1. Na forma ativa, a IL-1β sai da célula e promove a inflamação nas células vizinhas.

Diversos estudos têm-se focado na modulação do mecanismo de ação desta interleucina, através de anticorpos anti-IL-1β ou através de antagonistas do seu recetor. Medicamentos que contêm substâncias como Anacinra (antagonista do recetor humano da interleucina-1) ou Canacinumab (anticorpo anti-IL-1β monoclonal totalmente humanizado) têm sido amplamente utilizados no tratamento de doenças relacionadas com o inflamassoma NLRP3, tal como a artrite reumatóide. No entanto, até 2016 ainda nenhum destes medicamentos tinha sido testado em doentes epilépticos. Casos clínicos reportados recentemente têm demonstrado a

eficácia destes medicamentos em doentes com epilepsia refratária. Até então, apenas se tinham realizado estudos com substâncias similares em modelos animais.

Adicionalmente, também foram desenvolvidos estudos para inibir a caspase-1, que tiveram sucesso na supressão de atividade epiléptica em modelos animais, mas não foram aprovados nos ensaios clínicos, ficando apenas na fase II.

O presente estudo teve como principal objetivo modular a ativação do inflamassoma NLRP3 e avaliar o impacto na atividade epiléptica de fatias organotípicas.

As fatias organotípicas são um ótimo modelo *ex vivo,* uma vez que preservam a arquitetura tridimensional, as conexões neuronais e as interações entre os neurónios e células gliais, por longos períodos. Além disso, também permitem testar potenciais fármacos de modo mais rápido, menos doloroso e menos dispendioso do que aconteceria em modelos animais.

Inicialmente foi estabelecido o modelo de ativação do inflamassoma NLRP3 em fatias organotípicas de hipocampo e córtex preparadas a partir dos cérebros de ratos Sprague-Dawley com 6/7 dias de vida, por exposição a diferentes concentrações de LPS (5, 10 e 20ng/mL) durante 3 e 6h ou a LPS (10ng/mL) e ATP (1mM) simultaneamente. Após uma pré-incubação apenas com LPS durante 3h, o ATP foi co-incubado com o LPS durante mais 3h. De modo a escolher a melhor condição de ativação do inflamassoma, estudou-se a expressão proteica da αII-espectrina, para avaliar a morte celular, de componentes do inflamassoma (NLRP3 e ASC), e de marcadores das células gliais (Iba1 e GFAP). Adicionalmente foram quantificados, no tecido e no meio de cultura, os níveis de duas citocinas pro-inflamatórias: a IL-1β e os Fatores de Necrose Tumoral Alfa (TNF-α). Verificou-se que a exposição das fatias organotípicas ao LPS/ATP promoveu a diminuição de necrose, bem como a potenciação da libertação de citocinas para o meio extracelular. Uma vez que estes processos são característicos da ativação do inflamassoma, optou-se por utilizar esta condição.

Posteriormente foi verificado o efeito da ativação do inflamassoma, pelo LPS/ATP, nas células gliais e na atividade epileptiforme. Através da técnica de imunohistoquímica foi possível observar a migração da microglia em direção ao meio de cultura. Na presença de LPS/ATP, a secção da fatia mais próxima do meio de cultura apresentava maior densidade celular, relativamente ao controlo, e maior ativação da microglia. Estas características correspondem a um processo de microgliose. Uma vez que existia elevada produção de IL-1β e microgliose nas fatias expostas a LPS/ATP antecipou-se um aumento na atividade epileptiforme nestas fatias. No entanto, tal não foi observado. As fatias expostas aos ativadores do inflamassoma apresentaram um número de bursts por fatia e características intrínsecas dos bursts semelhantes aos observados em fatias controlo. Os bursts são conjuntos de atividade neuronal excessiva que representam a fase ictal (correspondente à crise epiléptica).

Após uma avaliação cuidada verificou-se que as fatias controlo, não sujeitas à adição de fármacos, exibiam uma elevada atividade epileptiforme. As fatias denominadas controlo neste estudo sofreram apenas uma mudança do meio de cultura, processo este que já havia sido descrito por diversos estudos. Durante os primeiros 14 dias *in vitro*, as fatias foram cultivadas num meio que continha soro de cavalo (meio Opti-MEM). Como este soro não é quimicamente definido, ou seja, varia de lote para lote, o meio de cultura foi alterado para um meio sem soro (meio Neurobasal A) no dia antes da adição dos fármacos. No entanto, verificou-se que as fatias controlo apresentavam claramente mais atividade epiléptica, que as fatias cultivadas sempre em meio Opti-MEM.

Posteriormente foi avaliado o impacto da inibição do inflamassoma NLRP3 na produção da IL-1β e na microgliose, uma vez que tinham sido potenciadas na presença de LPS/ATP. De modo a inibir o inflamassoma, utilizou-se um inibidor seletivo deste complexo multiproteico denominado de MCC950 (10μM). Na presença dos ativadores do inflamassoma, o MCC950 não foi capaz de reverter a libertação da citocina pro-inflamatória nem a microgliose.

Por estudos electrofisiológicos verificou-se que na presença dos ativadores do inflamassoma, o MCC950 não foi capaz de reverter a atividade neuronal excessiva. No entanto, quando o MCC950 foi incubado sozinho, observou-se uma clara diminuição da atividade ictal nas fatias organotípicas. Conclui-se que a atividade epileptiforme induzida nas fatias organotípicas pela mudança do meio de cultura era dependente do inflamassoma, dado que foi revertida por incubação com o seu inibidor.

Em suma, os nossos resultados demonstram que o inflamassoma NLRP3 está relacionado com a indução e potenciação da atividade epileptiforme. Adicionalmente, também sugerem que o MCC950 é um potencial agente terapêutico para a epilepsia e que o inflamassoma NLRP3 deve continuar a ser meticulosamente estudado como potencial alvo terapêutico para a epilepsia.

Palavras - chave**|** Atividade epileptiforme, inflamassoma NLRP3, MCC950, neuroinflamação, fatias organotípicas.

ABSTRACT

Extensive evidence has supported the involvement of neuroinflammation in epileptic seizures. Recently, analysis of serum blood samples of epileptic patients revealed an increased production of several pro-inflammatory cytokines, namely interleukin-1β (IL-1β).This protein is produced by NLRP3 inflammasome, a cytosolic multiprotein complex involved in innate immune response. The canonic activation of NLRP3 inflammasome involves a priming signal (as lipopolysaccharides – LPS), which upregulates the expression of NLRP3 and pro-IL1β; and an activating signal (as adenosine triphosphate – ATP), which promotes the assembly of the complex.

The goals of this study were to enhance epileptiform activity of organotypic slices through LPS/ATP – activated NLRP3 inflammasome and to reduce this activity by selectively inhibiting the inflammasome.

Organotypic cortex-hippocampus slices of Sprague-Dawley rats with 6/7 days were exposed to different LPS concentrations (5, 10, 20ng/mL) at 3 or 6h or LPS (10ng/mL) plus ATP (1mM) to choose the best condition to activate the NLRP3 inflammasome. In order to inhibit the inflammasome, a selective inhibitor, MCC950 (10μM), was added 1h before co-incubation with LPS and ATP. Negative controls with each compound alone were carried out in some assays.

Regarding inflammasome activation, LPS and ATP together decreased necrosis (assessed by ratio SBDP120/α-IISpectrin) and potentiated the release of pro-inflammatory cytokines (interleukin-1β (IL-1β) and tumor necrosis factor α). These events are characteristics of NLRP3 inflammasome activation. Expression of inflammasome components (NLRP3 e ASC) and glial cells markers (Iba1 e GFAP) were also evaluated, but did not show differences.

In LPS/ATP presence, slices presented microgliosis in the layers near the culture medium. However, they depicted a similar epileptiform activity when compared with control slices, which were not exposed to drugs. In this study was possible to verify that control slices, that only underwent culture medium exchange, had an exacerbated synchronous neuronal activity, when compared with slices that did not undergo this process.

In slices treated with MCC950 in the presence of LPS/ATP, neither IL-1β release nor microgliosis were reversed by MCC950. Moreover, NLRP3 inflammasome inhibitor did not affect epileptiform activity in the presence of LPS/ATP. Nevertheless, when MCC950 was incubated alone, the epileptiform activity was dramatically reduced. That is, MCC950 reversed the epileptiform activity induced by medium exchange, suggesting that this process involved the NLRP3 inflammasome.

Our findings demonstrate the important role of NLRP3 inflammasome in the promotion of epileptiform activity and begin to unravel a potential target for antiepileptic therapy.

Keywords| Epileptiform activity, NLRP3 inflammasome, MCC950, neuroinflammation, organotypic slices.

INDEX

LIST OF ABBREVIATIONS

AEDs	Antiepileptic drugs
ALS	Amyotrophic lateral sclerosis
ANOVA	Analysis of variance
ASC	Apoptosis-associated speck-like protein containing a CARD
ATP	Adenosine triphosphate
BBB	Blood-brain barrier
BSA	Bovine serum albumin
CA	Cornu Ammonis
CA1	Cornu Ammonis 1
CA3	Cornu Ammonis 3
CARD	Caspase activation and recruitment domain
CAPS	Cryopyrin-associated periodic syndromes
CBA	Cytometric bead array
CNS	Central nervous system
DAMPs	Danger-associated molecular patterns
DG	Dentate Gyrus
DIV	Days *in vitro*
DMSO	Dimethyl sulfoxide
ELISA	Enzyme-linked immunosorbent assay
EAE	Experimental autoimmune encephalomyelitis
$GABA_A$	Gamma-aminobutyric acid type A
GAPDH	Glyceraldehyde 3-phosphate dehydrogenase
GBSS	Gey's Balanced Salt Solution
GFAP	Glial fibrillary acidic protein
HMGB1	High-mobility group box-1
HRP	Horseradish peroxidase
Iba1	Ionized calcium binding adaptor molecule 1
IL-1β	Interleukin-1β
IL-18	Interleukin-18
IL-1R1	Type 1 IL-1 receptor
IL-1RA	IL-1 receptor antagonist
ILAE	International league against epilepsy
LPS	Lipopolysaccharides
LRR	Leucine-rich repeat
MTLE	Mesial temporal lobe epilepsy
NACHT	Nucleotide-binding and oligomerization domain
NBA	Neurobasal A
NF-kB	Nuclear factor kappa B
NLR	Leucine-rich repeat containing
NLRP3	NACHT, LRR and PYD domains-containing protein 3
NMDA	N-methyl-D-aspartate
NR2B	NMDA receptor subunit 2B
OHSC	Organotypic hippocampal slice cultures
$P2X_7$	P2X purinergic receptors 7
PAMPs	Pathogen associated molecular patterns
PYD	Pyrin domain
PBS	Phosphate buffered saline
Pro-IL-1β	Pro-interleukin-1β

PRR	Pattern recognition receptor
RIPA	Ristocetin induced platelet aggregation
ROS	Reactive oxygen species
RT	Room temperature
siRNA	Small interfering RNAs
SBDP	Spectrin breakdown products
TLE	Temporal lobe epilepsy
TLRs	Toll-like receptors
TLR4	Toll-like receptor 4
TNF - α	Tumor necrosis factor - alpha
TNFR1	Tumor necrosis factor receptor 1

LIST OF FIGURES

LIST OF TABLES

1. INTRODUCTION

1.1. Epilepsy

Epilepsy is a neurological disease characterized by the occurrence of at least one epileptic seizure. This epileptic event is transient and happens due to abnormal and prolonged synchronization of neuronal electric activity in the brain (Fisher et al., 2014). The official definition of epilepsy formulated by a Task Force of the International League Against Epilepsy (ILAE) includes the occurrence of at least two seizures with more than 24h apart; one seizure and a risk comparable to those who have had two unprovoked seizures (at least 60%); or the diagnosis of an epilepsy syndrome (a clinical condition that is defined by a group of signs and symptoms such as type of epileptic seizure, age of onset, electroencephalogram pattern, and family history)(Fisher et al., 2014).

This brain disease is one of the most prevalent and disabling neurological disease affecting around 65 million people worldwide (Ngugi et al., 2010). In Portugal, according to *Liga Portuguesa Contra a Epilepsia* (LPCE), 40 to 70 thousand people may suffer from epilepsy, in a ratio of 1:200 (http://static.lvengine.net/epilepsia/Imgs/GENERALIDADES(1).pdf seen at 22.12.2017). Recent data showed that the number of patients, both adults and children, with active epilepsy (under treatment or with recent seizures) is rising, probably due to population growth (https://www.cdc.gov/media/releases/2017/p0810-epilepsy-prevalence.html seen at 22.12.2017).

After the patient has a first epileptic seizure it is important to know the cause of epilepsy. It is critical for the treatment to know if the epilepsy origin is structural, infectious, metabolic, immune, yet unknown or with more than one etiology (Scheffer et al., 2017).

1.1.1. Mesial Temporal Lobe Epilepsy and the hippocampus

Mesial temporal lobe epilepsy (MTLE) is an epilepsy syndrome characterized by epileptogenic abnormalities in mesial temporal lobe, especially in hippocampus. This is the most common form of resistant epilepsy to antiepileptic drugs. Only by surgical treatment is possible to abolish the disabling seizures. The histopathological hallmark of MTLE is hippocampal sclerosis that occurs due to pyramidal cell loss of Cornu Ammonis (CA), part of hippocampus, mainly in CA1 and CA4 (Blümcke et al., 2013) (Fig. 1). Associated with this neuronal cell loss is a severe pattern of astrogliosis (explained in the next chapters) that causes shrinkage and hardening of tissue (Chang and Lowenstein, 2003). In addition to these morphological features, neurogenesis (Brooks-Kayal et al., 1998) and alterations in the gamma-aminobutyric acid type A ($GABA_A$) receptors on the surface of hippocampal dentate granule cells (Parent et al., 1997) also occur.

In a normal hippocampus, excitatory inputs from entorhinal cortex go directly to dentate gyrus (DG), which in turn projects to CA3. However, in abnormal hippocampus, as a result of neuronal cell loss in CA3, mossy fiber axons from dentate granule cells start to sprout aberrantly and to synapse on dendrites of neighboring dentate granule cells, resulting in a excitatory feedback loop (Chang and Lowenstein, 2003). Moreover, there is a loss of inhibition due to death of interneurons (de Lanerolle et al., 1989). All these events, promote the appearance of hypersynchronous neuronal discharges that are responsible for generating spontaneous seizures.

Patients with MTLE normally have a history of febrile seizures (Choy et al., 2014) or injuries, such as head injury or infections, within the first 5 years of life, which suggest that during development brain insults play a major role in epileptogenic hippocampal damage (Engel, 2001). The time between a brain insult and onset of spontaneous recurrent seizures (i.e., the latent period) is highly variable, ranging from months to years. In this latent period a normal brains starts to develop epilepsy in a process called epileptogenesis (Herman, 2002).

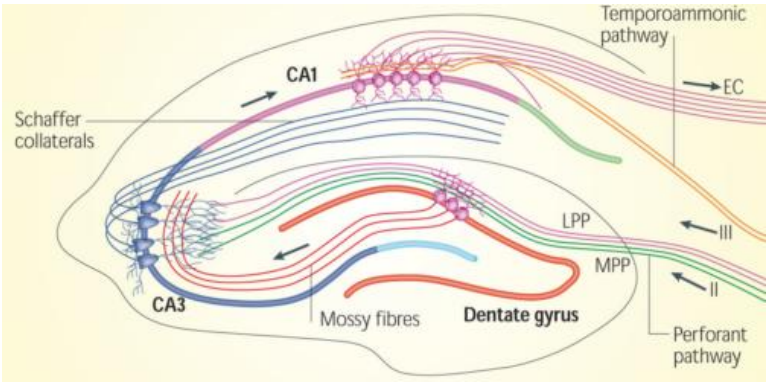

Fig. 1 - The neural circuitry in the hippocampus (Deng et al., 2010).

1.2. Experimental models of Epilepsy

To develop therapeutics that can interfere with epileptogenesis it is crucial to study the alterations that occur in the brain before epilepsy develops. It is not possible to determine these changes in human tissue because the only human samples derive from brain surgeries of refractory epilepsy patients, which means that at this point epilepsy is already very well establish. For this reason, over the last decades, experimental models of epilepsy have been developed, which have been crucial to improve the knowledge of the basic mechanisms of epileptogenesis and seizure generation.

Epilepsy consists of multiple heterogeneous syndromes with many etiologies and different age of onset. Therefore, experimental models, *in vivo* or *in vitro*, mimic different types of epileptic seizures, syndromes or just specific aspects of the disease.

In vivo animal models have been categorized into different seizure models: chemical or pharmacologic (induced by pilocarpine or kainic acid, for example); electrical stimulation (such as the kindling model); genetic (knock-out of genes related with dysfunction of ion channels, receptors, enzymes or transporters); developmental (like the febrile seizures model) and trauma (such as cortical undercut model) (Kandratavicius et al., 2014; Löshcer, 2002; Raol and Brooks-Kayal, 2012). The most commonly used models to mimic human temporal lobe epilepsy (TLE) are pilocarpine (an acetylcholine receptor agonist) model, kainate (a glutamate analogue) model and kindling model, a process that triggers epileptic seizure through repeated low-intensity electrical stimulation in a given brain region. All of them are used to study the mechanism of epileptogenesis, cognitive deficits and develop therapies (Raol and Brooks-Kayal 2012). Although there are many similarities between human epilepsy and these models, the research of epileptogenic mechanisms and antiepileptic drug screening is accomplish at the expense of high mortality of animals (rats or mice) and high variability in the spontaneous

seizures frequency and severity. Moreover, they are costly and time-consuming procedures, mainly the kindling model (Kandratavicius et al., 2014).

The mechanistic features of epilepsy can also be studied through *in vitro* models. Reduced biological systems, like brain slices, allow to detail cellular and molecular processes related with epileptogenesis. These systems maintain their tridimensional structure, allowing the preservation of neuronal circuits necessary for the development of spontaneous seizures (Wong, 2011). Brain slices can be acute, which means that they are maintained for several hours *ex-vivo*, mainly for electrophysiological activity recordings or release experiments after short incubation with stimuli. However, studies of chronic actions resulting from pharmacological intervention are not possible in these preparations (Humpel, 2015; Sundstrom et al., 2005). For longer studies is essential to use organotypic brain slices, which can be maintained in culture from one week up to 6 months (Gogolla et al., 2006).

1.2.2. Organotypic Hippocampal Slice Cultures (OHSC)

Organotypic slice cultures were established using the roller tube technique (Gähwiler, 1981), that later was modified and optimized by Stoppini et al. (1991), who developed the interface method. This last approach allows slices to be cultured on semipermeable membraned in a semi-three dimensional structure where as the original technique only generates a quasi-monolayer slice.

Both culturing techniques can be used to prepare organotypic slices from different parts of the brain, such as cerebellum (Ghoumari et al., 2003), thalamus (Molná and Blakemore, 1998) or striatum (Becq et al., 1999), but hippocampal slices, either from rats or mice, are the most used (Organotypic Hippocampal Slice Cultures - OHSC). The age of the animal from which the brain tissue is removed varies. Early postnatal pups with 6 or 7 days are easier to dissect. Cytoarchitecture is already established and nerve cells survive better to explantation (A De Simoni et al., 2006; Gähwiler et al., 1997). Moreover, slices obtained from animals between birth to 5 days, for mice, and to 15 days, for rats, show more reproducibility, survival, and morphological organization (Muller et al., 2001).

OHSC has a well-defined cellular architecture of the hippocampus and therefore preserves the *in vivo* organizational features. The neuronal connectivity, the glial-neuronal interactions, the synaptic circuitry, chemical signaling and neurotransmitter receptors distribution remain intact in this type of culture (Gähwiler, 1981; Gähwiler et al., 1997; Stoppini et al., 1991). The deafferentation and deefferentation occurring during tissue slicing is known to cause cell death. However, after 2 weeks in culture, slices recover from the altered metabolic state and dead cells are washed away. The surface cells are healthy, receiving and sending inputs from intact axons (A De Simoni et al., 2006; Gähwiler, 1981). It is worth noticing that as an *ex vivo* preparation, OHSC does not have a functional vascular compartment, so effects of blood flow or recruitment of inflammatory cells from peripheral nervous system cannot be considered (Sundstrom et al., 2005; Q Wang and Andreasson, 2010).

These preparations need to be cultured for at least 10 to 14 days to guarantee that they are not activated by endogenous release of calcium or glutamate and that reactive astrogliosis is minimized (Humpel, 2015). During this period, slices mature and intrinsic axonal projections become stabilized, while nerve cells continue to differentiate and to develop a tissue

organization that closely resembles that observed *in situ* (A De Simoni et al., 2006; Gähwiler et al., 1997).

These features, closely related to *in vivo,* enable the study of central nervous system (CNS) function and dysfunction and understand a variety of processes over time, like neurogenesis, synaptogenesis, neuronal loss, calcium homeostasis and epileptogenesis. OHSC, as a complex multicellular model that reflects the environment present *in vivo*, also allows to study a selection of compounds and to identify their mode of action for use in *in vivo* tests.

1.2.2.1. OHSC as a model of epileptogenesis

OHSC show many epileptogenic alterations that are also observed in human epileptic tissue. Studies of neuronal activity in these slices showed that CA1 and DG have higher percentage of cell death, but CA3 is spared (Laake et al., 1999; Noraberg et al., 1999; Vornov et al., 1991). As a consequence of this neuronal death, partly due to deafferentation occurring during tissue slicing, axons from mossy fiber pathway start to sprout leading to aberrant connections (Frotscher and Gähwiler, 1988) and consequentially to hyperexcitability. Additionally, there is a loss of inhibition due to death of interneurons (Cossart et al., 2001). Together these two events promote the development of spontaneous seizures. Nevertheless, it should be noted that cultures up to 30 days *in vitro* (DIV) with well-preserved inhibitory interneurons have been described (Dyhrfjeld-Johnsen et al., 2010).

Dyhrfjeld-Johnsen et al. showed, in slices cultured in serum-free medium, the appearance of epileptiform activity related with slices age (Dyhrfjeld-Johnsen et al., 2010). This activity exhibit interictal discharges, which occur among seizures, or ictal discharges, which appear during a seizure. According to this study, epileptiform activity starts to develop after 7 DIV. Between 14 and 17 DIV, interictal-like spikes and bursts appear, preceding increasingly ictal-like discharges after 21 DIV. This resembles the latent period that occurs between an initial event of an injury and the appearance of spontaneous recurrent seizures that is characterized in MTLE patients (Herman, 2002). This peak of seizure-like activity at 14 DIV is coincidence with a later secondary peak of cell death, being the first after slicing (Berdichevsky et al., 2012). It is widely accepted that severe and prolonged seizures (i.e. *status epilepticus*) result in neuronal death even in humans (Dam, 1980; Henshall and Meldrum, 2012). Hippocampal volume loss is proportional to the duration of epilepsy (Henshall and Meldrum, 2012).

Recent *in vivo* studies in mice have shown that under epileptic seizures neuronal stem cells start to divide symmetrically and undergo a conversion into reactive astrocytes (Sierra et al., 2015). In OHSC, a reactive astrocytic response during culturing process is described (Coltmann and Ide, 1996). This appearance of astrogliosis strongly influence the generation of new granule cells (a process called neurogenesis). Immediately after preparation, slices have a neurogenesis rate equivalent to *in vivo* condition. However, after one week of cultivation the rate of neurogenesis decreases dramatically (80-90%) (Namba et al. 2007; Alberi et al. 2016). Both these morphologic features, severe pattern of astrogliosis and loss of neurogenesis are observed in MTLE-patients.

1.3. Neuroinflammation related to Epilepsy

Neuroinflammation is classically a beneficial process that protects central nervous system by removing pathogens and helping in tissue healing. Nevertheless, when extent or duration of inflammation exceeds the homeostatic threshold, the beneficial effects turn into toxic and harmful effects, contributing to a range of disorders including Alzheimer's disease, Parkinson's disease and epilepsy (Lénárt et al., 2016; Vezzani et al., 2013).

Pre-clinical and clinical studies reinforce the idea of a positive feedback loop between epilepsy and inflammation (Ravizza and Vezzani, 2006; Turrin and Rivest, 2004; Xu et al., 2013). Epileptic seizures increase the production of pro-inflammatory cytokines, like interleukin-1β (Il-1β) and tumor necrosis factor-alpha (TNF-α), by glial cells (microglia and astrocytes). Also induce an upregulation of pro-inflammatory molecules such as chemokines, prostaglandins and toll-like receptors (TLRs). These inflammatory mediators, in turn, can trigger neuronal hyperexcitability, through modulations of ion channels in neurons and glutamate release in glial cells, decrease seizure threshold and induce the breakdown of the blood-brain barrier (BBB) (Shimada et al., 2014).

1.3.1. Microglia

Microglia are the innate immune cells in the CNS. These glial cells are the resident macrophages in the brain and spinal cord and its major function is the body defense against injury, infections and diseases.

The distribution of these cells differs between species and brain structures. In mouse brain, the number of microglial cells varies between 5 and 12% of total neural cells (Lawson et al., 1990) and, in human brain, its ranges between 0.5 and 16% (Mittelbronn et al., 2001). Regarding brain structures, hippocampus has one of the most densely populated regions of microglia. Particularly, DG appears to have more microglia than CA (Lawson et al., 1990).

With their macrophage capacity for phagocytosis, microglia destroy damaged and dying neurons who suffered excitotoxicity to protect the nearby healthy cells. These cells also facilitate local tissue repairing and the recovery of injured neurons through release of proinflammatory mediators, neuroprotective and trophic factors (Mirrione and Tsirka, 2011). Besides neuroprotective function, microglia can also be neurotoxic, since inflammatory molecules, when released for too long or in high quantities, are toxic to neurons and have a negative impact in their function. Moreover, microglia release other toxic factors (as nitric oxide) which leads to oxidative stress and, consequently, to extensive neuroinflammation and recruitment of peripheral immune cells into the damaged brain, compromising the BBB (Mirrione and Tsirka, 2011).

Unlike macrophages of the peripheral immune system elsewhere, microglia have a specialized phenotype. The microglia resting, or quiescent ramified state, is characterized by cells with elongated processes. When the microglia detect a potentially danger insult to the CNS (as inflammation, altered neuronal activity, trauma), retract their processes and change to a rounded amoeboid morphology, thus becoming activated. In that phase, microglia become phagocytic, proliferative and migratory, moving to the lesion site, exhibiting the capacity to release chemokines, cytokines, neurotrophic factors and to present antigens (Kettenmann et

al., 2011; Mirrione and Tsirka, 2011). Sometimes when this activation is too extensive is called 'microgliosis'.

Evidences suggest that microglial activation is heterogeneous. In a way to simplify, its activation has been categorized into two groups: M1 ("classical") or M2 ("alternative"), depending on the nature of the triggered stimulus. M1 produces pro-inflammatory mediators, developing a classical inflammatory reaction, whereas M2 produces anti-inflammatory mediators, being associated to tissue repairing and homeostasis restoration (Tang and Le 2017; Sousa, et al. 2017).

Although not able to differentiate between microglia phenotypes, ionized calcium binding adaptor molecule 1 (Iba1) is one of the most used markers to detect all forms of microglia both in rodents and humans (Sousa et al., 2017). However, it should be noted that Iba1 does not differentiate microglia from macrophages, neutrophils or monocytes upon infiltration of these cells into the CNS (Kettenmann et al., 2011; Sousa et al., 2017).

1.3.2. Astrocytes

Astrocytes are the major glial cell population within the CNS. In the cortex of the rodents there is one astrocyte for three neurons and in human cortex this proportion is 1.4 astrocytes for every neuron (Nedergaard et al., 2003), which means that there is an increasing number of these glial cells with brain evolution.

In XIX century, astrocytes were seen as supportive cells of neural tissue, they were just the glue of the brain and a sensitive marker of diseased tissue. The word "glial" originates from the word "gliok", which means "glue" or slime in Greek. However, over the past 25 years it has become clear that astrocytes are a specialized type of cells responsible for a wide variety of complex and essential functions in the healthy CNS. These glial cells regulate blood flow, release energy substrates directly in node of Ranvier and other substances, like transmitters and growth factors, into synapses, participating in synaptic function and plasticity. Also maintain extracellular balance of ions, fluid balance and cellular transmitters (Nedergaard et al., 2003; Perea et al., 2009; Sofroniew, 2009; Sofroniew and Vinters, 2010).

Besides these functions, astrocytes have a major role in the response to CNS insults (infection, trauma, neurodegenerative disease and ischemia), which involves changes in their molecular expression and morphology (Sofroniew, 2009, 2015).

Astrocytes are a very heterogeneous group of cells but they can be divided in two main subtypes, protoplasmic or fibrous, depending on cellular morphology and anatomical locations. Protoplasmic astrocytes are localized in gray matter, such as CA and DG in the hippocampus, and exhibit numerous fine processes in a uniform globoid distribution. Fibrous astrocytes are found throughout all white matter, like Schaffer collateral in hippocampus, and exhibit fewer and longer processes than protoplasmic ones (Andriezen, 1893).

In CNS, astrocytes are orderly and well organized, in a non-overlapping manner. Nevertheless, when these glial cells detect an insult they start to proliferate and to extend their process beyond their own individual domain, resulting in a highly overlapping net of processes. Additionally, astrocytes' cell body hypertrophy also occurs. This modification, called reactive astrogliosis, is not an all-or-none phenomenon, is a set of gradual changes depending on the type of insult. Sometimes, when this reactive astrogliosis is too severe there is a glial scar formation, which is a narrow and compact scar that can act as neuroprotective barrier to

inflammatory cells and infectious agents (Sofroniew and Vinters, 2010; Sofroniew, 2015). It is noteworthy that recently, Liddelow suggested the existence of two (or more types) of reactive astrocytes, one type being helpful and the other being harmful (Liddelow and Barres, 2017). Nevertheless, this division is still poorly understood and is not yet widely used.

The morphological changes can be perceived through immunohistochemical techniques. Glial Fibrillary Acidic Protein (GFAP), an intermediate filament protein, is the most used marker for astrocytes. When astrocytes are hypertrophic, an upregulation of this protein occurs (Ben Haim et al., 2015). However, it is now clear that not all astrocytes express GFAP and not all cells in the CNS that express GFAP are astrocytes (Oberheim et al., 2012; Sofroniew and Vinters, 2010).

1.3.3. Cytokines

1.3.3.1. Interleukin -1β (IL-1β)

IL-1β is a proinflammatory cytokine rapidly synthesized and released primarily by microglia (Giulian et al., 1986) and later by astrocytes (W Zhang et al., 2000) under pathological conditions. High levels of IL-1β were detected in epileptic patients (Uludag et al., 2015). After precipitating events like infections or inflammation, the systemic host, especially young children, responds with fever. Sometimes, this fever provokes convulsions (febrile seizures) by a mechanism that involves IL-1β but is not fully understood. It is known that IL-1β intracerebral administration in immature rodents decreases the threshold for induction of experimental febrile seizures (Dubé et al., 2005). Moreover, in mice, the ablation of the gene for IL-1β receptor, type 1 IL-1 receptor (IL-1R1), gave them resistance to experimental febrile seizures (Dubé et al., 2005).

In pharmacologic or kindling models, the rapid increase of IL-1β levels during acute seizures subsisted after seizure reduction (MG De Simoni et al., 2000; Ravizza et al., 2008). Furthermore, these levels did not return to basal levels during epileptogenesis or in chronic epileptic tissue, which prompted the development of spontaneous seizures. These long-lasting high levels of IL-1β were expressed by astrocytes and not by microglia, which also happens in human TLE tissue. The chronic IL-1β expressing astrocytes suggest that astrocytes and IL-1β play a predominant role in sustaining chronic inflammation underlying the spontaneous seizures onset (Ravizza et al., 2008).

When seizures evoke rapid production of this cytokine, the expression of endogenous IL-1R antagonist (IL-1RA) should rapidly increase and occlude the activation of the IL-1R1, which is what happens in typical peripheral inflammatory reactions. Nevertheless, in this pathologic situation IL-1RA is upregulated to a far lower extent and with a substantial delay (MG De Simoni et al., 2000; Oprica et al., 2003; Vezzani and Baram, 2007). Thus, the brain is less efficient in shutting down the effects of a sustained rise in endogenous IL-1β once IL-1R1, expressed in hippocampal neurons, is activated repetitively.

IL-1β promotes excitability and excitotoxicity in hippocampal pyramidal cells through a pathway that also involves another proinflammatory cytokine, the high-mobility group box- 1 (HMGB1). Interaction between IL-1R1 and Toll-like receptor 4 (TLR4), a receptor activated by HMGB1, enhances calcium influx athwart phosphorylation of N-methyl-D-aspartate (NMDA) receptor subunit 2B (NR2B). This increased calcium permeability of NMDA receptor plays a role in neuronal excitability (Shimada et al., 2014; Vezzani et al., 2011). Also, *in vivo* experiments

clearly demonstrate IL-1β-induced hyperexcitability. Intracerebrally administration of IL-1β in pharmacological models exacerbates seizures (Vezzani et al., 1999) and administration of IL-1R1 antagonist reduces them (Vezzani et al., 2000). Besides, IL-1β inhibits $GABA_A$ inhibitory receptor functions in hippocampal neurons (S Wang et al., 2000).

IL-1β also plays a role in BBB permeability. When this cytokine is produced by seizures promotes neuronal cell death and the breakdown of BBB. This breakdown leads to BBB leakage and increases the permeability to different molecules (Shimada et al., 2014; Vezzani and Granata, 2005). One of them is albumin. This type of proteins, upon entrance into the brain, induces an upregulation in inflammatory mediators and reduces the potassium and glutamate uptake of astrocytes, leading to enhancement of neural excitability (Shimada et al., 2014). Although, both albumin and IL-1β inhibit the astrocytic reuptake of glutamate, IL-1β also increases its astrocytic release via TNF-α induction (Shimada et al., 2014; Vezzani et al., 2008).

Taken together, several lines of evidences support the role of IL-1β as an epileptogenic cytokine, enhancing hippocampal neurons hyperexcitability and decreasing seizure threshold.

1.3.3.2. Tumor Necrosis Factor-α (TNF-α)

TNF-α is another inflammatory factor scattered by glial cells, mainly by microglia (Chung and Benveniste, 1990; Welser-Alves and Milner, 2013). This cytokine acts as a proinflammatoy stimulus inducing the expression of the inactive IL-1β proform. However, IL-1β maturation and release are not related to TNF-α, but rather to protein complexes named inflammasomes (Schroder and Tschopp, 2010) (explained in the next chapter).

A number of studies, both clinical and pre-clinical, have revealed an increased expression of TNF-α in the brain of human epileptic patients (Sinha et al., 2008) and in mice with pilocarpine-induced seizures (Turrin and Rivest, 2004).

TNF-α and IL-1β act synergistically to promote neuronal hyperexcitability. IL-1β-induced TNF-α stimulates astrocytes to release glutamate, which will lead to increased levels of extracellular glutamate. This high concentration depolarizes the membrane potential of glutamatergic neurons, thus promoting their stimulation (Shimada et al., 2014). In addition, TNF-α regulates neuronal circuit homeostasis by modulating the frequency of different receptors. When this cytokine binds to one of its receptor, tumor necrosis receptor 1 (TNFR1), causes a rapid exocytosis of AMPA receptors, which have a high affinity to glutamate, in hippocampal pyramidal cells. Many of these newly exocytosed AMPA receptors lack GLUR2 subunit. As this subunit render the channel impermeable to Ca^{2+}, the lacking of it will make AMPA receptor more permeable to this cation (Stellwagen et al., 2005). Simultaneously, TNF-α can cause an endocytosis of $GABA_A$ receptors, promoting a decrease in inhibitory synaptic strength (Stellwagen et al., 2005). Summing up, this proinflammatory cytokine is able to alter the balance between excitation and inhibition in a manner that potentiates the appearing of spontaneous epileptic seizures.

It should be noted that TNF-α has been also associated with neuroprotective mechanisms. In OHSC prepared from mice, a high concentration of TNF-α enhanced excitotoxicity, however in lower concentrations promoted neuroprotection against AMPA-induced neuronal death (Bernardino et al., 2005). The TNF-α-induced mechanisms are mediated by its receptors.

TNFR1 is involved with toxicity, whereas tumor necrosis receptor 2 (TNFR2) is involved with neuroprotective effect.

1.4. Inflammasomes

The inflammasome concept was first described in 2002 by Tschopp and colleagues (Martinon et al., 2002). The authors identified a caspase-1 activating complex and called it inflammasome, stating that it was an important arm of the innate immunity.

An inflammasome is a cytosolic multiprotein complex that triggers the activation of inflammatory caspases, mainly caspase-1, allowing the cleavage and release of pro-inflammatory cytokines and subsequently an inflammatory response. The signaling cascades that are induced by cytokines promote immunopathogenic conditions that lead to neuronal death and a pro-inflammatory cell death known as pyroptosis (Bergsbaken et al., 2010). Therefore, inflammasomes play a pathogenic role in neurological diseases such as Alzheimer's disease, traumatic brain injury, multiple sclerosis (Freeman et al., 2017; Freeman and Ting, 2016), vascular disease (Lénárt et al., 2016) and epilepsy (Edye et al., 2014).

Each inflammasome contains a pattern recognition receptor (PRR) that senses the presence of microorganisms by recognizing invariant microbial motifs, which are called pathogen-associated molecular patterns (PAMPs), and endogenous molecules released from damaged cells, entitle danger-associated molecular patterns (DAMPs) (Takeuchi and Akira, 2010). Thus, these complexes direct the responses of the innate immune system to pathogenic stimuli. These PRR, expressed by different cell types (microglia, astrocytes, monocytes, macrophages and others), can be subdivided in two major classes according to their subcellular localization (Fig. 2A). Toll-like receptors (TLRs) and C-type lectin receptors (CTLs) are transmembrane proteins which sense extracellular milieu or endosomal signals. The second class, composed by intracellular proteins including RIG-I-like receptor (RLR), the AIM2-like-receptor (ALR, also called PYHIN or HIN200) and the nucleotide-binding domain and leucine-rich repeat containing (NLR) proteins (also called non-officially as NOD (nucleotide-binding oligomerization domain) - like receptor) (Ting et al., 2008), senses intracellular signals and are the only receptors involved in inflammasome formation.

The NLRs is a family of cytosolic receptors subdivided in two types depending on which N-terminal molecule they contain. If the member of NLR family contains an N-terminal pyrin domain (PYD) then is subcategorized into the NLRP family (previously also called "NALPs"). But if it possess a caspase activation and recruitment domain (CARD) in N-terminal end, is subcategorized as NLRC (previously also called NOD) (Ting et al., 2008). Beyond the N-terminal effector PYD or CARD, NLRs also contain a C-terminal leucine-rich repeat (LRR) domain and in the middle a conserved central nucleotide-binding and oligomerization domain (NACHT; also called with the broader name of NBD) (Ting et al., 2008)(Fig. 2B). The PYD or CARD domain mediates downstream signal transduction. The NACHT domain has ATPase activity and it is essential for forming oligomeric structures that are required for inflammasome assembly. Lastly, the LRR repetition has autoregulatory functions and it is involved in ligand interaction (Schroder and Tschopp, 2010).

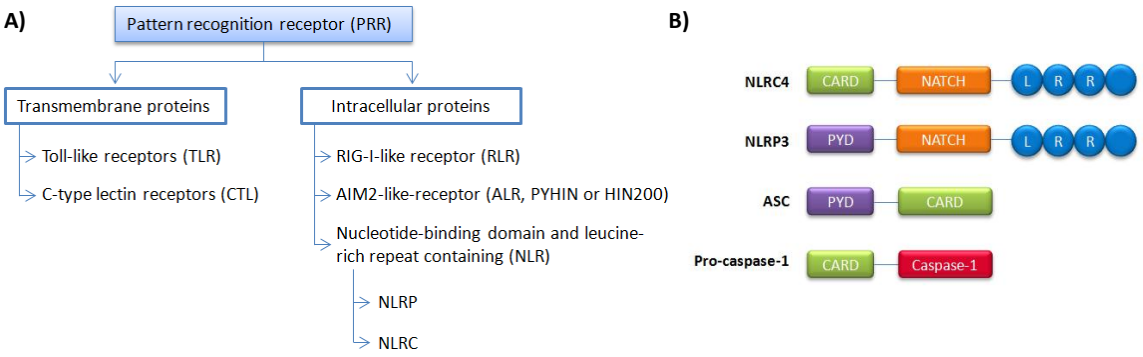

Fig. 2 - (A) Schematic organization of pattern recognition receptor (PRR) family. (B) Composition depiction of inflammasome components. Example of NLRP3 and NLRC4 as sensor proteins.

Normally, each inflammasome is composed by one sensor protein (like NLRP3), which gives it the name, an adaptor apoptosis-associated speck-like protein containing a CARD (ASC, also termed PYCARD) and a pro-caspase-1 (Fig. 2B). Nevertheless, there are some variations in the structure depending on the inflammasome (Lamkanfi and Dixit, 2014; Schroder and Tschopp, 2010). ASC is composed of two domains: a PYD and a CARD; and acts as a central adaptor between the PYD of the sensor protein and the CARD of pro-caspase-1.

Upon activation of inflammasome sensors mediated by PAMPS and DAMPS, ASC proteins assemble into multiple filamentous structures which form a platform termed ASC speck or pyroptosome (Hoss et al., 2017; Lu and Wu, 2015). When this ASC aggregate binds to sensor protein oligomers, ASC is able to recruit pro-caspase-1, leading to autoproteolytic conversion of the pro-enzyme into caspase-1. This active enzyme mediates the production of IL-1β and interleukin-18 (IL-18) pro-inflammatory cytokines and the initiation of a pro-inflammatory cell death named pyroptosis (Latz et al., 2013; Martinon et al., 2002). This type of cell death also requires cleavage of gasdermin D, which forms pores in the plasma membrane, and can be activated either by caspase-1 (W-T He et al., 2015; J Shi et al., 2015) or caspase-11 (Kayagaki et al., 2011).

There are different inflammasomes clearly identified, such as NLRC4, NLRP1, NLRP3 or AIM2, which respond to different priming stimuli (Place et al., 2018; Schroder and Tschopp, 2010). NLRP1 is activated by *Bacillus anthracis* anthrax lethal toxin, where as NLRC4 responds to a protein appendage (called type three secretion system-T3SS) found in several Gram-positive and to flagellin proteins of Gram-negative bacteria. Moreover, AIM2 detects bacterial and viral dsDNA as well as self-DNA. Finally, the NLRP3 is activated by a wide and varied range of stimuli, which will be discussed later. It should be noted that the mechanisms associated with the activation of inflammasomes are still under debate.

1.4.1. NLRP3 Inflammasome

The NLRP3 inflammasome is the most studied inflammasome, since it was described in 2004 (Agostini et al., 2004), and has gathered attention in neuroscience. *nlrp3* gene is defined as NLR family pyrin domain containing 3, while NLRP3 protein is usually designated as NATCH, LRR and PYD domains-containing protein 3. Before this nomenclature, *nlrp3* gene was previously approved by RGD (from NHLBI, NIH) and HUGO Gene Nomenclature Committee (HGNC) as CIAS1 (Hoffman et al., 2001), C1orf7 and “cold autoinflammatory syndrome 1”.

There are others aliases for *nlrp3* gene, at least more sixteen. The most common are: cryopyrin, NALP3, Nucleotide-Binding Oligomerization Domain, Leucine Rich Repeat and Pyrin Domain Containing, PYRIN-Containing APAF1-Like Protein 1, FCAS1.

Mutations in the inflammasome sensor NLRP3 is related with inherited cryopyrin-associated periodic syndromes (CAPS), which include familial cold autoinflammatory syndrome (FACS), Muckle-Wells syndrome (MWS) and neonatal-onset multisystem inflammatory disease (Abderrazak et al., 2015; Ozaki et al., 2015). Furthermore, deregulation of NLRP3 inflammasome activation underlies other multifactorial diseases, including gout, type 2 diabetes mellitus, atherosclerosis, Parkinson's Disease, Alzheimer's Disease, multiple sclerosis, traumatic brain injury and amyotrophic lateral sclerosis (ALS) (Abderrazak et al., 2015; Baroja-Mazo et al., 2014; Freeman and Ting, 2016; Ozaki et al., 2015).

Regarding NLRP3 inflammasome localization in the brain, it is still a debated subject and needs further studies to confirm it. Although there are a countless number of articles looking at NLRP3 inflammasome, there are few that address the thematic of its location. It seems widely accepted that NLRP3 inflammasome is expressed in microglia (Edye et al., 2014; Song et al., 2017; Walsh et al., 2014). However it remains controversial whether astrocytes and neurons express it. Nevertheless is necessary to understand that inflammasome components and active inflammasome are expressed differently.

In microglia, there are evidences that NLRP3 is not constitutively expressed in healthy conditions. It is only upregulated after priming or in disease models (Gustin et al., 2015; Zendedel et al., 2016). Although, it seems not to be expressed in mice models of ALS (Debye et al., 2018; Johann et al., 2015). Contrariwise, caspase-1 and ASC are constitutively express without any stimuli. ASC is also expressed in microglia in animal models of spinal cord injury (Zendedel et al., 2016) and ALS (Debye et al., 2018; Johann et al., 2015). Altogether, these evidences indicate that microglia, in need of defending the body, has all the necessary components for a functional NLRP3 inflammasome (Gustin et al., 2015; Heneka et al., 2013).

In astrocytes, NLRP3 expression depends on stimuli. In cell culture from C57BL/6JOlaHsd mice primed with LPS or cytokines mix, very weak levels of NLRP3 transcript and almost no protein were detected (Gustin et al., 2015). However, there are a minor expression of this inflammasome component in a spinal cord injury model (Zendedel et al., 2016) and a strongly expression in ALS (Debye et al., 2018; Johann et al., 2015) and in primary cultured astrocytes treated chronically with ethanol (Alfonso-Loeches et al., 2014). ASC resembles NLRP3 in these cells. Caspase-1 is expressed at low levels in healthy astrocytes (Alfonso-Loeches et al., 2014; Gustin et al., 2015), but at higher levels in primary cultured astrocytes treated chronically with ethanol (Alfonso-Loeches et al., 2014). In short, there are contradictory evidences on the lack of inflammatory components in these glial cells. Further understanding about when or if all NLRP3 components are present in astrocytes will enlighten its function in these cells. NLRP3 is related to many disorders, but lipopolysaccharides (LPS) still is the stimulus par excellence of this inflammasome.

Lastly, there are reports congruently showing the presence of NLRP3 in healthy (Gustin et al., 2015) and non-healthy neurons (Debye et al., 2018; Zendedel et al., 2016). ASC and caspase-1 (Gustin et al., 2015) are weakly expressed in healthy primary cortical neurons and neuronal ASC expression is also described in disease models (Debye et al., 2018; Zendedel et al., 2016). Altogether, these results appear to point to the presence of all inflammasome

components in neurons, albeit in small amounts, indicating that the inflammasome may be functional in these cells.

In summary, under certain conditions, astrocytes and neurons may also express a functional NLRP3 inflammasome. Nevertheless, it is unclear whether the inflammasome is expressed equally by all cells containing its components, regardless of the activating stimulus. Co-localization and mRNA studies of these proteins have recently started and will help to understand the relevance of NLRP3 inflammasome in each type of brain cell.

Beyond the cellular location of this multiprotein complex, a subcellular characterization of each inflammasome component has also started and it is controversial. Although further studies are required, each protein has been found in different organelles, which make this inflammasome assembly highly regulated, in addition to the fact that each protein is auto-inhibited in the absent of stimulation (Place et al., 2018).

Under resting conditions NLRP3 localizes at the cytoplasm, but not within mitochondria, in primary cultured astrocytes treated chronically with ethanol (Alfonso-Loeches et al., 2014) and in human embryonic kidney cells and bone marrow derived macrophages (Subramanian et al., 2013). Another study suggest that endoplasmic reticulum structures are the sites containing this protein in human monocytic cell line (Zhou et al., 2011). Regarding basal location of ASC, it is dispersed in the cell, either in the nucleus or in the cytoplasm in mouse macrophages (Y Wang et al., 2013). Finally, it is very well known that inactive proform of caspase-1 is located in the cytosol (Miao et al., 2011).

In the presence of NLRP3 activators, all the components need to assembly to form a functional inflammasome. There are two theories: one suggests that NLRP3 inflammasome has an organelle-free cytoplasmic localization in nigericin or ATP-primed macrophages (Baroja-Mazo et al., 2014; Y Wang et al., 2013), and the other reiterates that both NLRP3 and ASC co-localize with endoplasmic reticulum and mitochondria organelle clusters in nigericin-primed human monocytic and embryonic kidney cells (Subramanian et al., 2013; Zhou et al., 2011) and in ethanol-primed astrocytes (Alfonso-Loeches et al., 2014). Supporting this last theory, it was described, in bone marrow-derived macrophages, that microtubules are responsible to drive the approximation of mitochondria to endoplasmic reticulum facilitating the NLRP3/ASC assembly and subsequent recruitment of pro-caspase-1 (Misawa et al., 2013). However, as a confounding factor, all inflammasome components were found in the extracellular mileu functioning as a danger signaling that amplifies the inflammatory response (Baroja-Mazo et al., 2014).

Overall, further studies are needed to understand the dynamics of NLRP3 inflammasome since the first triggering signal. Perhaps these subcellular locations are not mutually exclusive or vary depending on the upstream trigger or cell type. To my knowledge, these studies were never conducted in microglia, which would be interesting.

1.4.1.1. Activation and assembly of NLRP3 inflammasome

NLRP3 inflammasome is activated by a wide variety of microbe or host derived triggers. The exact mechanism by which different stimuli activate NLRP3 remains unclear. However, it is widely accepted that NLRP3 can be activated through canonical or non-canonical pathways. Recent studies also include an alternative pathway of NLRP3 inflammasome activation (Y He, Hara et al., 2016).

Canonical pathway

In the canonical pathway, NLRP3 activation is highly regulated and demands two independent signals (Fig. 3). The first signal, such as TLR ligands or endogenous molecules, drive the upregulation of NLRP3 and pro-IL-1β through the activation of nuclear factor kappa B (NF-kB) (Lamkanfi and Dixit, 2014; Ozaki et al., 2015; Place et al., 2018). Subsequently, post-transcriptional changes occur in NLRP3 protein. Although these regulatory mechanisms are poorly understood, it is known that TLR4 adaptors, such as MYD88, are involved and NLRP3 is deubiquitinated by K63-specific deubiquitinase BRCC3 in order to become active (Y He, Hara et al., 2016; Place et al., 2018). Bacteria and bacterial components like LPS, viruses, TNF-α and others PAMPs and DAMPS can act as first trigger (Franchi et al., 2009; Y He, Hara et al., 2016; Ozaki et al., 2015).

Once primed, a second signal allows assembly and activation of the NLRP3 inflammasome. A range of molecules act as NLRP3 activators, among them extracellular adenosine triphosphate (ATP), uric acid crystals, β-amyloid (Aβ), free fatty acids, cholesterol crystals, bacterial pore-forming toxins, bacteria, viruses, fungal or protozoan pathogens (Y He, Hara et al., 2016; Ozaki et al., 2015; Place et al., 2018). Without interacting directly with inflammasome, these stimuli induce one or more downstream cellular events that lead to NLRP3 inflammasome activation. The most consensual events among the scientific community are potassium efflux (Muñoz-Planillo et al., 2013; Rivers-Auty and Brough, 2015), generation of mitochondrial reactive oxygen species (ROS) (Zhou et al., 2011), cathepsin release as a result of phagolysosomal membrane destabilization (Hornung et al., 2008), release of mitochondrial DNA or cardiolipsin (Nakahira et al., 2011) and changes in osmotic pressure and cell volume (Compan et al., 2012).

Focusing only on potassium efflux model, it has been proposed that extracellular ATP that activates P2X purinergic receptors 7 ($P2X_7$) ATP-gated ion channels results in potassium efflux and simultaneously sodium influx through the cell membrane (Kahlenberg and Dubyak, 2004). Also, low potassium ion concentrations results in ASC speck formation (Fernandes-Alnemri et al., 2007) and spontaneous NLRP3 inflammasome assembly (Pétrilli et al., 2007). In recent studies (Y He, Zeng et al., 2016; Schmid-Burgk et al., 2016; H Shi et al., 2016) a novel protein has emerged as an essential regulator of NLRP3 inflammasome activation downstream of potassium efflux. This protein is Nek7 (never-in-mitosis A-related kinase 7), a kinase related with mitotic progression and DNA damage response, which binds to LRR of NLRP3 and it is necessary for the recruitment of ASC by NLRP3 and the formation of ASC oligomers.

$P2X_7$ receptors are also linked to a hemichannel protein, called pannexin-1, which stimulates the formation of a large pore, allowing the entry of inflammasome activators (Pelegrin and Surprenant, 2006). Extracellular ATP-derived catabolism products also play a role in NLRP3 inflammasome activation. Adenosine diphosphate (ADP) through purinergic receptor $P2Y_1$ activate phospholipase C-β, which modulates Ca^{2+} and K^+ flux, and consequently activate the inflammasome. Adenosine also promotes this event by activating P1 receptors (A_{2A}, A_{2B} and A3) and modulating cyclic adenosine monophosphate (Baron et al., 2015). Although adenosine is often described as anticonvulsant agent when coupled with receptor A_1 (Boison and Dow, 2012), extracellular catabolism of ATP is associated with the activation of A_{2A} receptors rather than A1 receptors (Cunha et al., 1996).

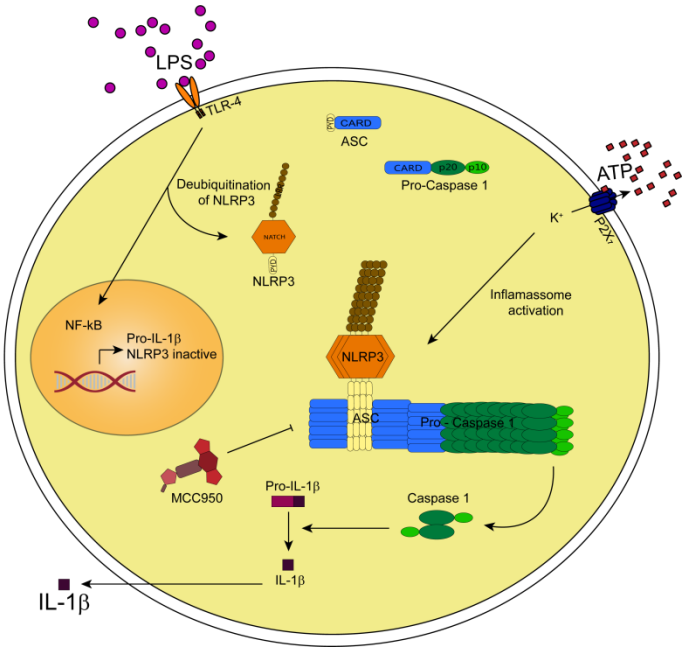

Fig. 3 - Priming and activation signals of the NLRP3 inflammasome.

Non-canonical and alternative pathways

In non-canonical pathway, caspase-11 (caspase-4 and caspase-5 in humans) is activated resulting in NLRP3-dependent release of IL-1β/IL-18 and in NLRP3-independent pyroptosis through gasdermin D N domain (Y He, Hara et al., 2016; Kayagaki et al., 2015). Additionally, activated caspase-11 cleaves pannexin-1 which also promotes $P2X_7$-mediated pyroptosis (Yang et al., 2015).

Most gram-negative bacteria, but not gram-positive bacteria, activate caspase-11; however the signaling mechanism upstream of caspase activation remains controversial (Y He, Hara et al., 2016). Studies suggest that LPS has also a role in this pathway. Cytosolic LPS binds selectively to CARD domain of caspase-11 (Hagar et al., 2013; J Shi et al., 2015), whereas, in canonical NLRP3 inflammasome pathway, extracellular LPS binds to TLR4.

The activation of NLRP3 inflammasome can also occur in response to TLR ligands alone, in the alternative pathway. Although not often mentioned, this pathway was described in human monocytes (Gaidt et al., 2016) and mouse bone marrow-derived dendritic cells (Y He et al., 2013). In this pathway cell death-related molecules like Receptor-interacting serine/threonine-protein kinase (RIPK1), Fas-associated protein with death domain (FADD) and caspase-8 are involved (Gaidt et al., 2016). Moreover, there is no evidence for ASC speck formation or pyroptosis (Gaidt et al., 2016).

1.4.1.2. NLRP3 inflammasome inhibition – a particular case of MCC950

Given the evidence that NLRP3 inflammasome mediates several inflammatory diseases, it makes sense to think of its inhibition and inhibition of its components or end products. In fact targeting IL-1 has been proved to be a successful method for CAPs treatment. Current treatments used are: anakinra, a recombinant IL-1RA; canakinumab, a fully humanized IL-1β antibody; or rilonacept, a soluble decoy IL-1 receptor (Ozaki et al., 2015). These biological

agents can also be used in other NLRP3-related disorders (H Zhang, 2011). Recently, clinical cases of patients with refractory epilepsy who had their seizures controlled by anakinra treatment have been reported (DeSena et al., 2018; Jyonouchi and Geng, 2016; Kenney-Jung et al., 2016) .

In animal models of epilepsy, modulation of IL-1β production pathway also interfered with seizures. Administration of IL-1RA, either peripherally or intracerebrally, reduced the incidence of seizures (Marchi et al., 2009; Vezzani et al., 2000). In the same way, administration of caspase-1 inhibitor (VX-765) reduced seizures and delayed their onset in rodents models of acute seizures induced by electrical stimulation or kainate (Maroso et al., 2011; Ravizza et al., 2006). However, VX-765 (also called Belnacasan) was tested in clinical trials for treatment-resistant partial epilepsy, but only reached phase II and was subsequently terminated.

Besides targeting the main pyrogenic product of NLRP3 inflammasome, alternative methods of inhibiting NLRP3 inflammasome activation are being proposed as a possible therapeutics for epilepsy. The administration of small interfering RNAs (siRNA) to knock out NLRP3 and caspase-1 in the brain of *status epilepticus* rat models showed a clearly reduction of hippocampal neuronal loss and attenuated the severity of spontaneous recurrent seizures (Meng et al., 2014).

NLRP3 inflammasome is also inhibited, indirectly, by a sulfonylurea drug called glyburide. This compound, used in the treatment of type 2 diabetes mellitus, acts downstream of $P2X_7$ receptor but upstream of NLRP3 activation. However, this drug is being associated with hypoglycemia *in vivo*, thus excluding its use in the treatment of other diseases (Ozaki et al., 2015).

Identification of a novel class of sulfonylurea containing compounds has revealed cytokine release inhibitory drugs (CRIDs). CRID3 (CP-456,773) belongs to this family of diarylsulfonylurea-containing compound. CRID3, also known as MCC950, was recently been described, by Coll et al. and colleagues, as a selective inhibitor of NLRP3 inflammasome (Coll et al., 2015). It inhibits both canonical and non-canonical activation of NLRP3 inflammasome, by blocking NLRP3-induced ASC oligomerization. This synthetic small molecule is capable of inhibiting NLRP3, but does not block other inflammasomes, such as AIM2, NLRC4 or NLRP1. Therefore, antimicrobial responses may remain intact, reducing the immunosuppressive effects that occur in drugs like canakinumab.

Evidences suggest that MCC950 attenuates the severity of experimental autoimmune encephalomyelitis (EAE) in mouse (a model of human multiple sclerosis), and effectively inhibits NLRP3 inflammasome activation in a mouse model of Muckle-Wells syndrome and in cells from subjects with the same disease (Coll et al., 2015). Moreover, MCC950 reverses hypertension in mice (Krishnan et al., 2016), preserves cardiac function in animal myocardial infarction model (Van Hout et al., 2017), improves blood–brain barrier integrity in mice with intracerebral hemorrhage (Ren et al., 2018) and ameliorates the behavioral and molecular dysfunctions related to diabetic encephalopathy in a mice model of type 2 diabetes mellitus (Zhai et al., 2018).

Pharmacokinetic and pharmacodynamic studies of MCC950 have already been performed (Coll et al., 2015). MCC950 is a stable compound, remaining more than 70% after 60 minutes in liver microsomes. The five major cytochrome P450 enzymes were only <15% inhibited. MCC950 has a half-live of 3.27h and an oral bioavailability of 68%. As MCC950 has a shorter half-life compared with canakinumab or rilonacept, it can be withdrawn if infections occur.

Like MCC950, ketone metabolite β-hydroxybutyrate (BHB) also selectively inhibits NLRP3 inflammasome activation (Youm et al., 2015). BHB is a molecule exploited by heart and brain as an alternative energy source during exercise or caloric deficiency. Nevertheless, this metabolite only blocks canonical NLRP3 activation and inhibits potassium efflux from macrophages (Shao et al., 2015).

A recently described compound, CY-09, appears to be promising for the therapy of inflammatory diseases. It blocks NLRP3 ATPase activity, resulting in the inhibition of assembly and activation of NLRP3 inflammasome. CY-09 showed therapeutic effects in mouse models of CAPS and type 2 diabetes (Jiang et al., 2017).

Several additional biological or synthetic molecules may provide other ways for inhibiting the NLRP3 inflammasome in different inflammasome-related diseases (Dorfleutner et al., 2015; Haneklaus et al., 2013; Ozaki et al., 2015; Shao et al., 2015).

1.5. Treatment options in Epilepsy

People with epilepsy face cognitive and learning problems, work and driving limitations, sleeping problems, symptoms of depression, anxiety or mood changes. This disease can also affect relationships and motherhood. The risk of death in these patients is higher if not appropriately treated. Although it's necessary to make medication adjustments, the use of antiepileptic drugs (AED) allows an improvement of the life quality of these patients. In the majority of the cases, these drugs can effectively suppress the seizures. It is noteworthy that AED are purely symptomatic, they are neither preventive nor curative. Classical AED are mainly based on three mechanisms of action: modulation of voltage-gated ion channels, increase of inhibitory neurotransmission mediated by GABA, or decrease of excitatory neurotransmission mediated by glutamate (Shimada et al., 2014).

Nevertheless, despite of more than 30 AED on the market (Basic, 2016), about 30-40% of patients with epilepsy remain resistant to pharmacotherapy, continuing to experience incapacitating seizures (Basic, 2016; Klein et al., 2018). According to ILAE, drug-resistant epilepsy is defined as failure of adequate drug trials of two tolerated and appropriately chosen and used AED regimens to achieve seizure freedom, whether as monotherapy or in combination (Kwan et al., 2009).

Therefore, there is an urgent need for new therapies that prevent or modify the epileptogenic process and not only stop seizures. This means that antiepileptogenic drugs are needed instead of antiepileptic (also called anticonvulsant or anti-seizure) drugs. Moreover, it is necessary to drive the attention to glial cells and not focus exclusively on neurons. Literature has clarified that the pathogenesis of epilepsy is more than a neuronal disorder; it is also associated with glial cells and inflammatory processes. Furthermore, the treatment of pediatric epilepsies with corticosteroids and adrenocorticotrophic hormone (ACTH) was one of the first clinical evidences of an immune inflammatory presence in epilepsy (Xu et al., 2013).

In the last decade, there has been a growing interest in understanding the anti-inflammatory effects of AED already on the market. The non-classical anti-seizure drug vinpocetine and the classical anti-seizure drug, carbamazepine, whose mechanisms of action involve the sodium channels, reduce inflammatory IL-1β and TNF-α expression in rat hippocampus (Gómez et al., 2014). Vipocetine also inhibits NF-kB-dependent inflammation (Jeon et al., 2010). Another epileptic drug that has been extensively studied for its anti-

inflammatory effects is levetiracetam. It modulates the gene expression and secretion of cytokines, like IL-1β and transforming growth factor beta 1 (Haghikia et al., 2008), and normalizes the resting membrane potential of astrocytes (Thöne et al., 2012). However, these AED have only a minor anti-inflammatory effect.

As a new potential strategy to prevent the onset or progression of the disease, it is necessary to focus on immunomodulatory drugs, which present more anti-inflammatory effects than the current AED.

Emerging research highlighting the relationship between IL-1β and epileptic patients raises a new inflammation pathway as a possible therapeutic target. Modulating the pathway of IL-1β production dependent of inflammasome NLRP3 has been a constant bet for the discovery of new therapeutics. Nevertheless, the effect of the inflammasome NLRP3 inhibition is still poorly studied. To my knowledge, only one study explored the effect of NLRP3 inhibition, through siRNA against NLRP3 and caspase-1, in rats with *status epilepticus* (Meng et al., 2014). Therefore, further studies are needed to clearly understand the impact of NLRP3 inflammasome inhibition in epilepsy models.

In an era of growing drug development targeting the inflammasome as a potential treatment for a wide range of severe diseases with an inflammatory component, it is exciting to study its use also as antiepileptogenic therapy.

2. AIM OF THE WORK

In the current study, we aimed to understand the outcome of NLRP3 inflammasome modulation upon the epileptiform activity of organotypic cortex-hippocampus slice cultures, an *ex vivo* model of epileptogenesis.

In order to accomplish this main objective, the project was divided in three tasks:

- ✓ Establish a NLRP3-mediated inflammation model, through:
  - Cell death assessment;
  - Expression of inflammatory markers.

- ✓ Assess the effect of NLRP3 inflammasome activation on epileptogenesis progression, through:
  - Morphology of glial cells;
  - Co-localization of NLRP3 in astrocytes;
  - Extracellular recordings;
  - CTL slices in serum-free medium (Neurobasal A) *vs* CTL slices in serum-containing medium (Opti-MEM): best control condition.

- ✓ Evaluate the impact of NLRP3 inflammasome inhibition on epileptogenesis progression, by:
  - IL-1β production;
  - Morphology of glial cells;
  - Extracellular recordings.

3. MATERIALS AND METHODS

3.1. Animals

Pregnant female Sprague-Dawley rats were acquired from Charles River Laboratories (Barcelona, Spain). Pregnant rats had a period of one week for acclimatization before the birth of the offspring. Pups were housed with their dams at constant temperature (20 ± 2ºC) and relative humidity (60%) with a fixed 14h light–10h dark cycle (lights on between 7a.m. and 9p.m.) and free access to food and water *ad libitum*.

All experimental procedures were conducted in compliance with the current Portuguese Laws and with the Directive 2010/63/EU of the European Parliament and of the council on the protection of animals used for scientific purposes. Experiments were approved by the Ethical Committee of the Faculdade de Medicina da Universidade de Lisboa. All efforts were made to use the minimum number of animals and to minimize animal suffering.

3.2. Organotypic cortex-hippocampus slice cultures

Organotypic slice cultures were prepared according to the modified interface culture method described by Stoppini et al. (Stoppini et al., 1991). Slices were a combination of hippocampus and cortex (Magalhães et al., 2018).

Postnatal day 6–7 (P6– P7) Sprague-Dawley rat pups (Fig. 4A) were decapitated, and the brains (Fig. 4B) were rapidly dissected and placed in a 60mm cell culture dish with cold Gey's balanced salt solution (GBSS) (Biological Industries, Israel) supplemented with 25mM D-(+)-glucose (Sigma-Aldrich, Missouri, USA). Under sterile conditions, a sharp forceps was inserted into the eye sockets to hold the head. Using thin scissors, the skin/scalp was cut along the midline from the vertebral foramen towards the frontal lobes and removed. Then, the skull was cut in the same way and along the cerebral transverse fissure (space between brain and cerebellum). After taking apart the skull, the olfactory bulbs were discarded using a spatula and the brain was removed to a cell culture dish with cold GBSS.

Fig. 4 - Preparation of organotypic cortex-hippocampus slices cultures. **(A)** P7 rat. **(B)** Intact brain from a pup. **(C)** McIlwain tissue chopper used for cutting the tissue. **(D)** Slices individuallization with round-tipped electrodes. **(E)** The six well culture plate with inserts carrying four slices per insert. **(F)** Incubator.

Under a dissecting microscope, cerebellum was used to hold the cerebrum while the hemispheres were separated along the midline. After individualizing each hemisphere, the main meninge over the hippocampus was removed. Both hemispheres were placed with hippocampus facing up and parallel to each other onto a filter paper. Hemispheres were placed perpendicular to blade and were sliced transversely at 350µm using a McIlwain tissue chopper (Fig. 4C). Sliced hemispheres were placed in cold GBSS. It is noteworthy that GBSS was always cold and renewed throughout all process.

Slices were individualized with round-tipped glass micropipette electrodes (Fig. 4D) so as not to damage them. The first four/five slices were discarded until the hippocampus displayed its typical cytoarchitecture. Usually 6-9 slices with intact hippocampal cytoarchitecture were collected per hemisphere. Well defined and undamaged slices were placed onto porous

(0.4µm) insert membranes (EDM Milipore, Massachusetts, USA) in six-well culture trays (Corning, New York, USA) (Fig. 4E). Each well contained four slices and 1mL of Opti-MEM culture medium (Table 1) (Bernardino et al., 2005, 2008).

The six-well culture trays with culture medium were placed overnight into an incubator (37ºC, 5% CO_2 and 95% atmospheric air) (Fig. 4F) to enable the medium to warm up and condition before plating. Slices were maintained at these conditions for the following 2 weeks. The culture medium was changed every 2-3days with Opti-MEM medium pre-heated at 37 ºC.

The day before the treatment, at 14 DIV, the Opti-MEM medium was changed to a chemically defined medium, Neurobasal A (NBA) medium (Table 1), to avoid potential variability due to different lots of heat-inactivated horse serum (Bernardino et al., 2005, 2008). At 15 DIV, in the end of the treatment, the slices were either stored for further processing or analyzed. If stored at –80°C, cortex and hippocampus from each slice were separated and collected in cryogenic vials (Corning). Tissue was pooled from one well (with four slices) per experimental group. The respective culture media were collected in duplicate for 0.5 ml in the cryogenic vials. For immunohistochemistry assays slices were fixated at the end of the experiment. Electrophysiology recordings, which require fresh tissue, were performed at 15-17 DIV.

Table 1 - Culture medium composition.

Opti-MEM Medium	Reference	Neurobasal A (NBA) Medium	Reference
50% OPTIMEM™ I Reduced Serum Medium	31985-047*	Neurobasal™- A medium	10888-022*
25% Hank's Balanced Salt Solution (HBSS)	24020-091*	2% B27 serum-free supplement	17504-044*
25% heat-inactivated horse serum	26050-088*	1mM L-Glutamine solution [200 mM]	25030-024*
25 mM D-(+)-Glucose solution, 45% in water	G8769**	30 µg/ml Gentamycin solution [50 mg/mL]	15750-037*
30 µg/ml Gentamycin solution [50 mg/mL]	15750-037*		
(*)Thermo Fisher, Massachusetts, EUA (**) Sigma-Aldrich. Note: penicillin and streptomycin (100 µg/ml) (15140-122(*)) were also used in some cultures instead of Gentamycin solution.			

3.3. Model of inflammation driven by LPS

LPS is used to induced inflammation either in OHSC (Huuskonen et al., 2005) or in *in vivo* rat models. *In vivo,* LPS decreases the seizure threshold (Sayyah et al., 2003), thus promoting febrile convulsions, which is a trigger of MTLE (Heida et al., 2004; Zhang et al., 2014).

At 15 DIV, with slices embedded in NBA medium, pro-inflammatory drugs were added directly into the culture medium.

To establish the inflammation model in organotypic cortex-hippocampus slices and determine whether LPS had an effect on NLRP3 inflammasome activation, a time and concentration study was performed. LPS (*Escherichia coli* serotype 055:B5) (Table 2) was incubated alone at final concentrations of 5, 10 and 20ng/mL over 3 or 6h (Fig. 5).

Although there is endogenous ATP in the slice, we decided to add ATP as a second stimulus for inflammasome activation (Y He, Hara et al., 2016). Thus, another condition was added.

After 3h of incubation with LPS (10ng/mL) alone, 1mM of ATP (Table 2) was co-incubated with LPS for another 3h. Control slices were maintained in drug-free NBA medium.

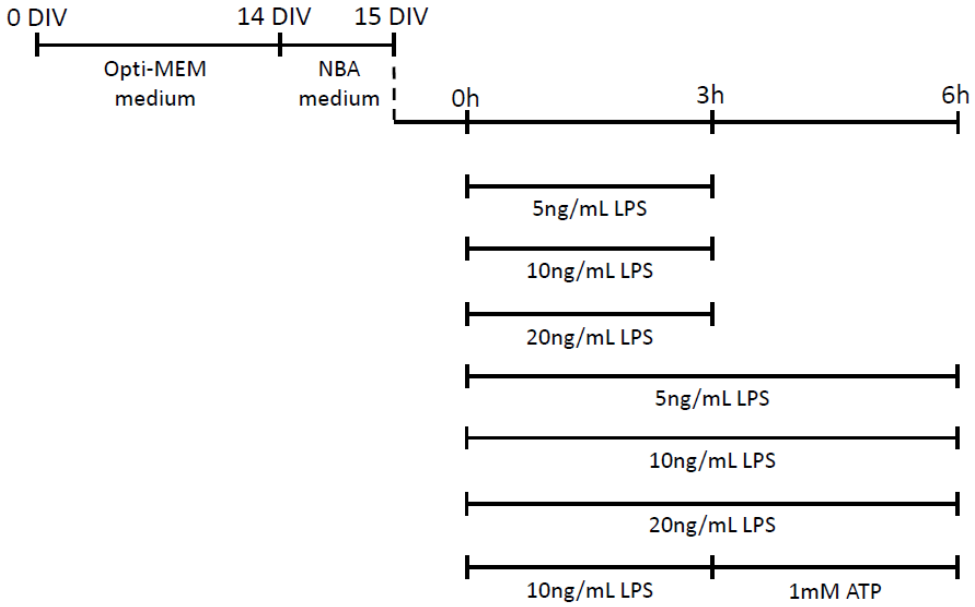

Fig. 5 - Schematic representation of the protocol for LPS-driven inflammation.

3.4. Pharmacological inhibition of NLRP3 inflammasome

After choosing the best condition for NLRP3 inflammasome activation, a pharmacological approach with an inhibitor of this multiprotein complex was performed. The aim of this experiment was to ascertain if inflammation promoted epileptiform activity through NLRP3 inflammasome or through another mechanism.

At 15 DIV, slices were incubated with MCC950, a NLRP3 inflammasome selective inhibitor, in the established inflammatory context, LPS (10ng/mL) with ATP (1mM). In this way, all the activating stimuli were present and if there was no inflammation and/or epileptiform activity, it would not be due to lack of triggers, but rather by the action of the inhibitor. MCC950 (10µM) was added to the culture medium. 1h after incubation with MCC950 only, LPS (10ng/mL) was added followed by ATP (1mM), 3h after LPS being added. Thus, slices were in MCC950 presence for a total time of 7h. A negative control condition, the MCC950 vehicle, dimethyl sulfoxide (DMSO; 0.1% in NBA medium), was incubated alone for the same time (Fig. 6, Table 2).

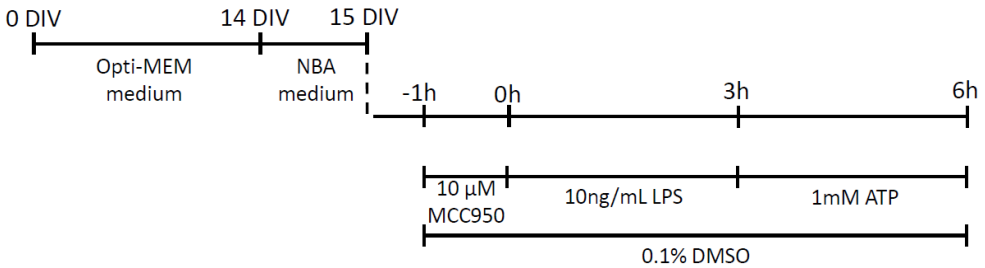

Fig. 6 - Schematic representation of the pharmacological approach for NLRP3 inflammasome inhibition.

3.5. Tissue lysates and protein quantification

The hippocampal tissue was homogenized in 130µL of RIPA (Ristocetin Induced Platelet Aggregation) buffer containing 50mM Tris pH 8.0 (EDM Milipore), 1mM Ethylenediamine tetraacetic acid (EDTA; Sigma-Aldrich), 150mM NaCl (EDM Milipore), 1% Nonyl phenoxlpoylethanol (NP-40; Fluka Biochemika, Switzerland) and 10% glycerol (Sigma-Aldrich). Protease inhibitors were also added to lysis buffer, namely protease inhibitor cocktail (Complete Mini-EDTA free, Roche, Germany) and 1mM phenylmethylsulfonyl fluoride (PMSF; Sigma-Aldrich), to prevent protein degradation by endogenous proteases, mainly serine and cysteine proteases, released in cell disruption processes.

After adding the complete RIPA, the tissue was dissociated with a pipette tip and then with a needle through up and down movements, for 5-6 times. Subsequently, the samples were incubated at 4°C with slow agitation for 15 min, followed by centrifugation at 13000 rpm for 10 min (4°C). Finally, the supernatant was collected into a new eppendorf tube and stored at -20°C, until further use.

Total protein was quantified using the Bio-Rad DC Protein Assay Kit (Bio-Rad, California, USA), which is a colorimetric assay for protein concentration following detergent solubilization. Briefly, 10µl of protein standard and samples were added in duplicate in a 96 well flat bottom plate (Corning). Bovine Serum Albumin (BSA; NZYtech, Lisbon, Portugal) was used as protein standard. Ten dilutions of protein standard containing from 0mg/mL to 1mg/mL protein were prepared in Milli-Q water. Samples were also diluted 1:5 in Milli-Q water. Later, 25µl of reagent A' (20µl of reagent S per each ml of reagent A) was added followed by 200µl of reagent B. The plate was covered and gentle agitated to mix all reagents. If there were bubbles, they were ruptured with a clean needle. After 15 min, absorbance was read at 750nm in Infinite M200 (Tecan, Switzerland).

3.6. Western Blot

Samples were mixed with 6x sample buffer (12% sodium dodecyl sulfate-SDS, 0.015% bromophenol blue, 36% glycerol, 720mM dithiothreitol, 420mM Tris pH 6.8) and boiled for 10 min. Subsequently, samples (40µg total protein/well) and protein size marker (Protein Marker II, NZYtech) were resolved on 12% SDS-PAGE gel, at 80 volts, until marker starts to separate and then at 120 volts during approximately 1h.

SDS-PAGE-separated proteins were transferred to PVDF membrane (Immun-Blot®PVDF Membranes for Protein Blotting, Bio-Rad) using a semi-dry transfer system (Bio-Rad) at a constant current of 300 Amps for 1h. After the blotting step, the membranes were stained with Ponceau S (Sigma-Aldrich), which is an acidic solution that identifies the presence of protein bands directly on the membrane. Ponceau solution was thoroughly removed with distilled water.

Membranes were then blocked in 5% (wt/vol) nonfat-dried milk (Nestlé, Portugal) in TBS-T (200mM Tris/HCL pH7.6, 1.5M NaCl and 0.1% Tween-20 (Sigma-Aldrich)) for 1h at room temperature (RT). Milk proteins cover the entire membrane surface ensuring non-specific binding of the antibodies.

Later, membranes were incubated overnight, at 4ºC, on a rotating shaker with primary antibodies (Table 3) diluted in 3% (wt/vol) BSA in TBS-T and then with the appropriate

horseradish peroxidase (HRP)-conjugated secondary antibodies (Table 4) diluted in 3% (wt/vol) BSA in TBS-T for 1h at RT.

Between blocking, first and second incubation, the blot was rinsed in TBS-T (3 times x 10 min), in sufficient volume to keep the membrane submerged and with gentle agitation to remove unspecific bonds.

Chemiluminescence signals were developed using ECL (enhanced chemiluminescence) detection (Western Lightening® Plus-ECL, PerkinElmer, Massachusetts, USA). For ECL detection, the substrate luminol is oxidized by HRP in the presence of H_2O_2 and an enhancer, producing 3-aminophthalate that emits light. The emitted light was detected by exposing the membrane to ChemiDoc™ MP Imaging System (Bio-Rad). The exposure time was defined for each protein analysed.

Band intensities were measured with Image J software (National Institutes of Health, Maryland, USA). The image before signal saturation has appeared was used to quantitatively analyze relative expression. To account for possible loading errors, the intensity of each protein band was normalized against the glyceraldehyde 3-phosphate dehydrogenase (GAPDH) (Table 3) band intensity.

3.7. Enzyme-Linked Immunosorbent Assay (ELISA)

IL-1β was measured in tissue sample and culture medium by using an ELISA kit (R&D System, Minnesota USA) containing a selective antibody against murine IL-1β that recognizes both pro-Il-1β and Il-1β. This cytokine was measured accordingly to manufacturers' suggested protocol.

Briefly, the wells were coated with the capture antibody and incubated overnight at RT. This step allows immobilization of antigens to the surface of polystyrene microplate wells. After removing the antibody, washing the plate three times and patting the plate on a paper towel, blocking buffer (reagent diluent) was added to cover all unsaturated surface-binding sites. Incubation lasted 2h at RT and then the plate was washed again. Washing the plate with wash buffer (phosphate buffered saline (PBS) plus Milli-Q water) between steps allowed removal of unbound materials.

Subsequently, 50µl of serial dilutions of protein standards and samples were added to each well for 1h at RT, and thus any analyte present was bounded by the immobilized antibody. Standards were diluted in NBA medium, for the antigen quantification in culture medium, and in reagent diluent for quantifications in tissue samples. Medium samples were not diluted and tissue samples were diluted 1:10 in reagent diluent, except control condition that was not diluted.

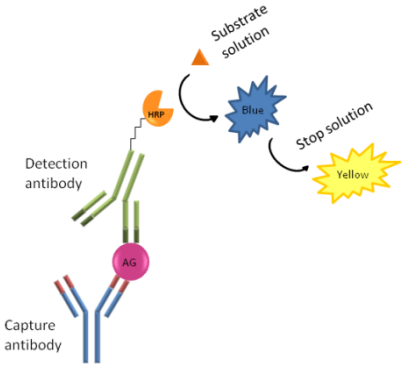

Fig. 7 - Schematic draw of ELISA.

After antigen incubation, a second HRP-labeled antibody (detection antibody) was incubated over 2h, at RT, to binds to the captured analyte (Fig. 7).

After rinsing with wash buffer again, the prepared solution of streptavidin protein conjugated with HRP was added and incubated over 1h at RT followed by washing and addition of tetramethylbenzidine (TMB) substrate solution. When this solution is added to the wells a

blue color develops in proportion to the amount of analyte present in the sample. The reaction is stopped by sulfuric acid, which turns the solution in the wells to yellow.

The optical density was detected at 450nm and 540nm in a microplate reader - Infinite M200 (Tecan). Readings at 540nm were substract from the readings at 450nm to correct optical imperfections in the plate. The detection limit was < 4 pg/mL.

A standard curve was prepared from the data produced from the serial dilutions on each plate with concentration on the x axis (log scale) versus absorbance on the Y axis (linear). The concentration of each sample was calculated with GraphPad Prism 6.0 (GraphPad Software Inc., California, USA) from the four-parameter logistic regression (4PL equation) which derived from the standard curve of known concentrations of the cytokine.

3.8. Cytometric bead array immunoassay

The cytometric bead array (CBA) technique is a method that captures a set of chemical substances, known as analytes, with beads of known size and fluorescence, making it possible to detect analytes using flow cytometry.

For the CBA measurements, the BD™ CBA Mouse Inflammation Kit (BD Biosciences, California, USA) was used to quantitatively measure Interleukin-6 (IL-6), Interleukin- 10 (IL-10), Monocyte Chemoattractant Protein-1 (MCP-1), Interferon-γ (IFN-γ), Tumor Necrosis Factor (TNF), and Interleukin-12p70 (IL-12p70) protein levels in a single sample. The assay was performed according to an adjusted manufacturer's protocol.

Briefly, each capture bead conjugated with a specific antibody was mixed in a single tube. The standard curve for each protein covered a defined set of concentrations from 0 to 5000 pg/mL. Inside the 96-well plate, 10µl of capture beads mixture was added to the same amount of recombinant standards or unknown samples and then incubated in the dark with 10µl of phycoerythrin (PE) - conjugated antibodies at RT for 2h. This PE detection reagent provides a fluorescent signal in proportion to the concentration of a specific cytokine, which is quantified from a calibration curve. Posteriorly, each well was washed with wash buffer and the plate was centrifuged at 400g for 5 minutes. After discarding the supernatant, each pellet was resuspended.

These sandwich complexes formed by capture bead plus analyte plus detection reagent were measured using a BD™ FACS Calibur flow cytometer (BD Biosciences) either through the 96-well plate or 12 × 75-mm tubes. Each tissue lysate or medium sample was quantified three times in different days.

Data were obtained and analyzed by FCAP Array software in dot-plot FL-2 channel vs. FL-3 channel. FL-2 detects PE, which emits at 585 nm, and FL-3 detects the particles that were dyed with six different fluorescence intensities and has a maximal emission wavelength of approximately 650 nm. The six FL-3 particles dyed to different intensities were distributed along the y-axis. The concentration of the cytokine calibrators was expressed (y-axis) vs. medium fluorescence intensity (FL-2) in the standard curves. The concentrations of cytokines that were below the limit of detection of the assay were given zero value of concentration.

3.9. Immunohistochemistry

Immunohistochemistry demonstrates the presence and location of proteins in an intact tissue. In this sensitive technique, a primary antibody recognizes specifically the target protein. This interaction can be later detected by a fluorochrome-conjugated secondary antibody and visualized using fluorescence microscopy.

Slices were fixed after treatment at 15 DIV. The NBA culture medium was removed and 1mL of 4% paraformaldehyde (PFA; VWR, Pennsylvania, USA) diluted in PBS (137mM NaCl, 2.1mM KCl, 1.8mM KH_2PO_4 and 10mM $Na_2HPO_4.2H_2O$, at pH 7.40) was added beneath and above the slices in each well of the culture tray. Later, slices were sequentially incubated for 1h in increasing concentrations of sucrose in PBS (10%, 20% and 30%), to cryoprotect the tissue. Slices were maintained (for a maximum of one week) at 4ºC soaked in 30% sucrose until further use.

In the beginning of the immunohistochemical staining procedure, the insert membrane was cut with a scalpel to individualize each slice and then each slice was transferred to a microscope slides (Thermo Fisher). In each slide, two individual slices were surrounded by a hydrophobic pen, DAKO pen (Dako, Glostrup, Denmark), to protect slices from drying out. Also to prevent the tissue from drying out, all incubations were carried out in a humidified chamber. Drying at any stage promotes non-specific binding and high background staining. After 3 times of PBS washes, 10min each, slices were permeabilized with 1% Triton X-100 (Sigma-Aldrich) in PBS for 1h at RT and then blocked with 20% Donkey Serum (D9663, Sigma-Aldrich) and 1% BSA in Milli-Q water for 3h at RT. Serum raised in donkey was chosen since it was the host of all secondary antibodies, thus minimizing the cross reactions with endogenous immunoglobulins in the tissue. BSA was also included to reduce non-specific binding caused by hydrophobic reactions. Primary antibodies (Table 3) diluted in PBS were applied and incubated overnight at 4ºC.

In the ensuing day, after washed 3 times for 10min with PBST (PBS with 0.1% Tween-20), slices were incubated with the fluorophores-labeled secondary antibodies (Table 4) in PBS for 5h at RT. Following rinse again with PBST (3 times) in the dark to avoid photobleaching, DAPI (D9564, Sigma-Aldrich) solution (1:1000 dilution in PBS) was added over 40 min at RT to stain the nuclei. To finalize, slices were rinsed 3 times with PBST and one with PBS and then mounted in Mowiol Solution (2,4g Polyvinylalcohol 4-88, 600 mM glycerol, 200mM tris, pH 8.0, in Milli-Q water). It is noteworthy to state that in the wash, the sections were wiped around with a tissue paper to drain the excess liquid.

Slices were observed in a confocal laser scanning microscope (Zeiss LSM 710, Carl Zeiss MicroImaging, Germany), using either an EC plan-NeoFluar 10x, a Plan-Apochromat 20x or a Plan-Apochromat 63x, with a frame size of 1024 x 1024 pixels. Furthermore, the imaging-settings were kept constant for all images.

To determine the co-localization between NLRP3 and astrocytes a rough analysis was carried out. Due to the lack of negative control, without primary antibody, in these immunofluorescence conditions to set a threshold in Alexa Fluor 568 channel (which shows NLRP3 staining), a threshold below the most saturated pixels was applied. The percentage of co-localization was calculated by the area of NLRP3 saturated pixels which co-localized with GFAP divided by the area of the all saturated pixels in a confocal image. The threshold was set at 100 for the red channel and at 30 for the green channel.

3.10. Electrophysiology – extracellular recordings

At 15-17 DIV, slices were removed from the incubator and placed in a petri dish with heated NBA medium. To individualize one slice at a time, the insert membrane was cut with a scalpel and the slice was transferred to an interface recording chamber with a humidified 95% O_2/5% CO_2 atmosphere at 37° C. Unlike the immersion chamber, this interface chamber allows the medium to pass under the slice as it was in the incubator. The NBA medium was superfused and recirculated at a rate of 2mL/min.

Recordings were obtained with an Axoclamp 2B amplifier (Axon Instruments, Foster City, California, USA), digitized and continuously stored on a personal computer with the WinLTP software (WinLTP Ltd., Bristol, UK)(Anderson and Collingridge, 2001). The pCLAMP Software Version 10.7 (Molecular Devices Corporation, California, USA) was used for data analysis. All recordings were band-pass filtered (eight-pole Bessel filter at 60 Hz and Gaussian filter at 600 Hz).

As the entorhinal cortex is included in these slices and its projections are intact, ictal discharges are originated in entorhinal cortex and propagate through DG to CA3 and CA1. Also, interictal discharges initiate in the CA3 and propagate via CA1 and subiculum to the entorhinal cortex and return to the hippocampus through the DG (Barbarosie and Avoli, 1997; Rutecki and Yang, 1998; Walther et al., 1986). As discharges can lose power in CA1 and this hippocampal region has more percentage of neuronal death in OHSC, the extracellular recordings to monitor the electrical activity of neurons were made in CA3 pyramidal cell region (Fig. 8). The viability of slices was routinely tested by recording population spikes from CA3 pyramidal cell population (Fig. 8).

Fig. 8 - Extracellular recording of one organotypic cortex-hippocampus slice. Bipolar concentric wire stimulating electrode was placed onto mossy fibers. Recording electrode (glass micropipette) was placed onto CA3 region.

3.10.1. Population spikes

Population spike is the synchronous discharge of neuron populations (Dyhrfjeld-Johnsen et al., 2010). Mossy fiber projections to CA3 pyramidal cells were electrically stimulated for the purpose of recording a biological response in the form of a population spike.

Extracellular recordings of population responses in the CA3 area were made using glass micropipettes electrode (2–4 MΩ) filled with artificial cerebrospinal fluid (ACSF) composed by: 124mM NaCl, 3mM KCl, 1.2mM NaH_2PO_4, 25mM $NaHCO_3$, 10mM glucose, 2mM $CaCl_2$, 1mM $MgSO_4$ with pH 7.4.

A bipolar concentric wire stimulating electrode was placed on mossy fibers and rectangular pulses of 0.1ms duration at every 15s were evoked. The average of 8 consecutive population spikes was obtained for representative purposes. Slices were stimulated with intensity between 1 and 4 volts. If there was no response, the recording or stimulating electrode was repositioned. After this second attempt if there was still no response the slice was discarded.

WinLTP 2.20b Reanalysis software (WinLTP Ltd., Bristol, UK)(Anderson and Collingridge, 2001) was used to visualize the population response.

3.10.2. Epileptiform activity

Extracellular recordings of epileptiform activity in the CA3 pyramidal cell region were performed using the same glass micropipette electrode used to record the population response, without changing the place (Fig. 8). The activity was recorded for at least 40 minutes.

In this study, interictal epileptiform discharges were defined as individual paroxysmal discharges clearly distinguished from the baseline, with an abrupt change in polarity occurring within several milliseconds (Berdichevsky et al., 2012). Ictal-like discharges were defined as continuous discharges lasting more than 6s (bursts). The end of a burst was defined when inter-spike interval was longer than 600ms. Continuous spike activity with duration lower then 6s was not accounted as burst activity. Slices with this type of activity and interictal discharges were classified as slices with interictal activity.

To quantify the epileptiform activity different parameters were assessed. The number of burst per slice was evaluated manually in slices with interictal-like discharges and in slices with mixed interictal-like and ictal-like discharges. To further characterize the bursts of the latest slices, the frequency of events within burst and the average positive peak amplitude (this is the amplitude between the baseline and the peak of the spike) was evaluated. The number of events per burst, the duration of each burst and the positive peak amplitude were auto-detected by pCLAMP Software, which allows a more reliable and automatic detection of events. The baseline used to detect these events was specific to each recording and was settled right above the end of noise oscillations.

3.10.3. Experimental conditions recorded in electrophysiology

In a first set of experiments, recording conditions included the drug free control condition (CTL), the inflammasome activation condition (LPS/ATP) and the inflammasome inhibition condition in an inflammatory context (MCC950/LPS/ATP). As negative controls, slices incubated with LPS (10ng/mL) alone over 3h or with ATP (1mM) alone over 3h were also evaluated (Fig. 9).

After these initial electrophysiological recordings, it was hypothesized that the change in culture medium on the day before the treatment was an inflammatory trigger of epileptiform activity. Therefore, studies were performed on slices maintained in Opti-MEM medium, without undergoing the change to NBA, and on slices exposed only to MCC950, incubated in NBA for 7h (Fig. 9). It should be noted that the neuronal electrical activity of the slices was recorded on time or 1h after the end of incubation, since more than one slice per insert was recorded.

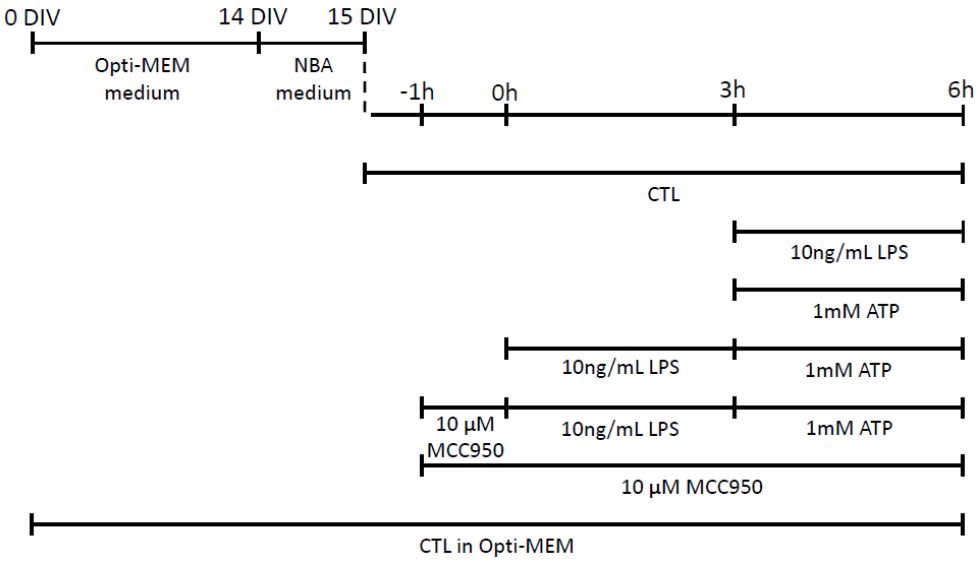

Fig. 9 - Schematic representation of the conditions used in electrophysiology.

3.11. Drugs and antibodies

Table 2 - Drugs used for slices treatment.

Drugs	Vehicle	Stock concentration	Final concentration	Reference	Supplier
Lipopolysaccharide (LPS)	Milli-Q water	5mg/ml	5, 10 or 20 ng/mL	L6529	Sigma-Aldrich
Adenosine 5'-triphosphate disodium salt hydrate (ATP)	NBA	50mg/mL	1 mM	A7699	Sigma-Aldrich
MCC950	DMSO	10mM	10 µM	17510	Cayman chemical company
Dimethyl sulfoxide (DMSO)	-	Density: 1.10 g/mL	0.1%	D2650	Sigma-Aldrich

Table 3 - Primary antibodies used in western blot and immunohistochemistry assays.

Protein	Antibody	Technique and Dilution	Reference	Supplier
αII-Spectrin	Mouse monoclonal	WB - 1:500	sc-48382	Santa Cruz Biotechnology
ASC	Rabbit polyclonal	WB - 1:1000	AL177	AdipoGen Life Sciences
GAPDH	Mouse monoclonal	WB - 1:1000	AM4300	Invitrogen
GFAP	Rabbit polyclonal	WB - 1:5000	G9269	Sigma-Aldrich
GFAP	Mouse monoclonal	IHC - 1:500	MAB360	EDM Milipore
Iba1	Goat polyclonal	WB - 1:1000	ab5076	Abcam
Iba1	Rabbit polyclonal	IHC – 1:250	ab108539	Abcam
NLRP3	Rabbit polyclonal	WB - 1:300 IHC - 1:500	ab214185	Abcam

Table 4 - Secondary antibodies used in western blot and immunohistochemistry assays.

Secondary Antibodies	Technique and Dilution	Reference	Supplier
Donkey anti-Goat IgG -HRP	WB - 1:10000	sc-2020	Santa Cruz Biotechnology
Goat anti-Mouse IgG -HRP	WB - 1:10000	sc-2005	Santa Cruz Biotechnology
Goat anti -Rabbit IgG -HRP	WB - 1:10000	1706515	Bio-Rad
Donkey anti-Rabbit Alexa Fluor® 488	IHC - 1:500	A21206	Invitrogen
Donkey anti-Mouse Alexa Fluor® 488	IHC - 1:500	A21202	Invitrogen
Donkey anti -Rabbit Alexa Fluor® 568	IHC - 1:750	A10042	Invitrogen

3.12. Statistical Analysis

All statistical analyses were performed with GraphPad Prism 6.0. Statistical significance was determined by using one-way analysis of variance (ANOVA) followed by Tukey's test for multiple comparisons, with $p<0.05$ considered to represent statistical significance. Data were expressed as means ± standard error of mean (SEM), except when n=2.

4. RESULTS

4.1. Establishment of NLRP3-mediated inflammation model

LPS is a potent bacterial endotoxin widely used to establish inflammation models. LPS is an excellent trigger of inflammation either in CNS or peripheral nervous system (PNS) and it has been used in different models, both *in vitro* and *in vivo*. Moreover, LPS was already described as an enhancer of seizure susceptibility (Sayyah et al., 2003) and an activator of NLRP3 inflammasome in *in vivo* models (F Zhang et al., 2016; Z-T Zhang et al., 2016).

In our study we aimed to establish an inflammatory phenotype in organotypic slices, but without damaging extensively the slices. Inflammation induction was tested with several LPS concentrations, ranging from 5 to 20ng/ml, over two-time periods, 3h and 6h. Furthermore, because NLRP3 inflammasome activation is described as a two-step process which requires two triggers, an extra condition which included ATP, was added to ensure that NLRP3 inflammasome was activated in our system.

Therefore, at 14 DIV, organotypic slices were exposed to 5, 10 and 20ng/mL of LPS over 3h and 6h, or to 10ng/mL of LPS alone for 3h followed by 3h co-incubation with 1mM of ATP.

4.1.1. Cell death assessment

Cell death was characterized through the expression of αII-Spectrin, a structural protein of the cell cytoskeleton mainly found in neurons (J He et al., 2016; Riederer et al., 1986). αII-Spectrin is a substrate for two cysteine proteases: calpains, which are related with necrosis and excitotoxicity, and caspase-3, which is the main effector caspase for apoptosis. Spectrin catabolism products are known as spectrin breakdown products (SBDP) and have distinct molecular sizes according to the enzyme responsible for the cleavage. Proteolysis by calpains forms fragments with 145kDa (SBDP145), whereas proteolysis by caspase-3 produces fragments with 120kDa. Another fragment with 150kDa (SBDP150) is produced by both proteases (Z Zhang et al., 2009).

Western blot analysis of tissue lysates from slices exposed to different LPS concentrations and to different time of exposure showed no differences in αII-Spectrin expression within conditions (Fig. 10A and B). Absence or presence of ATP also did not influence αII-Spectrin expression in these slices (Fig. 10C).

The effect of these different conditions in calpain-mediated necrosis was assessed through the ratio between SBDP145 and αII-Spectrin. It is important to note that SBDP150 and SBDP145 were analyzed as a single fragment. There were no differences in necrosis within slices exposed to the different concentrations of LPS and distinct exposure time (Fig. 10D). However, ATP significantly decreased the ratio SBDP145/αII-Spectrin (0.8925±0.1586, n=4), when compared with slices incubated with the same concentration of LPS but in the absence of ATP (1.368±0.1692, n=4, $^{\#}p<0.05$, Fig. 10E). This decrease can be due to the occurence of another form of cell death, called pyroptosis, in slices exposed to LPS/ATP, which is closely related with NLRP3 inflammasome activation and release of IL-1β (Bergsbaken et al., 2010).

Regarding the effect of LPS in different conditions or in presence of ATP in caspase-3-mediated apoptosis, the ratio SBDP120/αII-Spectrin remained unchanged between conditions (Fig. 10F and G).

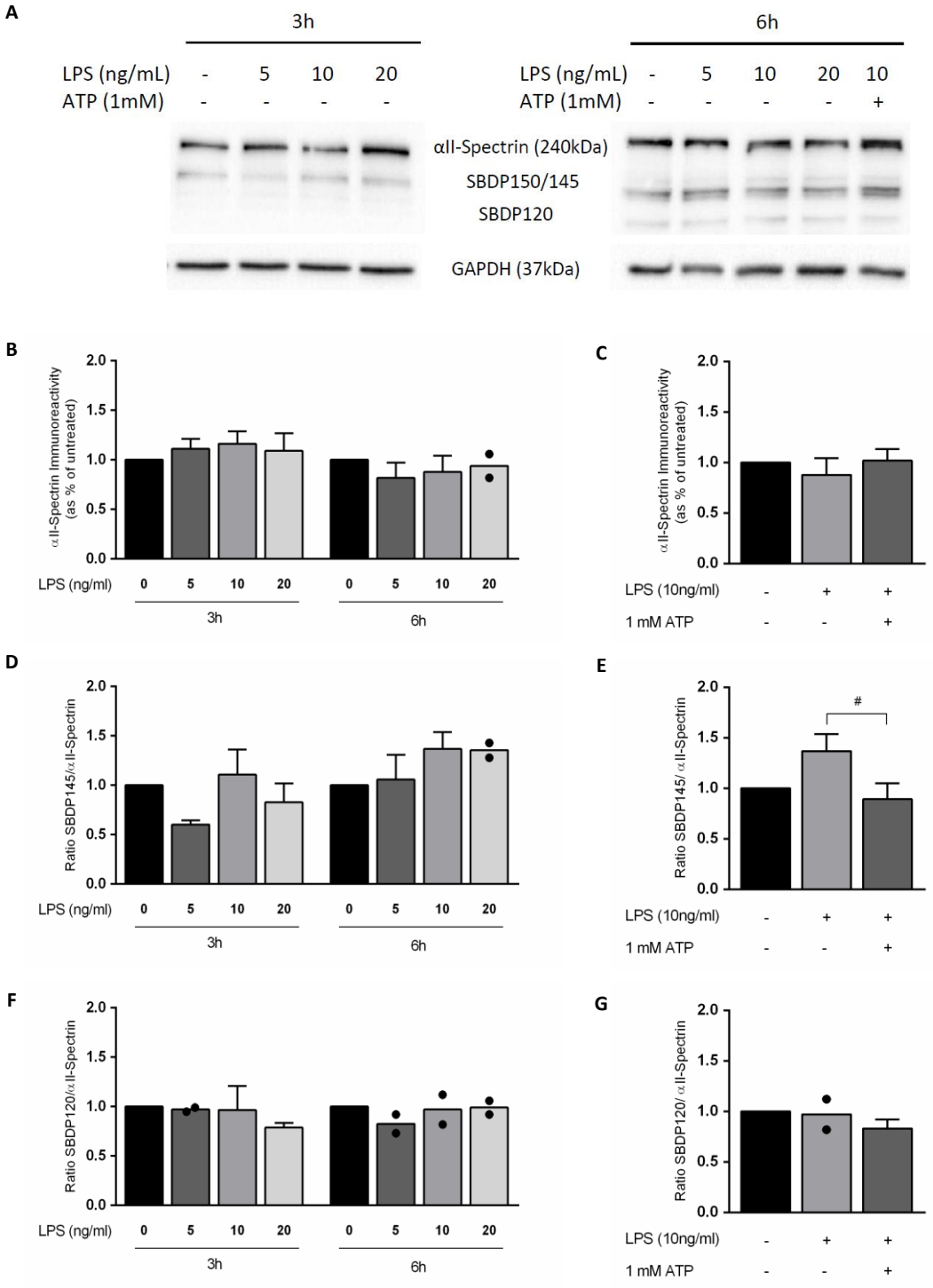

Fig. 10 - Expression profiles of αII-Spectrin and SBDPs in organotypic cortex-hippocampus slices following LPS exposure in presence or absence of ATP. **(A)** Representative immunoblots for αII-Spectrin, SBDPs and GAPDH after 3h or 6h of LPS incubation at different concentrations, and co-incubated with ATP (1mM). **(B-G)** Western blot analysis of αII-Spectrin [n=2-6] **(B)**, ratio SBDP145/αII-Spectrin [n=2-6] **(D)** and ratio SBDP120/αII-Spectrin [n=2-4] **(F)** of different concentrations of LPS in distinct timepoints, or co-incubated with ATP [n=4-5] **(C)**, [n=4] **(E)**, [n=2-4] **(G)**, respectively. GAPDH was used as the loading control. Data are presented as mean ± SEM (except when n=2). $^{\#}p<0.05$ LPS vs LPS+ ATP by one-way ANOVA followed by Tukey's test.

4.1.2. Expression of inflammatory markers

4.1.2.1. NLRP3/ ASC

NLRP3 inflammasome is a multiprotein complex formed by three distinct proteins: NLRP3 itself, ASC and pro-caspase-1. NLRP3 and ASC are the first to assembly together and subsequently recruit pro-caspase-1 (Hoss et al., 2017). Therefore, to evaluate NLRP3 inflammasome activation, the expression of NLRP3 and ASC subunits were assessed.

Contrariety to expected, there were no statistical differences in NLRP3 and ASC expression, neither between different LPS concentrations at 3h or 6h (Fig. 11B and Fig. 12B, respectively), nor between presence or absence of ATP (Fig. 11C and Fig. 12C, respectively). However, although the results do not confirm the NLRP3 inflammasome activation, they are also not sufficient to sustain that the inflammasome is not activated. Moreover, if we look carefully to the western blotting representative bands (Fig. 11A) it is possible to observe a similar expression of control conditions when compared with the others. Data described elsewhere has shown less NLRP3 expression in basal conditions (Meng et al., 2014; F Zhang et al., 2016).

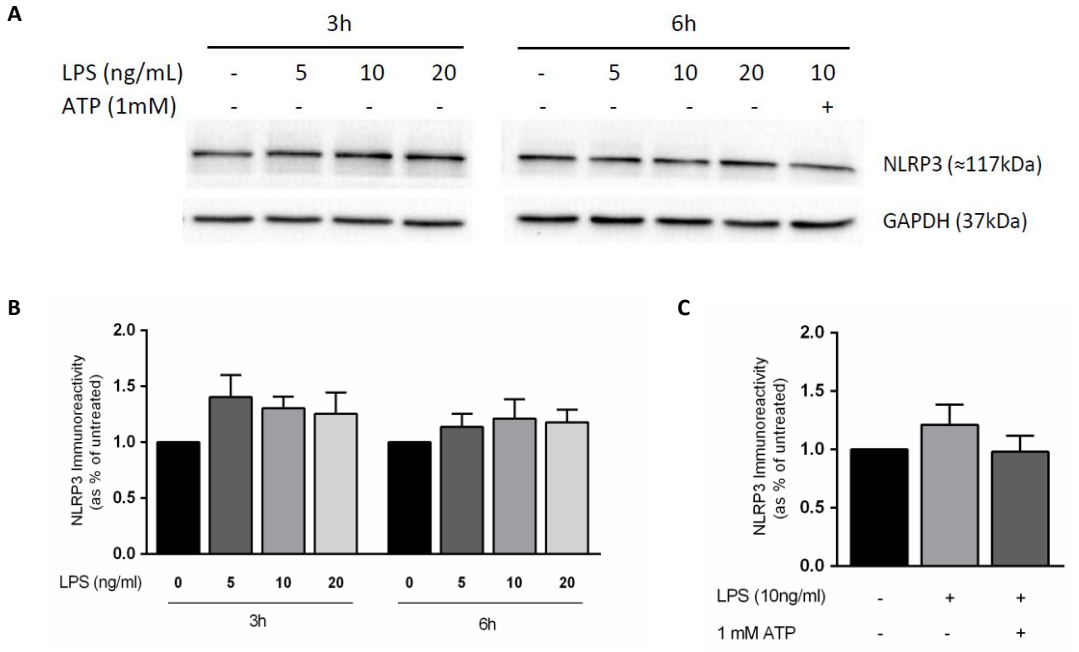

Fig. 11 - Expression profile of NLRP3 in organotypic cortex-hippocampus slices following LPS exposure in presence or absence of ATP. **(A)** Representative immunoblots for NLRP3 and GAPDH after 3h or 6h of LPS incubation at different concentrations, and co-incubated with ATP (1mM). Western blot analysis of NLRP3 expression in slices exposed to different concentrations of LPS at 3h and 6h [n=6-8] **(B)** and in presence of ATP [n=7-8] **(C)**. GAPDH was used as the loading control. Data are presented as mean ± SEM.

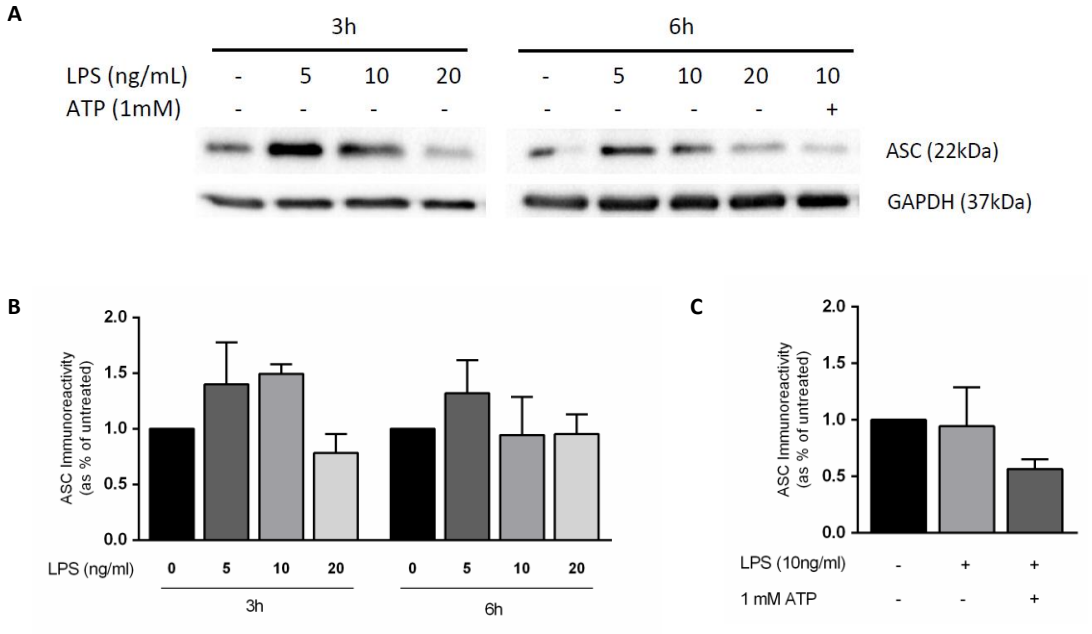

Fig. 12 - Expression profile of ASC in organotypic cortex-hippocampus slices following LPS exposure in presence or absence of ATP. **(A)** Representative immunoblots for ASC and GAPDH after 3h or 6h of LPS incubation at different concentrations, and co-incubated with ATP (1mM). Western blot analysis of ASC expression in slices exposed to different concentrations of LPS at 3h and 6h [n=3-5] **(B)** and in presence of ATP [n=3-5] **(C)**. GAPDH was used as the loading control. Data are presented as mean ± SEM.

4.1.2.2. Iba1/GFAP

Under dangerous or pathogenic conditions, glial cells are the key mediators of neuroinflammation. Therefore, activation of microglia and astrocytes is considered a hallmark of neuroinflammation. Changes in the activation state of microglia and astrocytes are known to increase the expression of their markers, Iba1 and GFAP, respectively (Bederson et al., 2001; Ben Haim et al., 2015). Thus, a western blotting analysis was performed to evaluate Iba1 and GFAP expression within the various conditions tested.

After 3h or 6h of exposure to different concentrations of LPS, slices did not have alterations in Iba1 or GFAP expression in relation to control condition (Fig. 13B and Fig. 14B). Furthermore, by comparing slices incubated with LPS in absence or presence of ATP, there were also no differences in expression of glial cells markers (Fig. 13C and Fig. 14C). Similarly to NLRP3 and ASC discussed in the previous section, Iba1 and GFAP expression in control condition was identical to the other conditions (Fig. 13A and Fig. 14A). In summary, the conditions tested did not induce an upregulation in microglia and astrocytes markers.

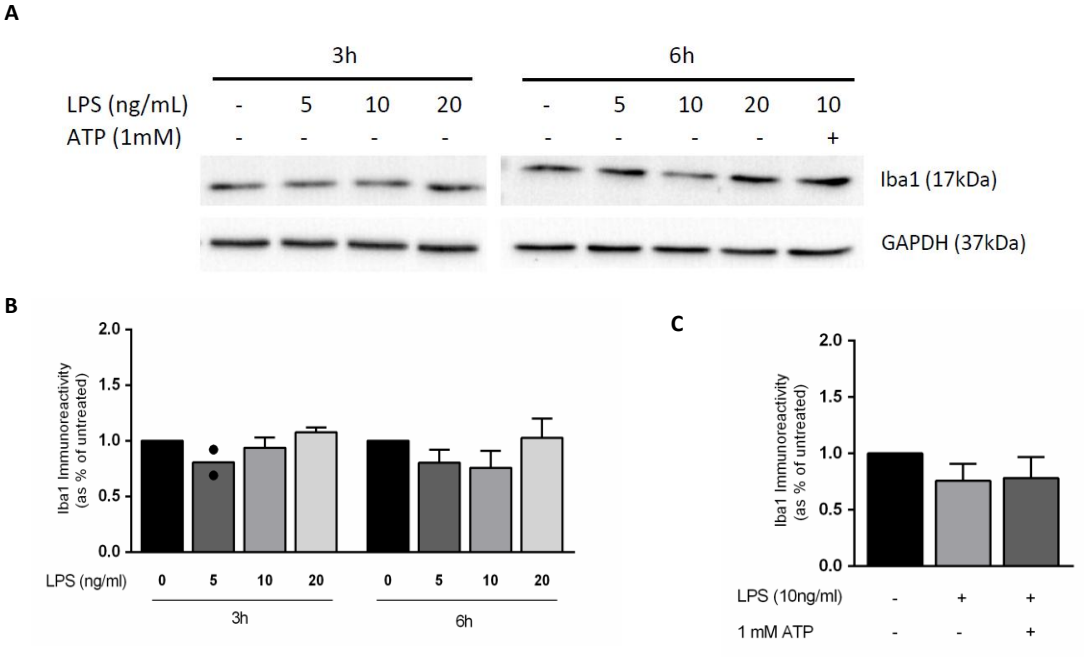

Fig. 13 - Expression profile of Iba1 in organotypic cortex-hippocampus slices following LPS exposure in presence or absence of ATP. **(A)** Representative immunoblots for Iba1 and GAPDH after 3h or 6h of LPS incubation at different concentrations, and co-incubated with ATP (1mM). Western blot analysis of Iba1 expression in slices exposed to different concentrations of LPS at 3h and 6h [n=2-6] **(B)** and in presence of ATP [n=4-6] **(C)**. GAPDH was used as the loading control. Data are presented as mean ± SEM (except when n=2).

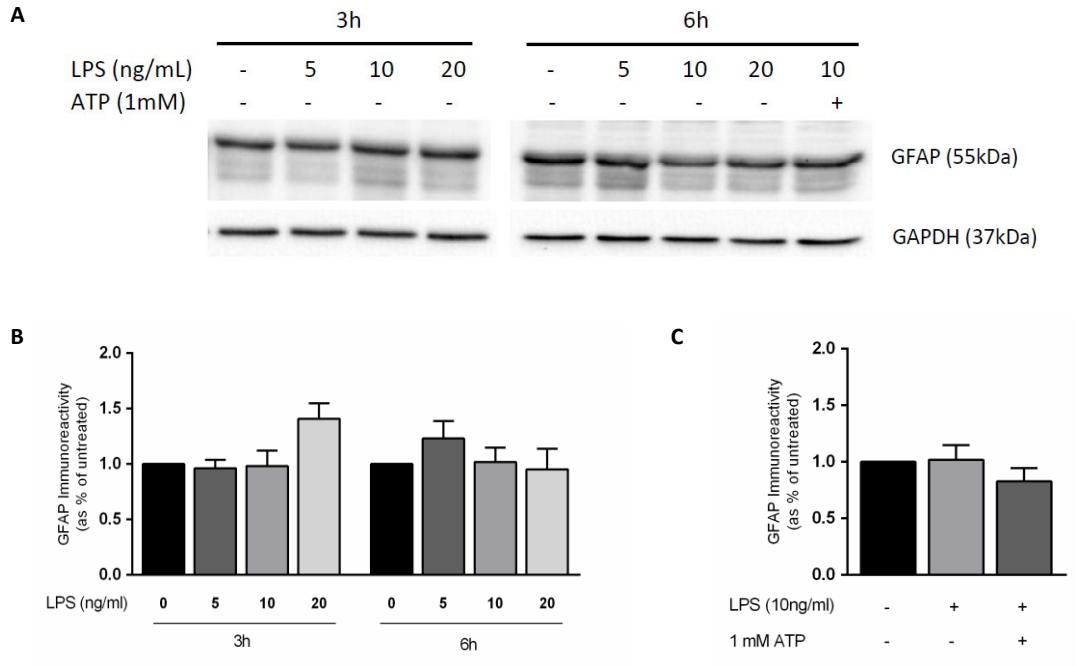

Fig. 14 - Expression profile of GFAP in organotypic cortex-hippocampus slices following LPS exposure in presence or absence of ATP. **(A)** Representative immunoblots for GFAP and GAPDH after 3h or 6h of LPS incubation at different concentrations, and co-incubated with ATP (1mM). Western blot analysis of GFAP expression in slices exposed to different concentrations of LPS at 3h and 6h [n=3-7] **(B)** and in presence of ATP [n=4-7] **(C)**. GAPDH was used as the loading control. Data are presented as mean ± SEM.

4.1.2.3. IL-1β production

Il-1β is the main pyrogenic product from NLRP3 inflammasome activation. It is well established that LPS through Nf-kB upregulates Il-1β gene resulting in the increase of pro-Il-1β, the inactive form. In the presence of ATP, the second stimulus, caspase-1 is activated to process pro-Il-1β, forming an active and mature form which can be released into the medium. Therefore, to further assess the activation of NLRP3 inflammasome, Il-1β levels were quantified.

Fig. 15A shows that hippocampal Il-1β levels increased with increasing concentration of LPS. Slices exposed for 3h to 10ng/mL (3229±721.0, n=3, *p<0.05) or 20ng/mL (3504±663.04, n=3, *p<0.05) of LPS had higher expression of this cytokine when compared with control slices (371.8± 162.0, n=3). Similarly, slices exposed for 6h to any concentration of LPS (5ng/mL: 4964±354.0, n=3; *p<0.05; 10ng/mL: 6038±444.4, n=3; *p<0.05; 20ng/mL: 11824±1826, n=5; ****p<0.0001) presented significantly higher Il-1β levels when compared with control (305.9±63.0, n=7). Moreover, exposure to 20ng/mL over 6h induces the highest levels of Il-1β when compared with 5ng/mL ($^{\#\#}$p<0.01) and 10ng/mL ($^{\#}$p<0.05) of LPS. However, it should be noticed that Il-1β levels in the tissue quantified by an ELISA kit are mostly represented by pro-IL-1β (Ravizza et al., 2006).

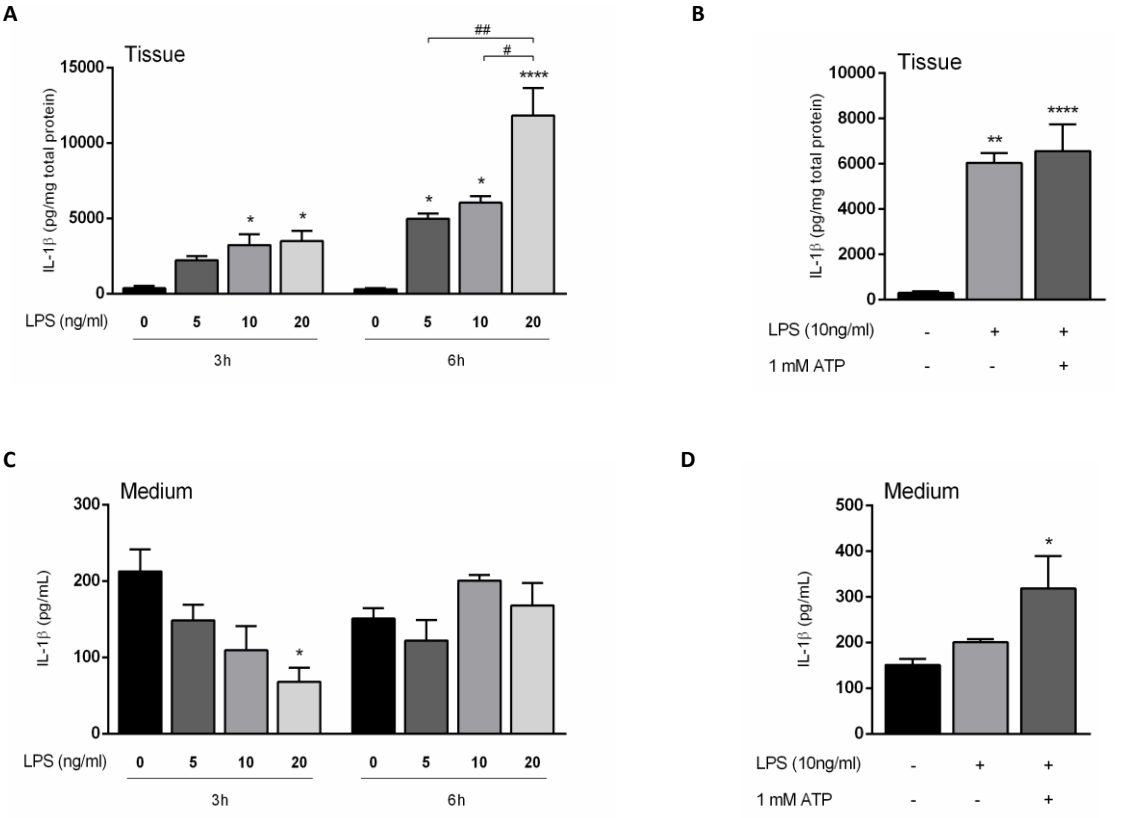

Fig. 15 - Effects of LPS exposure and LPS/ATP co-exposure on Il-1β levels. **(A, B)** Il-1β levels in organotypic slices exposed to different concentrations of LPS at 3h and 6h [n=3-7] **(A)** and co-incubated with ATP (1mM) [n=3-7] **(B). (C, D)** Il-1β released to the culture medium from slices exposed to different concentrations of LPS at 3h and 6h [n=3-6] **(C)** and co-incubated with ATP [n=6-7] **(D)**. Data are presented as mean ± SEM. *p<0.05, **p<0.01, ****p<0.0001 vs control; $^{\#}$p<0.05, $^{\#\#}$p<0.01 vs other treated condition, by one-way ANOVA followed by Tukey's test.

Although LPS induced Il-1β (and pro-Il-1β) levels in the tissue, this increase was not accompanied by increased Il-1β release. None of the LPS treated conditions was able to increase the levels of mature and released Il-1β (Fig. 15C). In fact, exposure to 20ng/mL of LPS during 3h reverted the release of Il-1β (67.76±18.58, n=4, *p<0.05) when compared with control (212.6±28.94, n=4).

In slices exposed to LPS (6038±444.4, n=3, **p<0.01) or co-exposed to LPS/ATP (6566±1174, n=6, ****p<0.0001), increased Il-1β levels in a similar extent were observed, when compared with control (305.9±63.0, n=7) (Fig. 15B). However, a significant release of Il-1β was only observed in slices co-exposed to LPS/ATP (Fig. 15D).

These results demonstrate that ATP is required for inducing maturation and release of Il-1β in the presence of LPS, as described before (Bernardino et al., 2008; Ravizza et al., 2006). LPS alone can also increase Il-1β release in a less potent manner in other similar models (Bernardino et al., 2008; Ravizza et al., 2006). Nevertheless, the basal level of this cytokine in the reported models was barely or not detectable, contrary to what was obtained in our model.

4.1.2.4. TNF-α production

During inflammatory process, different mediators are produced to promote inflammatory responses in order to fight against dangerous or pathogenic agents, or to defend the organism itself by controlling the pro-inflammatory response. Among these inflammatory mediators are small molecules like cytokines and chemokines.

To better characterize the LPS-induced inflammation in organotypic cortex-hippocampus slices, in presence or absence of ATP, a large range of inflammatory mediators was assessed through CBA assay. This technique was performed in Tarja Malm's Lab at the University of Eastern Finland, Kuopio, Finland. The anti-inflammatory cytokine interleukin-10 (IL-10), the chemokine monocyte chemoattractant protein-1 (MCP-1), as well as, pro-inflammatory cytokines interleukin-6 (IL-6), interferon-γ (IFN-γ), TNF-α, and interleukin-12p70 (IL-12p70) were evaluated using a CBA mouse inflammation kit. All of these small molecules can be produced by microglia and/or astrocytes under certain conditions (Kawanokuchi et al., 2006; Lau and Yu, 2001; Lobo-Silva et al., 2016; C Wang et al., 2016; Welser-Alves and Milner, 2013). Moreover, these molecules were already related with epilepsy in different studies (Alsharafi et al., 2015; Sinha et al., 2008; Strauss and Elisevich, 2016; Turrin and Rivest, 2004).

Not all cytokines tested in the tissue and in the medium of slices exposed to LPS, in presence of absence of ATP, were detected. This mouse inflammation kit was able to recognize TNF-α, although the sample had a distinct origin. Mouse TNF-α bears a high degree of homology (94%) with rat.

Fig. 16 shows the effect of LPS or LPS co-incubated with ATP on TNF-α levels in tissue and culture medium. The quantification of TNF-α levels in slices exposed to different LPS concentrations was not performed. Co-incubation with LPS and ATP increased the TNF-α levels in the tissue (154.8±51.37, n=3, *p<0.05), when compared with control slices (3.141±1.088, n=3, Fig. 16A). LPS was able to increase the release of TNF-α, comparing with basal levels (4.200±0.070, n=3), both in absence (631.8±27.03, n=3, **p<0.01) or presence of ATP (1157±157.7, n=3, ***p<0.001, Fig. 16B). However, ATP further enhanced the release of this pro-inflammatory cytokine when compared to LPS alone ($^{\#}$p<0.05, Fig. 16B).

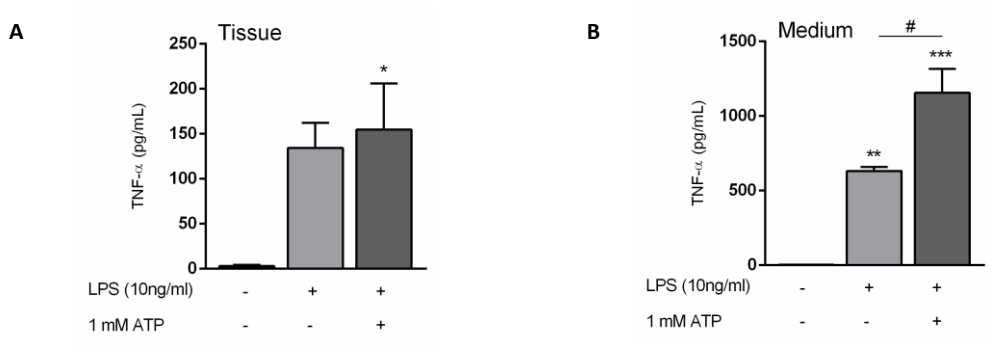

Fig. 16 - Effects of ATP co-exposure with LPS on TNF-α levels. **(A, B)** TNF-α levels in slices exposed to LPS in absence or presence of ATP [n=3] **(A)** and in the culture medium [n=3] **(B).** Data are presented as mean ± SEM. *p<0.05, **p<0.01, ***p<0.001 vs control; #p<0.05 LPS vs LPS plus ATP, by one-way ANOVA followed by Tukey's test.

4.2. Effect of NLRP3 inflammasome activation

Taking in account the results demonstrated in the previous section, the co-incubation LPS/ATP was selected, in detriment of the remaining, to induce the NLRP3-mediated inflammasome model. LPS incubated alone did not promote IL-1β release, at any of the concentrations or time of exposure used. These results suggested that in this model and at the concentrations used LPS acts only upstream of NLRP3 inflammasome activation. Whereas, ATP in presence of LPS was able to potentiates the release of the pro-inflammatory cytokines IL-1β and TNF-α. As described by others, an increased in the release of these cytokines, mainly of IL-1β, is indicative of the NLRP3 inflammasome assembly and activation.

Therefore, in all subsequent experiments, co-incubation with 10ng/ml of LPS and 1mM of ATP was used as an activating condition of NLRP3 inflammasome.

4.2.1. Morphology of glial cells

Glial cells activation can be evaluated by increased expression of microglia and astrocytes markers (Iba1 and GFAP, respectively), and by changes in their morphology.

The results obtained by western blot showed that at the conditions tested, Iba1 and GFAP expression was not altered. But this does not discard the activation of glial cells. Indeed, the expression of the glial markers may not change when the hippocampal lysate is analyzed as a whole, as in the western blotting technique.

In order to fully address this subject, an immunohistochemical assay was performed, which allows to compare the morphology of microglia and astrocytes between control slices and treated ones.

In slices with Iba1 positive cells, different microglia distribution was observed between distinct layers from the same slice (Fig. 17). Less microglia was observed on the top of the slices than on the bottom of the slices, which is nearest the culture medium. This gradient distribution suggests that these glial cells move towards the culture medium. The microglia movement is observed in different hippocampal regions (DG, CA3 and CA1) of control slices and LPS/ATP-treated slices, being more accentuated in the last ones (Fig. 17A, B and C).

In both conditions, the microglia furthest from the culture medium has a ramified morphology (a small soma with fine cellular processes) corroborating a resting state. However,

microglia closer to the culture medium has retracted coarse processes that resemble reactive state. In treated slices this reactive state indicative of microglial activation is more prominent when compared with control slices, since there are more and less dispersed cells. Therefore, it is plausible to affirm that LPS/ATP promote microgliosis in the hippocampal subregions and in the layers closer to the culture medium.

A

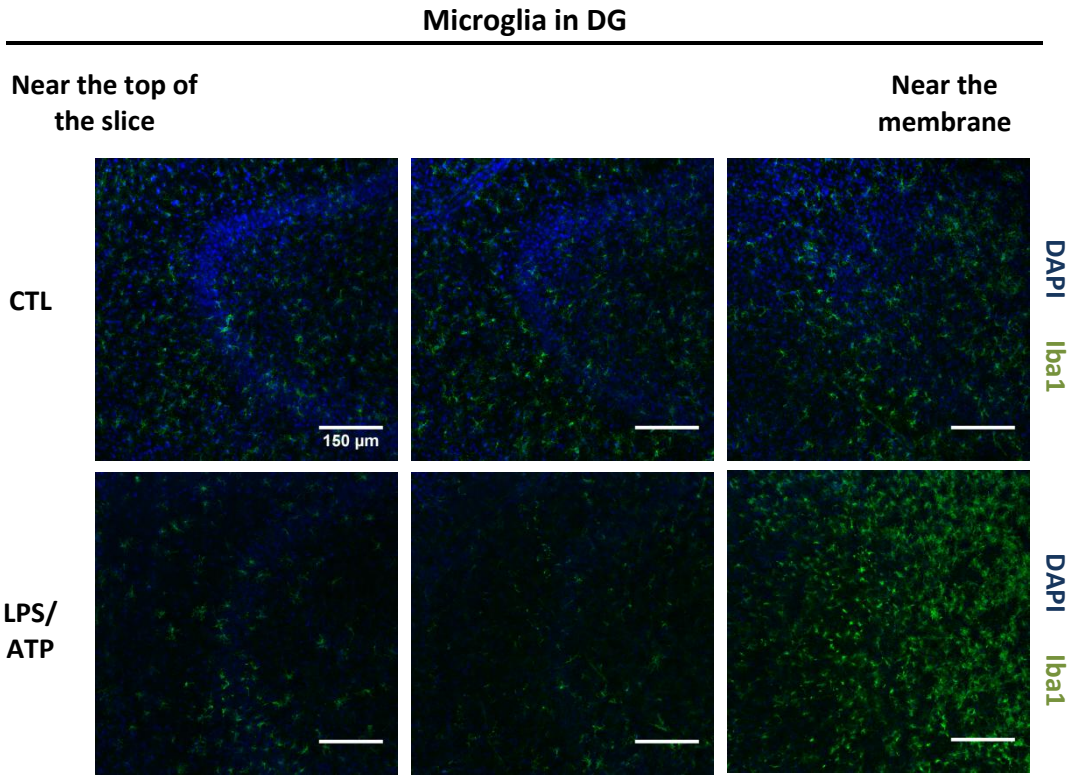

B

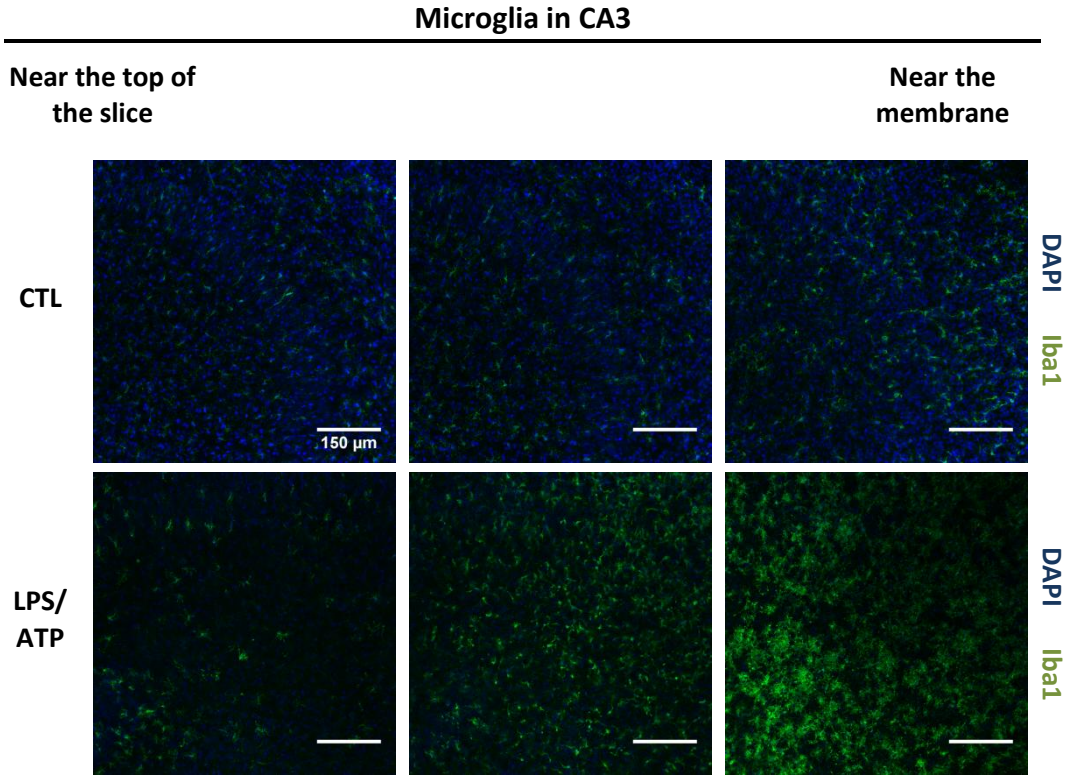

C

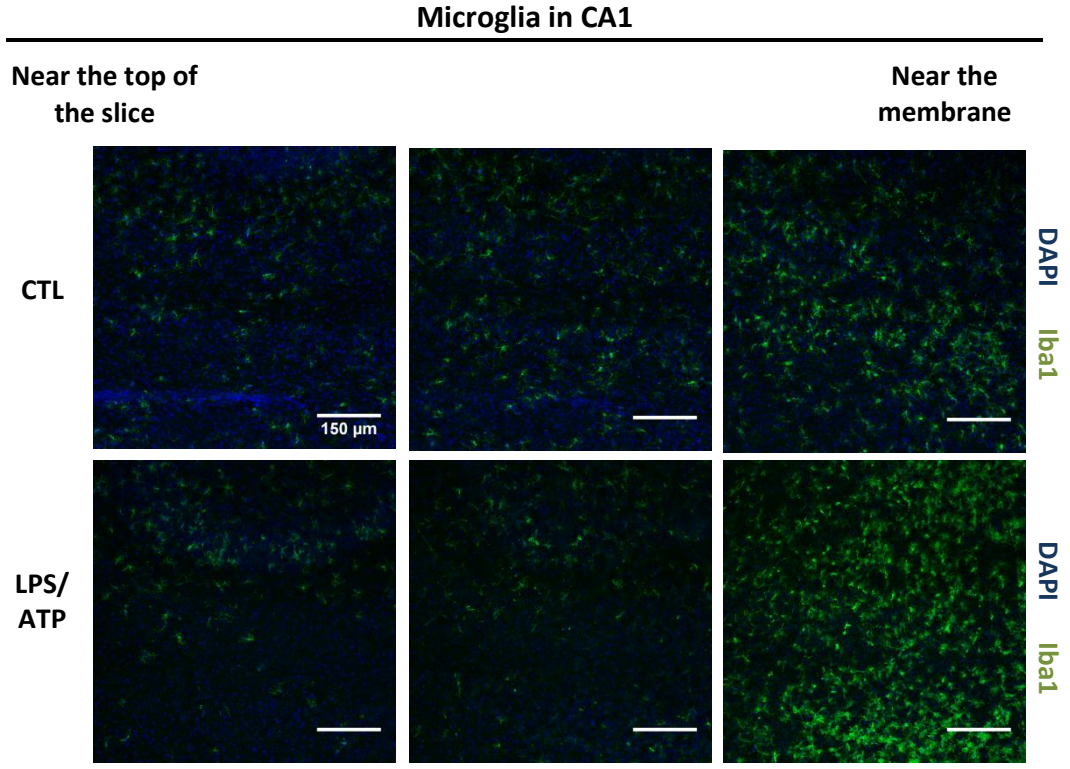

Fig. 17 – Microglia migration across organotypic cortex-hippocampus slices. Representative immunohistochemical staining for Iba1 (green) and DAPI (blue) fluorescence of control slices and slices exposed to LPS/ATP in DG **(A)**, CA3 **(B)** and CA1 **(C)**. Confocal images represent three optical sections from the same slice obtained with Plan-Apochromat 20x/0.8 M27 objective and 0.6 zoom. DG, Dentate gyrus. CA3, Cornu ammonis 3. CA1, Cornu ammonis 1. Scale bar, 150µm.

Regarding GFAP positive cells, no morphological differences were observed between astrocytes from control or treated slices, neither between different hippocampal regions (Fig. 18). In both conditions, astrocytes have large soma and thick processes forming a network which extends beyond the individual domain. This morphology is representative of a mild astrogliosis. Without quantitative measurements it was not possible to recognize the effect of LPS/ATP in organotypic slices. Contrary to microglia, astrocytes do not move towards culture medium (data not shown).

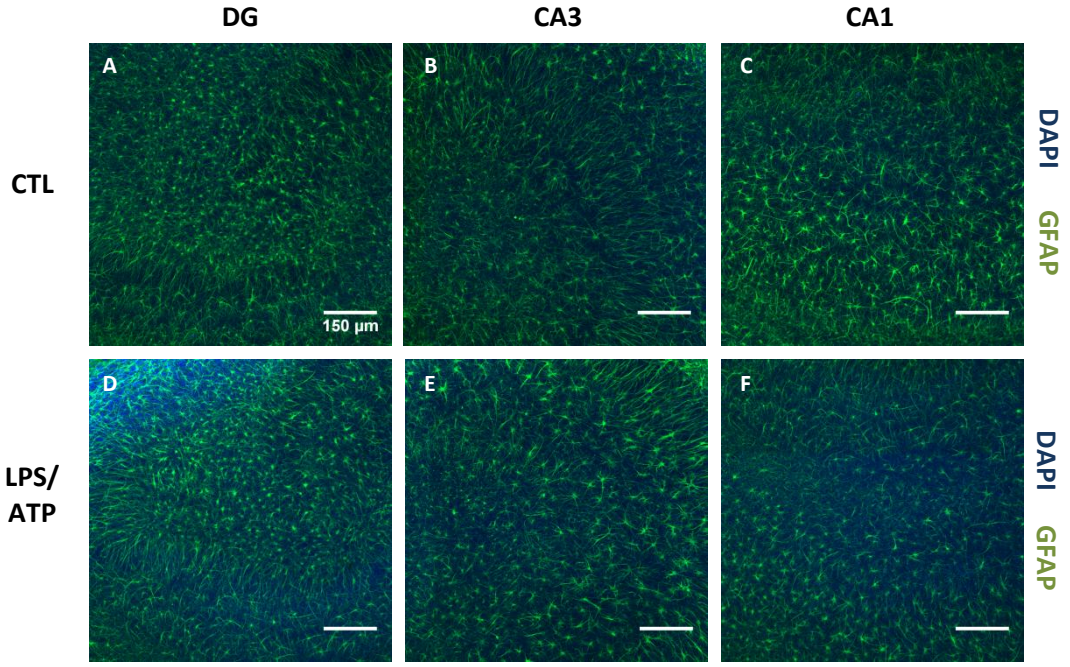

Fig. 18 - Astrocytes in organotypic cortex-hippocampus slices. Representative immunohistochemical staining for GFAP (green) and DAPI (blue) in hippocampal regions of control slices **(A, B, C)** and slices co-exposed to LPS/ATP **(D, E, F)**. Confocal images represent maximum intensity projections of optical sections obtained with EC Plan-Neofluar 10x/0.30 M27 objective and 1.0 zoom. DG, Dentate gyrus. CA3, Cornu ammonis 3. CA1, Cornu ammonis 1. Scale bar, 150µm.

4.2.2. Co-localization of NLRP3 in astrocytes

It is well established that microglia express all NLRP3 inflammasome components and is therefore capable of producing a functional multiprotein complex. However, it is not clear if NLRP3 is expressed by astrocytes or whether they produce a functional NLRP3 inflammasome. The expression appears to vary depending on the disease involved. In a way to clarify if astrocytes express NLRP3 in our organotypic slices a double-staining with GFAP and NLRP3 was performed.

The immunohistochemistry protocol of slices double labeled with GFAP and NLRP3 has been optimized. Changes in permeabilization and blocking solutions allowed to fully identify NLRP3 staining. Further optimizations must be performed, especially in antibody concentration, but a rough analysis was carried out to understand if NLRP3 co-localizes with astrocytes in these slices.

Preliminary results showed that NLRP3 is co-localized with astrocytes (Fig. 19). Even with the threshold chosen (which was not optimized, as explained in section 3.9) it was possible to observe co-localization in control slices and in slices incubated with LPS/ATP. The maximum percentage of NLRP3 and GFAP co-localization found in one layer of the slice was similar in both conditions, around 28%. The percentage of co-localization in 11 layers was 16.52±2.398 in control condition and 14.64±2.348 in LPS/ATP condition. NLRP3 expression differs between layers.

These preliminary results anticipate that NLRP3 is located in astrocytes processes and cell body. Moreover, this rough analysis means that with a lower threshold, that would be given by a negative control slice, the percentage of co-localization would be higher.

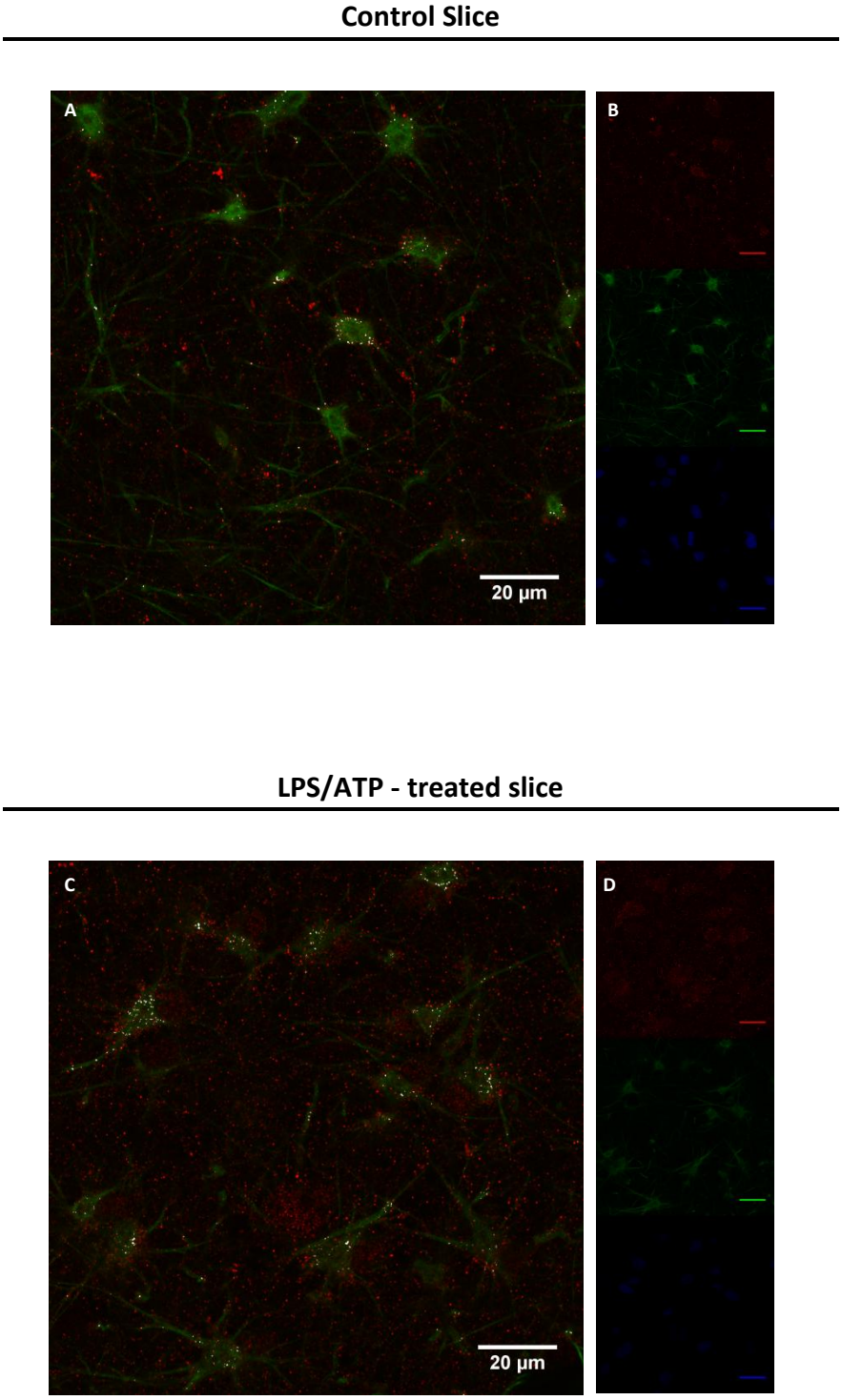

Fig. 19 - Co-localization of NLRP3 with astrocytes. Representative immunofluorescence staining for control slices (**A**, **B**) and LPS/ATP-treated slices (**C**, **D**). Double immunofluorescence of NLRP3 (red) and GFAP (green) in control slice **(A)** and in LPS/ATP-treated slice (**C**). White dots represent the points above the threshold that co-locate in the two channels. NLRP3 (red), GFAP (green) and DAPI (Blue) staining alone in control slice **(B)** and in LPS/ATP-treated slice (**D**). Confocal images were obtained with a Plan-Apochromat 63x/1.40 Oil DIC M27 objective and 1.0 zoom. Scale bar, 20 µm.

4.2.3. Extracellular recordings

In order to investigate the consequences of NLRP3 inflammasome activation in epileptiform activity, field potential recordings from CA3 region of organotypic slices were performed. Each slice was primarily stimulated in mossy fibers to ensure the occurrence of a biologic response. With the recording electrode placed in CA3 was possible to record population spikes (Fig. 20A). When no response was detected, the slice was discarded (see Methods).

After this screening, epileptiform activity was recorded continuously during 40 min. Organotypic slices revealed activity with no population discharges (Fig. 20B), activity with interictal-like discharges (Fig. 20C), or mixed activity with interictal-like and ictal-like discharges (Fig. 20D). These three types of activity were already described by others (Dyhrfjeld-Johnsen et al., 2010).

In inflammasome activation conditions, all slices displayed mostly mixed interictal-like and ictal-like activity. In slices incubated with LPS/ATP, the number of burst per slice was similar to that counted in control slices (Fig. 21A). Moreover, slices incubated with LPS or ATP alone behaved similarly. It should be noted that in slices incubated with LPS alone, this bacterial compound was exposed to slices for only 3h, instead of 6h. Regarding the bursts inner parameters, both frequency and amplitude of events per burst were also similar between control and treated slices (Fig. 21B and C).

Surprisingly, these results suggest that under the conditions evaluated, NLRP3 inflammasome manipulation is not increasing epileptiform activity when compared with control condition. Thus, this issue was further pursued.

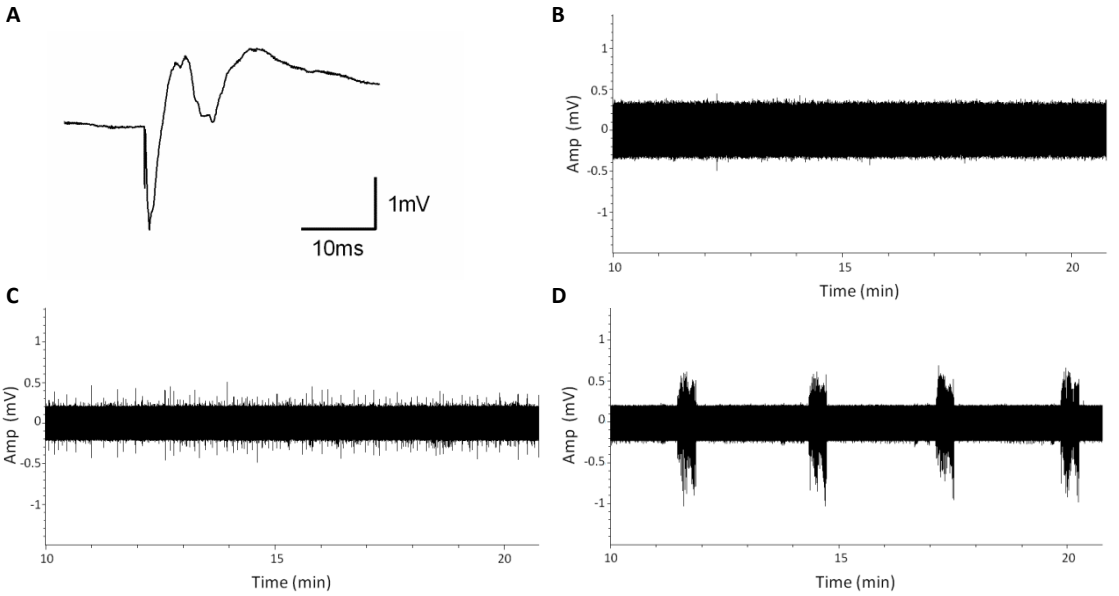

Fig. 20 - Extracellular recordings in organotypic cortex-hippocampus slices. **(A)** Representative population spike recorded after stimulation. **(B-D)** Field potential recordings of neuronal activity from CA3 region, which displayed no population discharges **(B)**, interictal-like discharges **(C)** and mixed interictal and ictal discharges **(D).**

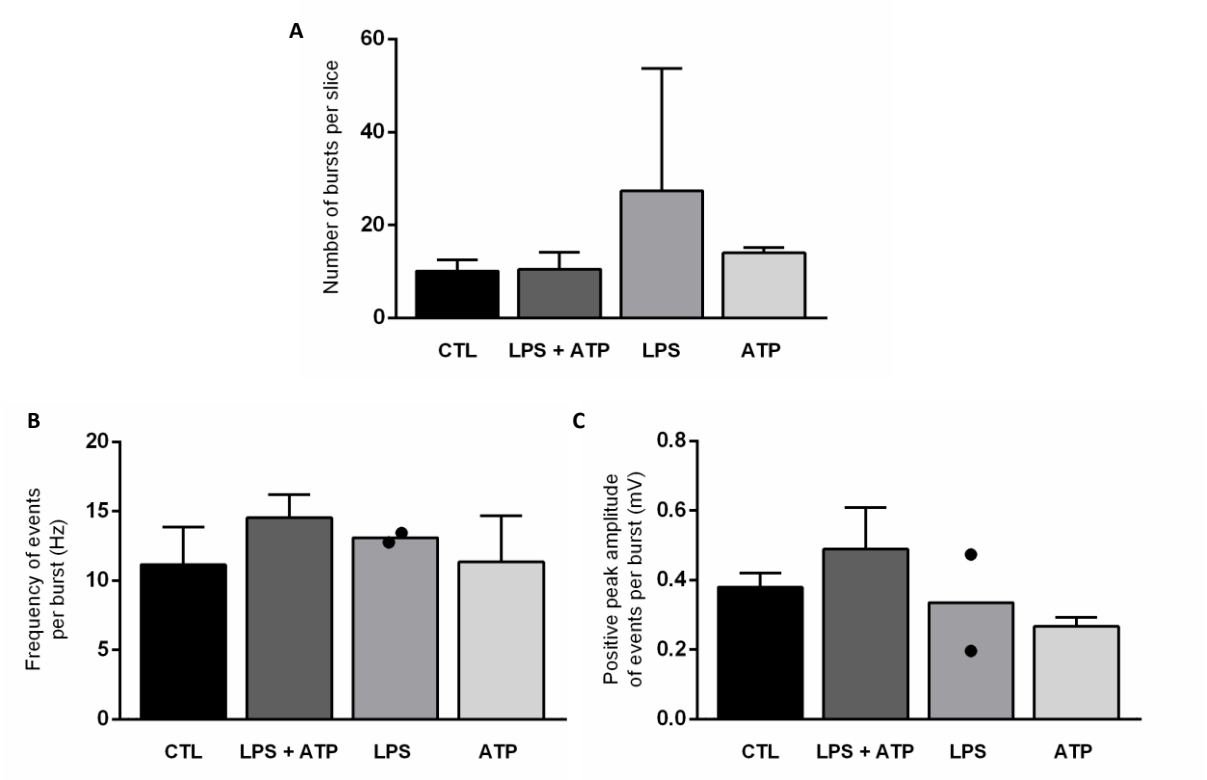

Fig. 21 - Analysis of epileptiform activity parameters in organotypic cortex-hippocampus slices under incubation with LPS or ATP alone, and LPS/ATP co-incubation. Number of bursts per slice [n=3-11] **(A)**, frequency [n=2-10] **(B)** and positive peak amplitude [n=2-10] **(C)** of events per burst are shown. Data are presented as mean ± SEM, except when n=2.

4.2.4. Slices in serum-free medium *vs* slices in serum-based medium: the best control condition

To fully understand if NLRP3 inflammasome manipulation did not affect epileptiform activity in relation to control condition, a careful assessment of control condition was performed.

Control slices were incubated throughout the whole culture time in a serum-containing medium (Opti-MEM), once horse serum allows the attachment of the slice on the membrane insert and the recovery from the explantation trauma (Gogolla et al., 2006; Muller et al., 2001). However, literature refers that this medium is not chemically well defined and should be exchange to a serum-free medium, like NBA. Therefore, the day before the experiments, all slices underwent a medium exchange, as described by others (Bernardino et al., 2008; Ravizza et al., 2006). Thus, the epileptiform activity of slices maintained in serum-based medium (CTL in Opti-MEM) was evaluated and compared with that of slices which underwent medium exchange to NBA (throughout this thesis denominated CTL).

CTL slices depicted a greater predominance of mixed interictal-like and ictal-like activity, when compared with slices incubated only in Opti-MEM medium (CTL in Opti-MEM) (Fig. 22 A). In slices that did not undergo medium exchange, the predominant activity was interictal-like. Only one slice out of 4 displayed mixed activity. Also, slices CTL in Opti-MEM (0.750±0.750,

n=4) had lower number of burst per slice than CTL slices (10.09±2.387, n=11, *p<0.05) (Fig. 22 B).

These results suggest that medium exchange at 14 DIV promotes epileptiform activity in these organotypic slices. In summary, our control condition already exhibited an exacerbated epileptiform activity when LPS and ATP were added.

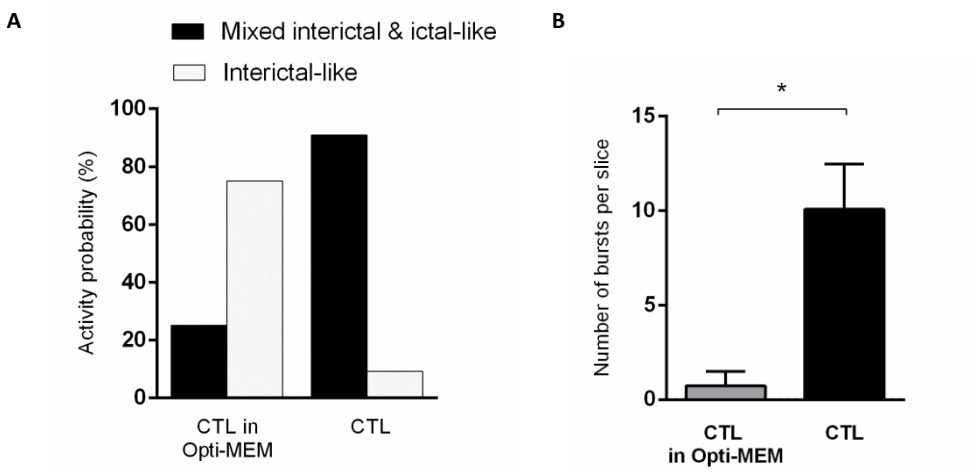

Fig. 22 - Differences in epileptiform activity of organotypic cortex-hippocampus slices according to culture media. (A) Activity probability of mixed interictal and ictal-like discharges or interictal-like discharges in control slices incubated only in serum-containing medium (CTL in Opti-MEM) and slices that underwent medium change (CTL). (B) Number of bursts per slice analysis between the two control conditions [n=4-11]. Data are presented as means ± SEM. *p<0.05by unpaired t-Test.

4.3. Impact of NLRP3 inflammasome inhibition

In the previous sections, NLRP3 inflammasome activation through LPS/ATP mediated the release of the pro-inflammatory cytokines, IL-1β and TNFα, and the activation of microglia. But, NLRP3 effect in epileptiform activity was not visible.

To verify if the inhibition of NLRP3 inflammasome decreased or reversed the parameters already evaluated, the slices were incubated with a selective inhibitor of this inflammasome, the MCC950.

4.2.1. IL-1β production

Fig. 23 shows the effect of MCC950 co-incubated with LPS/ATP upon Il-1β levels in organotypic slices and released to the culture medium.

In tissue samples, Il-1β levels increased both in absence (6566±1174, n=6, **p<0.01) and presence (8091±2218, n=4, **p<0.01) of MCC950, when compared with control slices (305.9±63.00, n=7, Fig. 23A). This result is in accordance with the literature once LPS potentiates the upregulation of pro-IL-1β, which is also detected by ELISA Kit as referred before. Moreover, MCC950 acts downstream LPS-mediated pro-IL-1β production, blocking only Il-1β production and not pro-Il-1β.

Furthermore, MCC950 had no effect upon Il-1β release (Fig. 23B). Although there was a downward trend MCC950 was not able to inhibit the LPS/ATP-mediated inflammasome activation and consequently the production and release of IL-1β.

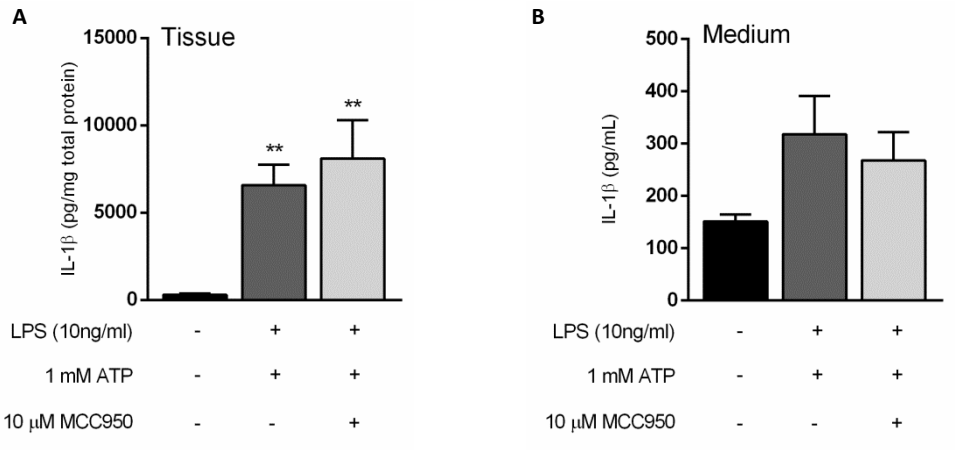

Fig. 23 - Effects of the NLRP3 inflammasome selective inhibitor, MCC950, on Il-1β levels produced and release by organotypic cortex-hippocampus slices. Il-1β levels in slices exposed to inflammasome activators, alone or together with MCC950 [n=4-7] **(A)** and in their culture medium [n=5-7] **(B).** Data are presented as mean ± SEM. **p<0.01 vs control, by one-way ANOVA followed by Tukey's test.

4.2.2. Morphology of glial cells

Fig. 24 shows that in slices incubated with MCC950 in inflammatory context and in slices treated with DMSO, the MCC950 vehicle, microglia distribution is different across the same slice in distinct hippocampal regions.

In slices co-incubated with MCC950/LPS/ATP, all hippocampal regions presented microgliosis in the layer nearest the insert membrane (Fig. 24). This inflammatory process did not appear to be qualitatively different from that observed in slices treated with the NLRP3 inflammasome activators. Therefore, MCC950 did not reverted LPS/ATP-induced microgliosis.

MCC950 vehicle was also evaluated to understand whether it could influence the action of MCC950. DMSO did not have an effect in microglia morphology or distribution. Microglia in DMSO-treated slices is similar to microglia found in control slices in DG and CA1 (Fig. 24A and C). In CA3 area is possible to observe more microglial cells in DMSO-treated slices that in control slices (Fig. 24B). However, this result has to be confirmed in more slices and quantitative measurements have to be performed.

Regarding astrocytes, no morphological differences were observed in these glial cells from slices co-exposed to LPS/ATP in absence or presence of NLRP3 inflammasome selective inhibitor (Fig. 25D-I). MCC950 does not appear to affect DG, CA3 and CA1 astrocytes (Fig. 25G-I). Neither did DMSO (Fig. 25J-L). In this *ex vivo* model of epileptogenesis, a mild astrogliosis seems to be always present at 15 DIV.

A

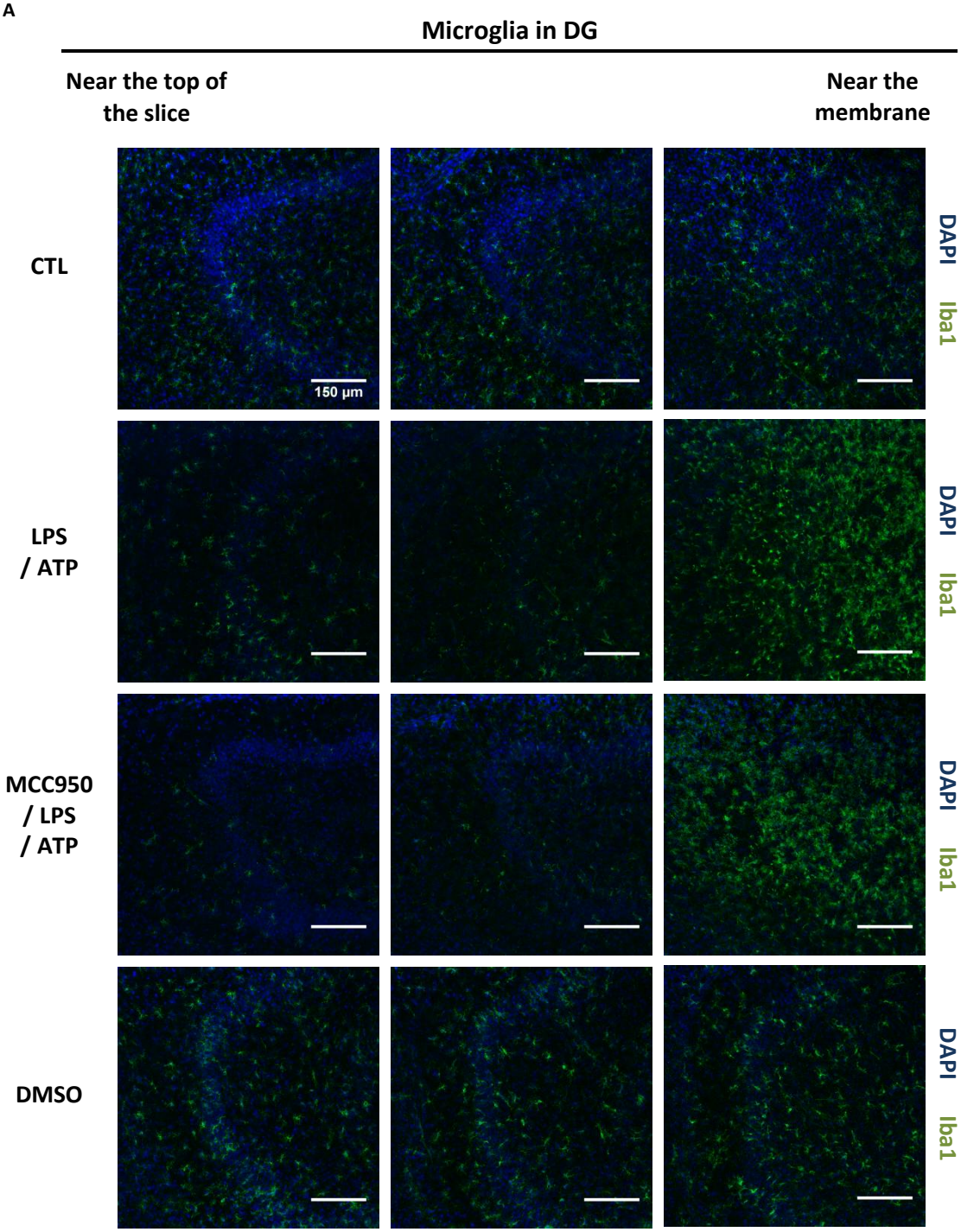
Microglia in DG
Near the top of the slice
Near the membrane
CTL
LPS / ATP
MCC950 / LPS / ATP
DMSO
150 µm
DAPI
Iba1

B

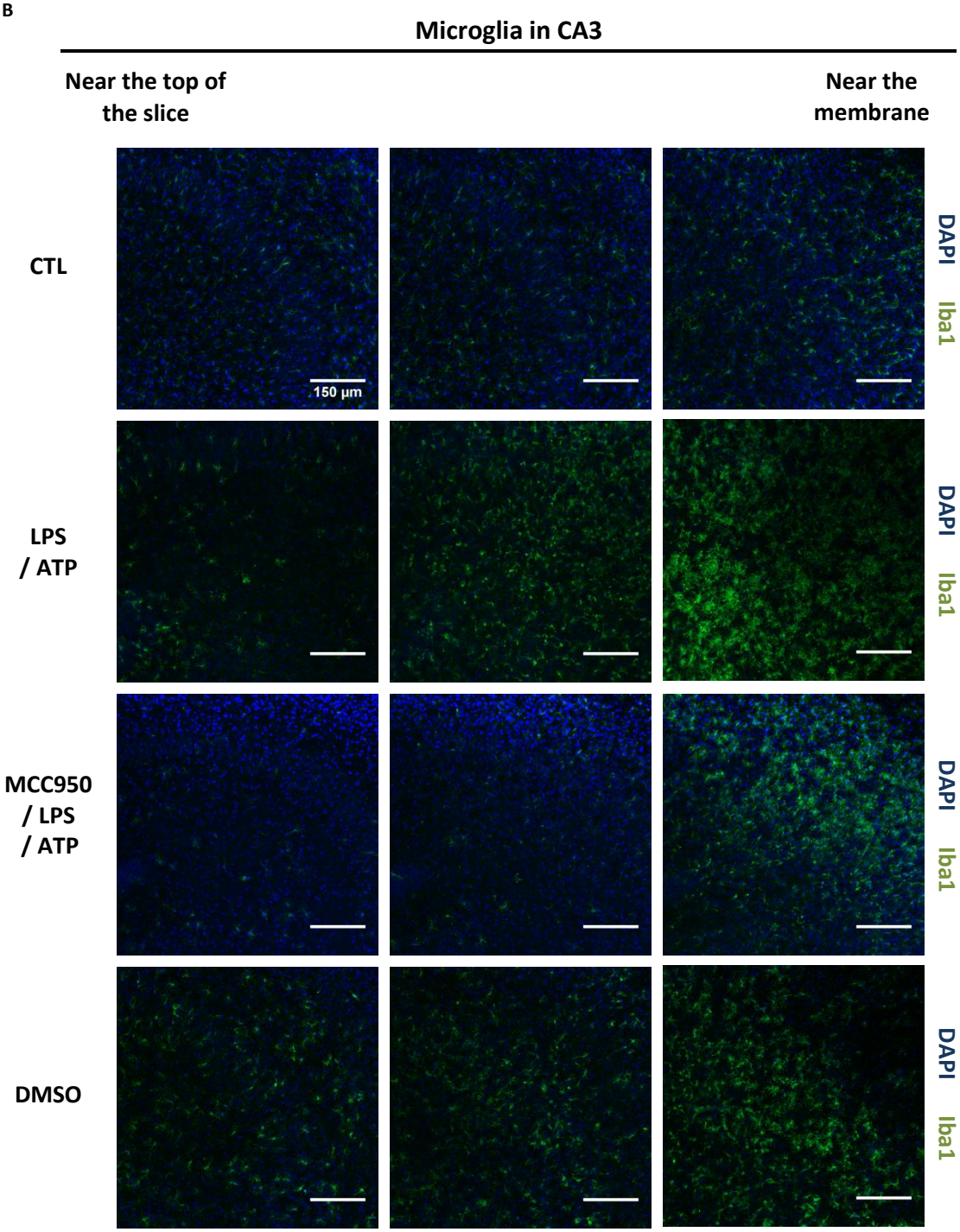
Microglia in CA3
Near the top of the slice
Near the membrane
CTL
LPS / ATP
MCC950 / LPS / ATP
DMSO
150 µm
DAPI
Iba1

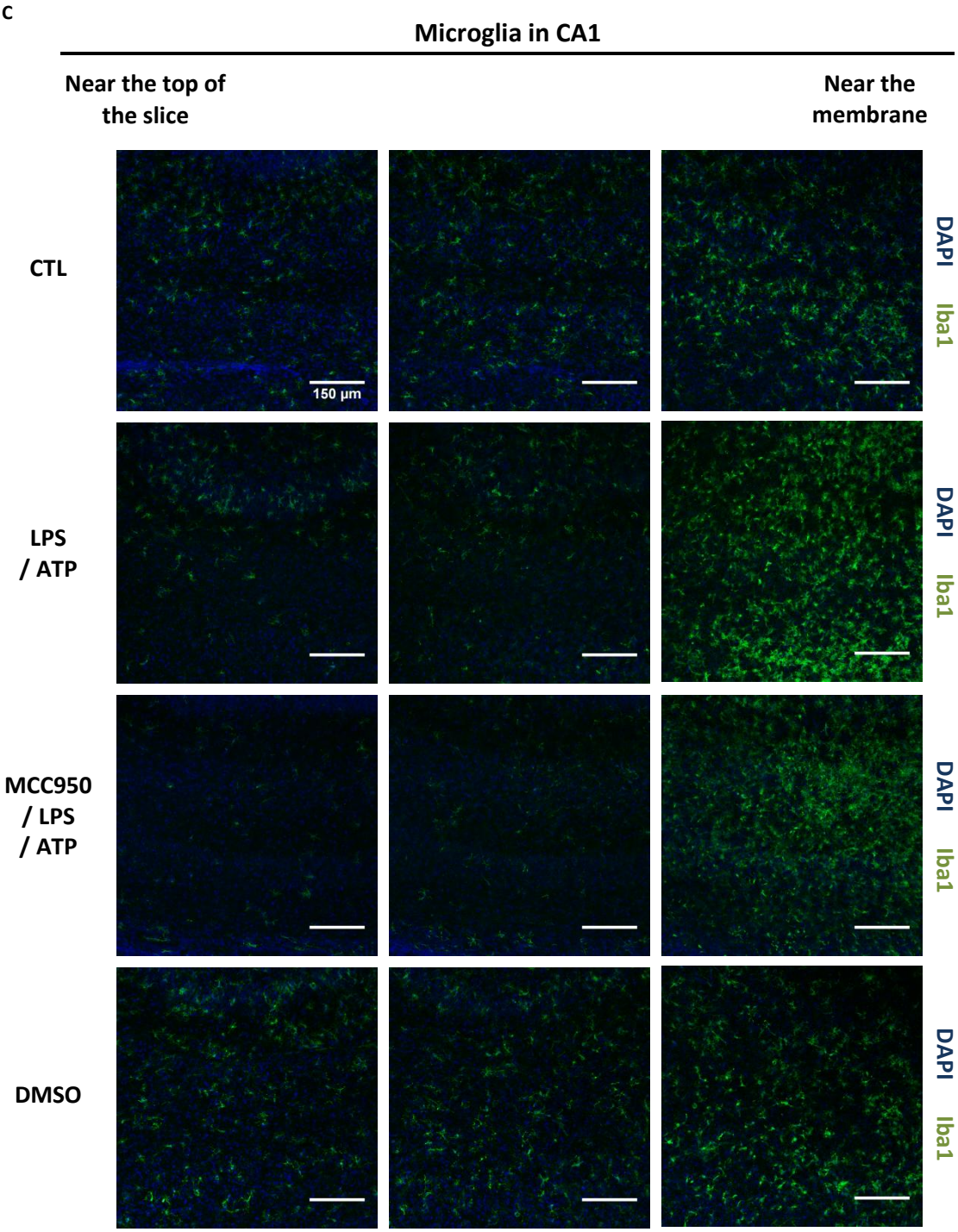

Fig. 24 - Microglia migration across organotypic cortex-hippocampus slices. Representative immunohistochemical staining for Iba1 (green) and DAPI (blue) of different conditions in DG **(A)**, CA3 **(B)** and CA1 **(C)**. Control slice, slice co-exposed to LPS/ATP, in absence and presence of MCC950, and a slice exposed to DMSO are shown. Confocal images represent three optical sections from the same slice obtained with Plan-Apochromat 20x/0.8 M27 objective and 0.6 zoom. DG, Dentate gyrus. CA3, Cornu ammonis 3. CA1, Cornu ammonis 1. Scale bar, 150µm.

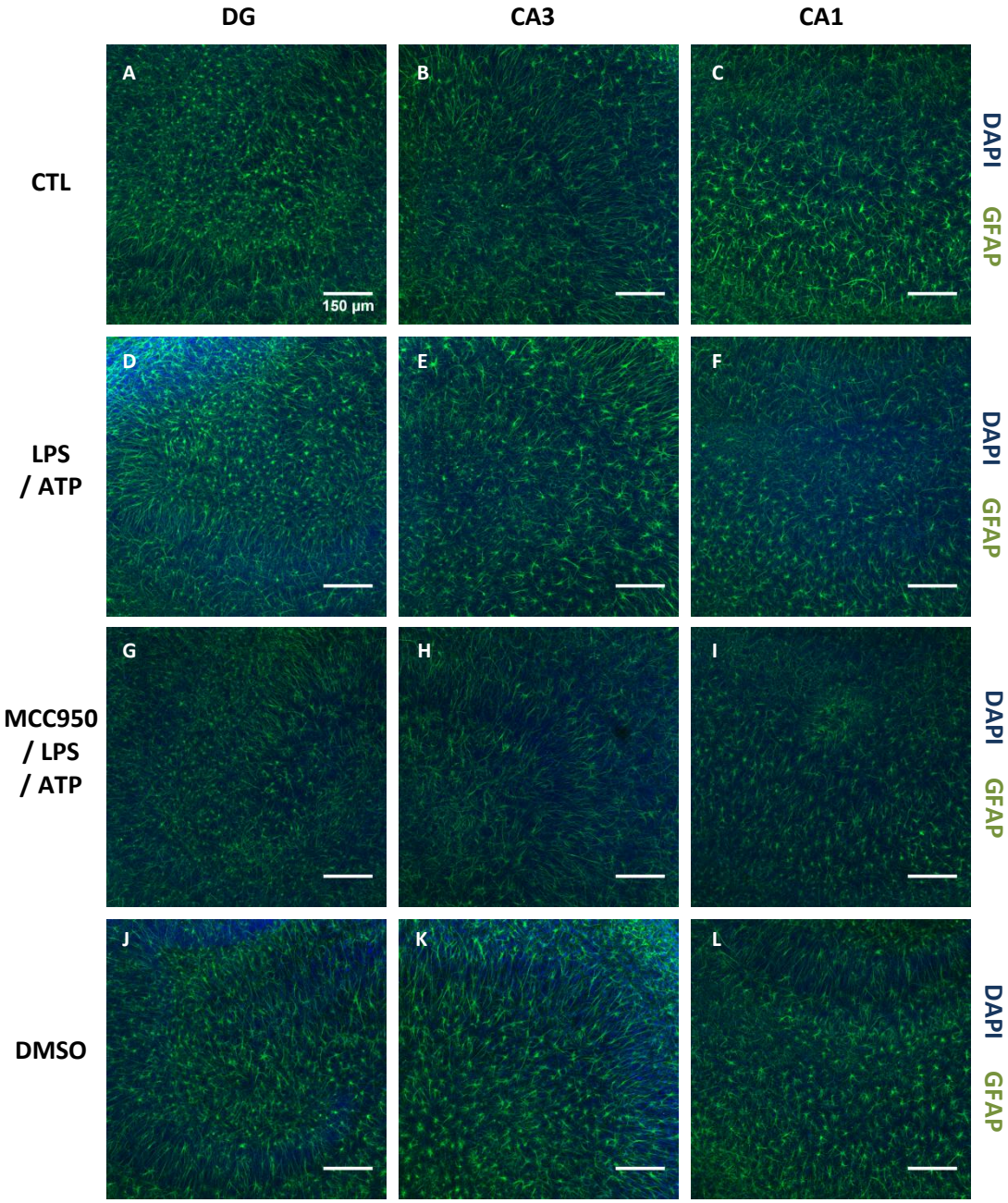

Fig. 25 - Astrocytes in organotypic cortex-hippocampus slices. Representative immunohistochemical staining for GFAP (green) and DAPI (blue) in hippocampal regions of control slice **(A, B, C)**, one slice co-exposed to LPS and ATP **(D, E, F),** one slice exposed to MCC950 in inflammatory context **(G, H, I)** and one slice exposed to DMSO, MCC950 vehicle **(J, K, L)**. Confocal images represent maximum intensity projections of optical sections obtained with EC Plan-Neofluar 10x/0.30 M27 objective and 1.0 zoom. DG, Dentate gyrus. CA3, Cornu ammonis 3. CA1, Cornu ammonis 1. Scale bar, 150µm.

4.2.3. Extracellular recordings

In order to investigate the effect of NLRP3 inflammasome inhibition, epileptiform activity was recorded in slices incubated with MCC950 alone or in an inflammatory context (LPS/ATP).

Fig. 26A shows that slices incubated with LPS/ATP in the presence or absence of MCC950 had a similar number of bursts per slice. Moreover, bursts inner characteristics also did not change significantly between these two conditions (Fig. 26B and C). Although a significant reduction in frequency and amplitude of events was not observed, there was a decreasing tendency in slices co-incubated with MCC950 and NLRP3 inflammasome activators. These results suggest that MCC950 was not able to decrease epileptiform activity at the concentrations used.

Comparing control slices with slices incubated only with MCC950, a decrease in the number of burst and in the frequency and amplitude of events was detected (Fig. 26A, B and C). Similar to slices incubated only in a serum-containing medium, the majority of the slices exposed to MCC950 had interictal-like activity instead of mixed interictal-like and ictal-like activity as in control slices (Fig. 26D and E). Moreover, the epileptiform activity induced by medium exchange in control slices was reverted by the NLRP3 selective inhibitor (Fig. 26F). Altogether, a new hypothesis rises up suggesting that epileptiform activity induced by serum withdrawal is NLRP3 dependent in these organotypic cortex-hippocampus slices.

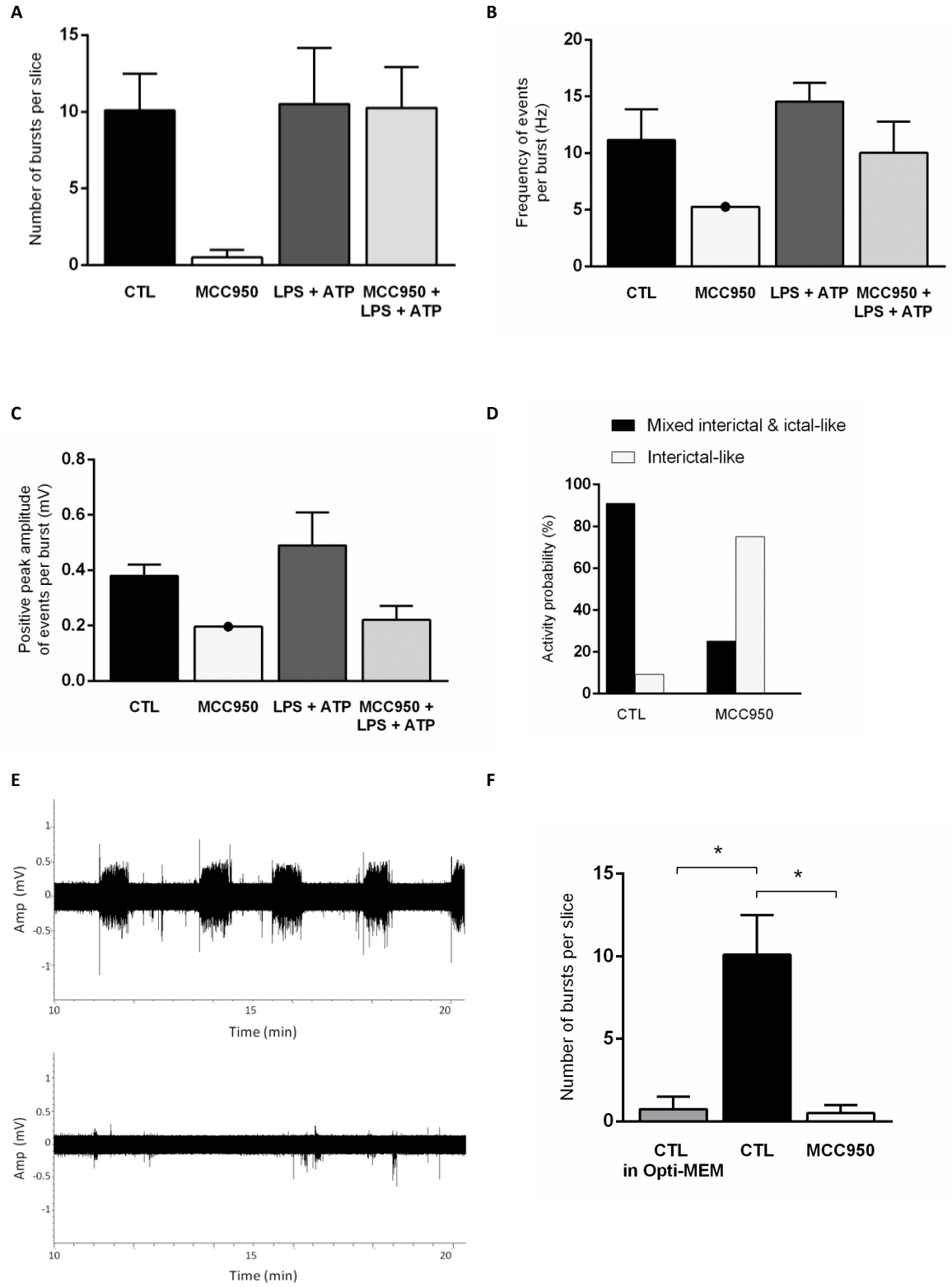

Fig. 26 - Extracellular recordings in organotypic cortex-hippocampus slices. **(A-E)** Analysis of epileptiform activity in NLRP3 inflammasome inhibition-related slices. Number of burst per slice [n=4-11] **(A)**, frequency [n=1-10] **(B)** and positive peak amplitude [n=1-10] **(C)** of events per burst were assessed. **(D)** Activity probability of mixed interictal and ictal-like discharges or interictal-like discharges in control slices and slices exposed only to MCC950. **(E)** Representative epileptiform activity recorded in control slice (upper image) and in MCC950-exposed slices (bottom image). **(F)** Number of bursts per slice in slices incubated only in serum-containing medium (CTL in Opti-MEM), in slices that underwent medium change (CTL) and in MCC950-exposed slices [n=4-11]. Data are presented as mean ± SEM, except when n=1. **p*<0.05 by one-way ANOVA followed by Tukey's test.

5. DISCUSSION

The main finding of this study is that activation of NLRP3 inflammasome is related with the enhancement of epileptiform activity. Although co-incubation with LPS and ATP did not influence epileptiform activity in our organotypic cortex-hippocampus slices (Fig. 21), culture medium exchange was able to increase this activity (Fig. 22). The transition, at 14 DIV, from a serum-containing medium to a serum-free medium potentiated the increasing of neuronal population discharges that were later reversed by MCC950 (Fig. 26F), a selective inhibitor of NLRP3 inflammasome. This result indicates that medium exchange triggered the activation of NLRP3 inflammasome, which in turn promoted epileptiform activity.

Through electrophysiological recordings it was possible to uncover the exacerbated epileptiform activity of our control slices when compared to slices incubated only in serum-containing medium. Thus, the use of control slices incubated in serum-free medium was not the most suitable condition, once NLRP3 inflammasome was already activated. This activation might have been triggered by the production of ROS caused by the serum removal from culture medium. It is described that ROS can also trigger the activation of NLRP3 inflammasome, working as a second stimulus (Zhou et al., 2011). Nevertheless, this theory still has to be tested. If ROS production is involved, then another compound should be working as a priming signal. It is noteworthy that medium composition is unlikely to be the cause of this epileptiform activity (Liu et al., 2017).

Knowing this, some of the results obtained throughout this study that appeared to be inconsistent with literature can now be understood and discussed.

Expression of different proteins in slices treated with LPS, in presence or absence of ATP

All proteins assessed through western blotting technique had a similar expression between control slices and treated slices. However, it was expected that control condition had lower levels of the proteins evaluated.

Although control slices had a similar expression of αII-spectrin when compared with treated slices, it was still possible to observe a lower SBDP145/ αII-spectrin ratio in slices co-incubated with LPS/ATP (Fig. 10). Both triggers promoted the decrease of necrosis, suggesting that they were able to further potentiate the NLRP3 inflammasome activation, which has been associated with a pro-inflammatory cell death called pyroptosis. It is thus plausible to speculate that cells were mainly dying by this form of cell death instead of necrosis. A less likely theory is that LPS and ATP under these conditions had protective actions that decreased premature cell death by autolysis.

Both NLRP3 and ASC expression did not change at different LPS concentrations and distinct timepoints or in presence of ATP (Fig. 11 and Fig. 12). Although changes can be masked by the high expression levels in the control condition, a decrease in NLRP3 and ASC expression in the presence of ATP can be observed (Fig. 11B). A similar decrease is also detected in ASC levels in the slices exposed to the highest concentrations of LPS (Fig. 12B). This tendency can yet reveal two hypotheses that need to be further studied. The first one is that NLRP3 and ASC are coupled to each other. It is described that this two proteins are linked by homotypic interactions between PYD domains (both NLRP3 and ASC have one PYD) (Oroz et al., 2016). If this bond has not been denatured during the preparation of the samples, PYD from ASC and PYD from NLRP3 are still linked and the antibodies against NLRP3 and ASC are not able to

recognize each PYD. The other hypothesis is that part of NLRP3 and ASC was released to extracellular medium. A study performed by Baroja-Mazo showed that 15 minutes after NLRP3 inflammasome activation, NLRP3, ASC, and other related proteins start to be released into the medium. Indeed, the majority of pool of NLRP3 was in tissue, but the highest levels of ASC were found in the medium (Baroja-Mazo et al., 2014).

NLRP3 inflammasome activation can be better studied using different techniques such as: size exclusion chromatography (SEC), co-immunoprecipitation (Co-IP), fluorometric caspase-1 activation assay or crosslinking (Coll et al., 2015; Khare et al., 2016). SEC allows the separation of the native protein complexes according to their size. Co-IP is a powerful technique used to identify protein-protein interactions. It targets a specific protein (like NLRP3) and allows the capture of others bound to it (as ASC). These proteins can be later separated by SDS-PAGE and detected by immunoblotting. The recruitment of ASC is used as the readout for inflammasome assembly. Fluorometric caspase-1 activation assay is used as complement to measure caspase-1 activity. In crosslinking technique, the crosslinking reagents bind to specific functional groups from, per example, ASC and capture with high sensitivity and stability the oligomeric state of this protein. ASC oligomerization is also used as the readout for NLRP3 inflammasome activation.

Regarding microglia and astrocytes markers assessed by western blotting, it was not possible to observe any alterations when comparing treated slices with control slices (Fig. 13 and Fig. 14). Once more, these results may have been masked by the use of control slices that underwent medium exchange. Beyond that, this *ex vivo* model is described to have a basal astrogliosis at the time of sampling. It is described that in organotypic hippocampal slices incubated in a serum-containing medium, a high hypertrophic astrocytic response takes place from 4 to 10 DIV, contrasting with the reduced number of GFAP-positive astrocytes observed at 2 DIV (Coltmann and Ide, 1996). These results were also corroborated by fluorescent intensity assessment of GFAP signal from slices incubated in serum-free medium (Gerlach et al., 2016).

Conversely, microglia has a mostly reactive morphology at 2 DIV (Coltmann and Ide, 1996; Gerlach et al., 2016) that, later, between 4 to 10 DIV, gives rise to a resting phenotype. These changes can be observed in slices incubated both in serum-containing (Coltmann and Ide, 1996) or serum-free medium (Czapiga and Colton, 1999). Nevertheless, microgliosis was already described at 15 DIV (Gerlach et al., 2016). The activation of the glial cells will be discussed again later.

Release of cytokines in slices treated with LPS, in presence or absence of ATP

Pro-inflammatory cytokine IL-1β is normally used as a readout of NLRP3 inflammasome activation once it is the main pyrogenic product produced by it. Comparing the IL-1β levels of slices that underwent medium exchange with slices incubated only in serum-containing medium, it was possible to verify higher levels of this cytokine in the first ones. IL-1β tissue levels, quantified in our laboratory in the same type of slices, but with different operator, was 77.08±6.842 pg of IL-1β/mg total protein in slices incubated only in serum-containing medium, at 14 DIV (Cláudia Cavacas' master thesis). These levels are around 4 times lower than that obtained in the control slices of this study. This confrontation also corroborates the results obtained in electrophysiological recordings.

Although NLRP3 inflammasome was already activated in control slices, it was possible to verify a further activation of this complex in slices co-exposed to LPS and ATP. With the results obtained in this study was possible to verify that LPS alone was not able to further potentiate IL-1β release in these slices (Fig. 15B), not even in a lower potent manner as described by others (Bernardino et al., 2008; Ravizza et al., 2006). Nevertheless, in ATP presence, both were able to potentiate further IL-1β production, corroborating the results obtained before in organotypic hippocampal cortex-free slices (Fig. 15B) (Bernardino et al., 2008; Ravizza et al., 2006).

In accordance with these results, another pro-inflammatory cytokine, TNF-α, was also increased in slices co-incubated with LPS and ATP (Fig. 16). To our knowledge, it was the first time that TNF-α levels were quantified in organotypic hippocampal slices incubated with LPS and ATP.

The close relationship between these two cytokines is known. IL-1β induces glutamate astrocytic release via TNF-α (Shimada et al., 2014; Vezzani et al., 2008) and this cytokine, in turn induces the expression of the inactive pro-IL-1β (Schroder and Tschopp, 2010). Both IL-1β and TNF-α promotes neuronal hyperexcitability and are increased in the brain of human epileptic patients (Sinha et al., 2008; Uludag et al., 2015).

Effect of LPS and ATP co-incubation in organotypic slices

The exposure of LPS and ATP, activators of NLRP3 inflammasome, promoted microgliosis in these organotypic cortex-hippocampus slices (Fig. 17). It was showed that microglia migrate from the top of the slice to the layers nearest the insert membrane, that is microglia move towards the culture medium. This process can be observed in control slices, especially in CA1, and in treated slices. In these last slices, it was possible to verify a severe microgliosis in the layers closest to the LPS/ATP-containing medium of all hippocampal regions. On the contrary, in presence of LPS and ATP, organotypic hippocampal slices exhibited reactive microglia randomly over the whole slice (Bernardino et al., 2008).

Microglial cells activation should be further investigated in this study. The quantitative analysis by counting the number of microglia was attempted through the Image J software. However, in the nearest layers of the insert membrane it was difficult to individualize and count the number of cells labelled with Iba1 due to its hyper-reactive morphology. Double immunolabeling for Iba1 and CD68 (a marker for activated microglia cells) could be performed to assess the percentage of resting microglia ($Iba1^+/CD68^-$) versus activated microglia ($Iba1^+/CD68^+$) (Gerlach et al., 2016). This method would also allow a better understanding of microglia activation state in control slices.

Regarding astrocytes, the exposure of LPS and ATP did not potentiate astrogliosis, since control slices already manifested this inflammatory process (Fig. 18). As mentioned before, it is known that astrogliosis is present in this type of slices in 15 DIV (Gerlach et al., 2016). A quantitative analysis of GFAP fluorescence intensity, as described by Gerlach et al., was thought but not implemented (Gerlach et al., 2016). Fluorescence intensity quantification is not a consensual method in the scientific community. Another analysis could be performed to better evaluate the astrocytes activation. Reverse transcription quantitative polymerase chain reaction (RT-qPCR) analysis of nestin and ciliary neurotrophic factor (CNTF) trancripts could also complement the immunohistochemical analysis. These two proteins are expressed by activated astrocytes (Gerlach et al., 2016).

Microgliosis and astrogliosis are associated with IL-1β production which has been related with epileptogenesis for some time (Vezzani et al., 2008; Vezzani and Baram, 2007). In the control slices used in this study, high levels of IL-1β were found and an unexpected high incidence of epileptiform activity was recorded, corroborating the relationship between these two. Slices co-exposed to LPS and ATP, which have had higher IL-1β levels when compared to control slices, did not display an increased epileptiform activity. The epileptiform activity recorded in the treated slices was similar to that recorded in the control (Fig. 21). No statistical differences were found in the number of burst per slice or in the bursts inner parameters. Therefore, LPS and ATP were not able to potentiate further the existing epileptiform activity. These results raise two theories: either epileptiform activity cannot be further potentiated once it reached the maximum level, or the concentrations of LPS and ATP used were not appropriate given the epileptiform basal state of the control slices.

The analysis carried out to evaluate epileptiform activity in these organotypic slices was developed by us. Articles demonstrating the presence of epileptiform activity in organotypic hippocampal slices used custom softwares for a sophisticated data analysis (Berdichevsky et al., 2012; Dyhrfjeld-Johnsen et al., 2010). In this study, bursts (ictal-like discharges) were defined as continuous discharges lasting more than 6 seconds. The threshold used to define ictal-like activity and interictal-like activity differs between models of epilepsy. Berdichevsky, in organotypic hippocampal cortex-free slices, defined bursts as paroxysmal discharges lasting more than 10 seconds or sequences of at least 20 paroxysmal spikes in 10 seconds (Berdichevsky et al., 2012). Rutecki, in acute hippocampal slices incubated with pilocarpine, defined bursts as discharges lasting more than 3s (Rutecki and Yang, 1998).

Taken together, NLRP3 inflammasome activators were not able to further potentiate astrogliosis and epileptiform activity displayed by control slices. However, they were able to promote microgliosis, a feature barely observed in control slices.

Co-localization of NLRP3 in astrocytes

This study showed, for the first time, co-localization between NLRP3 and astrocytes in a model of epileptogenesis (Fig. 19). To my knowledge until now there is no published article studying NLRP3 co-localization with other proteins in any model of epilepsy. The co-localization analysis performed was tight once it had a high threshold for the red channel, the one used for NLRP3. To the naked eye it was possible to see that there were still areas of co-location that were below the threshold. However, this threshold was suggested by iMM Bioimaging Unit, since there was no negative control without primary antibodies prepared under the same conditions and with the same fluorescence intensities.

Nevertheless, these preliminary results demonstrated that NLRP3 indeed co-localized with GFAP. If astrocytes express NLRP3 protein or produce a functional NLRP3 inflammasome is still controversial. In C57BL/6JOlaHsd mice primed with LPS or cytokines mix almost no NLRP3 protein were detected (Gustin et al., 2015), although it was detected in rat models of spinal cord injury model (Zendedel et al., 2016) and ALS (Debye et al., 2018; Johann et al., 2015). However, if astrocytes actually express nlrp3 mRNA and produces a NLRP3 protein or if they capture this protein from the extracellular medium it is still unclear. Our experiment also failed to elucidate this paradigm.

It would also be interesting to study the cellular co-localization between NLRP3 and ASC in order to understand in which cells it co-localizes. ASC-NLRP3 co-localization within a specific

cell would be used as readout for NLRP3 inflammasome activation. Yet, performing immunolabeling with NeuN (a neuronal specific nuclear protein) or Iba1 and NLRP3 inflammasome components would also be newsworthy in order to confirm a functional NLRP3 in these cells.

Impact of MCC950 co-incubated with LPS and ATP in organotypic slices

The treatment with MCC950, NLRP3 inflammasome selective inhibitor, did not attenuate the IL-1β release from organotypic slices in response to stimulation with LPS and ATP, at the concentrations tested (Fig. 23). Although MCC950 co-incubation with LPS and ATP has never been studied in organotypic slices, Coll et al. reported a decrease of IL-1β production from bone marrow derived macrophages (BMDMs), human monocyte–derived macrophages (HMDMs) and human peripheral blood mononuclear cells (PBMCs) stimulated with LPS and ATP and treated with MCC950 (Coll et al., 2015). Moreover, decrease of IL-1β levels in the serum was also verified in *in vivo* models of EAE exposed to MCC950 and LPS (Coll et al., 2015). I*n vitro* models have reported different concentrations of MCC950. In cells treated with LPS and ATP up to 1μM of this drug was applied, where as in cells treated with LPS and nigericin the maximum concentration applied was 10μM (Coll et al., 2015). Organotypic slices are a more robust model than isolated cells, thus the highest concentration of MCC950 described by Coll et al. was used in our slices. MCC950 at 10μM was diluted in 0.1% DMSO. This vehicle can be toxic to cells, but as the concentration used is considered to be safe for them.

Corroborating the results of LPS/ATP-induced IL-1β production, MCC950 did not affect LPS/ATP-promoted microgliosis neither epileptiform activity (Fig. 24). Although it is necessary to quantitatively evaluate the number of microglial cells to confirm these results, NLRP3 inflammasome selective inhibitor did not potentiate a clear reverse of microgliosis. At the time, it was the first time that this evaluation was carried out. A recent report showed that MCC950 attenuated Aβoligomers-evoked microglia reactivity in a mouse model of Alzheimer ’s disease, but IL-1β levels were not quantified in this study (Fekete et al., 2018).

In relation to epileptiform activity, MCC950 when co-incubated with LPS and ATP did not reduce the exacerbated neuronal activity (Fig. 26). As shown, control slices already depicted an exacerbated activity, and MCC950 was not able to attenuate the epileptiform activity generated by further activation of the inflammasome by LPS/ATP.

Taken together, these results suggests that, at the concentrations studied, MCC950 is not capable of ameliorate the effect of NLRP3 inflammasome activators in microglial cells and their related-cytokines. Furthermore, is not capable of decreasing epileptiform activity in an inflammatory context in these organotypic cortex-hippocampus slices. Nevertheless, if we look carefully for data depicted in the graphs related with IL-1β secretion and epileptiform activity analysis, it is possible to observe a consistent decrease in the MCC950 condition in inflammatory context. This raises a question about the concentrations used for each compound (MCC950, LPS and ATP), which certainly deserves further attention.

Slices treated with MCC950 alone resemble slices incubated in serum-containing medium and reverse the epileptiform activity

This discussion has already addressed the effect of exchanging culture media on neuronal activity in control slices. It was observed that slices that did not undergo this process, that is slices always incubated in serum-containing medium (Opti-MEM medium), have little or

almost no epileptiform activity (Fig. 22). The interictal discharges appear to be the most predominant in these slices. This small activity resembles that recorded from slices incubated with MCC950 alone. After medium exchange, slices depicted an exacerbated epileptiform activity, and the selective inhibitor was able to attenuate the effect of serum removal, obliterating almost all ictal-like discharges (Fig. 26F).

In organotypic hippocampal slices displaying ictal-like discharges, phenytoin suppressed ictal activity but not interictal activity (Berdichevsky et al., 2012; Dyhrfjeld-Johnsen et al., 2010). Phenytoin is an anticonvulsant drug widely used around the world to suppress some types of seizures. It is reported that this effect of phenytoin on organotypic slices is comparable to the effect observed in electroencephalogram (EEG) of patients with epilepsy (Berdichevsky et al., 2012; Dyhrfjeld-Johnsen et al., 2010). Nevertheless, this drug prevents seizures but does not prevent epileptogenesis. Phenytoin exerts an acute and reversible anticonvulsive effect. It would be interesting to address this issue in our model of epileptogenesis and evaluate the epileptiform activity of the slices upon MCC950 withdrawal.

6. Conclusion and Future Perspectives

Our study affirmed that NLRP3 inflammasome activation, which is associated with a massive release of IL-1β, is required for exacerbation of epileptiform activity and possible for epileptogenesis process.

It was the first time that a study reported that MCC950, a selective inhibitor of NLRP3 inflammasome, reversed epileptiform activity. In 2014, a study reported that inhibition of this particular inflammasome, through NLRP3 mRNA silencing, provided neuroprotection in rats following SE (Meng et al., 2014). However, this treatment was only effective in 44% of the rats from the treated group, contrasting with the 75% possible efficacy in this study. Although it is necessary to increase the number of experiments, these preliminary results unveil a potential antiepileptogenic therapy.

Future studies should focus on disentangling the NLRP3 inflammasome endogenous activator responsible for the epileptiform activity induced by serum withdrawal. Moreover, LPS/ATP concentrations should be increased to understand if this exacerbated neuronal activity has reached the maximum level by only medium exchange. It would also be interesting to observe the effect of LPS and ATP in organotypic slices maintained in serum-containing medium (Opti-MEM).

Future work could further detail the effect of MCC950 in organotypic slices. For instance increasing the MCC950 concentration in slices treated with LPS/ATP can enlighten the mechanism of action of this selective inhibitor. Also, evaluation of Il-1β secretion and microgliosis in slices treated with MCC950 alone would be helpful.

Furthermore, adding the AED phenytoin to organotypic slices and testing MCC950 in a wash in /wash out system would provide a better knowledge about its epileptogenic properties.

In a long-term future, it would also be exciting to assess the action of MCC950 beyond BBB and to evaluate its effects in *in vivo* models of epilepsy.

7. REFERENCES

Abderrazak, A., Syrovets, T., Couchie, D., El Hadri, K., Friguet, B., Simmet, T., and Rouis, M. (2015). NLRP3 inflammasome: From a danger signal sensor to a regulatory node of oxidative stress and inflammatory diseases. *Redox Biology*, *4*, 296–307.

Agostini, L., Martinon, F., Burns, K., McDermott, M. F., Hawkins, P. N., and Tschopp, J. (2004). NALP3 forms an IL-1β-processing inflammasome with increased activity in Muckle-Wells autoinflammatory disorder. *Immunity*, *20*(3), 319–325.

Alfonso-Loeches, S., Ureña-Peralta, J. R., Morillo-Bargues, M. J., Oliver-De La Cruz, J., and Guerri, C. (2014). Role of mitochondria ROS generation in ethanol-induced NLRP3 inflammasome activation and cell death in astroglial cells. *Frontiers in Cellular Neuroscience*, *8*.

Alsharafi, W. A., Xiao, B., Abuhamed, M. M., Bi, F.-F., Luo, Z.-H., Gambardella, A., Qiu, D.-L., and Zhang, Y.-W. (2015). Correlation Between IL-10 and microRNA-187 Expression in Epileptic Rat Hippocampus and Patients with Temporal Lobe Epilepsy. *Frontiers in Cellular Neuroscience*, *9*, 466.

Anderson, W. W., and Collingridge, G. L. (2001). The LTP Program: a data acquisition program for on-line analysis of long-term potentiation and other synaptic events. *Journal of Neuroscience Methods*, *108*, 71–83.

Andriezen, W. L. (1893). The Neuroglia Elements in the Human Brain. *British Medical Journal*, *2*(1700), 227–230.

Barbarosie, M., and Avoli, M. (1997). CA3-Driven Hippocampal-Entorhinal Loop Controls Rather than Sustains In Vitro Limbic Seizures. *The Journal of Neuroscience*, *17*(23), 9308–9314.

Baroja-Mazo, A., Martín-Sánchez, F., Gomez, A. I., Martínez, C. M., Amores-Iniesta, J., Compan, V., Barberà-Cremades, M., Yagüe, J., Ruiz-Ortiz, E., Antón, J., Buján, S., Couillin, I., Brough, D., Arostegui, J. I., and Pelegrín, P. (2014). The NLRP3 inflammasome is released as a particulate danger signal that amplifies the inflammatory response. *Nature Immunology*, *15*(8), 738–748.

Baron, L., Gombault, A., Fanny, M., Villeret, B., Savigny, F., Guillou, N., Panek, C., Le Bert, M., Lagente, V., Rassendren, F., Riteau, N., and Couillin, I. (2015). The NLRP3 inflammasome is activated by nanoparticles through ATP, ADP and adenosine. *Cell Death and Disease*, *6*, e1629.

Basic, S. (2016). Epilepsy Pharmacoresistance – Where Are We Now? *Journal of Neurology & Stroke*, *4*(6), 161.

Becq, H., Bosler, O., Geffard, M., Enjalbert, A., and Herman, J. P. (1999). Anatomical and functional reconstruction of the nigrostriatal system in vitro: Selective innervation of the striatum by dopaminergic neurons. *Journal of Neuroscience Research*, *58*(4), 553–566.

Bederson, J. B., Pitts, L. H., Tsuji, M., Nishimura, M. C., Davis, R. L., and Bartkowski, H. (2001). Rat middle cerebral artery occlusion: evaluation of the model and development of a neurologic examination. *Stroke*, *17*(3), 472–476.

Ben Haim, L., Ceyzériat, K., Carrillo-de Sauvage, M. A., Aubry, F., Auregan, G., Guillermier, M., Ruiz, M., Petit, F., Houitte, D., Faivre, E., Vandesquille, M., Aron-Badin, R., Dhenain, M., Déglon, N., Hantraye, P., Brouillet, E., Bonvento, G., and Escartin, C. (2015). The JAK/STAT3 pathway is a common inducer of astrocyte reactivity in Alzheimer's and Huntington's diseases. *The Journal of Neuroscience*, *35*(6), 2817–2829.

Berdichevsky, Y., Dzhala, V., Mail, M., and Staley, K. J. (2012). Interictal spikes, seizures and ictal cell death are not necessary for post-traumatic epileptogenesis in vitro. *Neurobiology of Disease*, *45*(2), 774–785.

Bergsbaken, T., Fink, S. L., and Cookson, B. T. (2010). Pyroptosis: host cell death and inflammation. *Nature Reviews Microbiology*, *7*(2), 99–109.

Bernardino, L., Balosso, S., Ravizza, T., Marchi, N., Ku, G., Randle, J. C., Malva, J. O., and Vezzani, A. (2008). Inflammatory events in hippocampal slice cultures prime neuronal

susceptibility to excitotoxic injury: A crucial role of P2X7 receptor-mediated IL-1β release. *Journal of Neurochemistry*, *106*(1), 271–280.

Bernardino, L., Xapelli, S., Silva, A. P., Jakobsen, B., Poulsen, F. R., Oliveira, C. R., Vezzani, A., Malva, O., and Zimmer, J. (2005). Modulator Effects of Interleukin-1β and Tumor Necrosis Factor α on AMPA-Induced Excitotoxicity in Mouse Organotypic Hippocampal Slice Cultures. *The Journal of Neuroscience*, *25*(29), 6734–6744.

Blümcke, I., Thom, M., Aronica, E., Armstrong, D. D., Bartolomei, F., Bernasconi, A., Bernasconi, N., Bien, C. G., Cendes, F., Coras, R., Cross, J. H., Jacques, T. S., Kahane, P., Mathern, G. W., Miyata, H., Moshé, S. L., Oz, B., … Spreafico, R. (2013). International consensus classification of hippocampal sclerosis in temporal lobe epilepsy: A Task Force report from the ILAE Commission on Diagnostic Methods. *Epilepsia*, *54*(7), 1315–1329.

Boison, D., and Dow, R. S. (2012). Adenosine dysfunction in epilepsy. *Glia*, *60*(8), 1234–1243.

Brooks-Kayal, A. R., Shumate, M. D., Jin, H., Rikhter, T. Y., and Coulter, D. A. (1998). Selective changes in single cell GABA A receptor subunit expression and function in temporal lobe epilepsy. *Nature Medicine*, *4*(10), 1166–1172.

Chang, B. S., and Lowenstein, D. H. (2003). Epilepsy. *The New England Journal of Medicine*, *349*, 1257–1266.

Choy, M., Dubé, C. M., Ehrengruber, M., and Baram, T. Z. (2014). Inflammatory processes, febrile seizures, and subsequent epileptogenesis. *Epilepsy Currents*, *14*(SUPPL.1), 15–22.

Chung, I. Y., and Benveniste, E. N. (1990). Tumor necrosis factor-alpha production by astrocytes. Induction by lipopolysaccharide, IFN-gamma, and IL-1 beta. *Journal of Immunology*, *144*(8), 2999–3007.

Coll, R. C., Robertson, A. A. B., Chae, J. J., Higgins, S. C., Muñoz-Planillo, R., Inserra, M. C., Vetter, I., Dungan, L. S., Monks, B. G., Stutz, A., Croker, D. E., Butler, M. S., Haneklaus, M., Sutton, C. E., Núñez, G., Latz, E., Kastner, D. L., … O'Neill, L. A. J. (2015). A small-molecule inhibitor of the NLRP3 inflammasome for the treatment of inflammatory diseases. *Nature Medicine*, *21*(3), 248–255.

Coltmann, B. W., and Ide, C. F. (1996). Temporal characterization of microglia, IL-1β-like immunoreactivity and astrocytes in the dentate gyrus of hippocampal organotypic slice cultures. *International Journal of Developmental Neuroscience*, *14*(6), 707–719.

Compan, V., Baroja-Mazo, A., Ló Pez-Castejó, G., Gomez, A. I., Martínez, C. M., Angosto, D., Montero, M. T., Herranz, A. S., Bazá, E., Reimers, D., Mulero, V., and Pelegrín, P. (2012). Cell Volume Regulation Modulates NLRP3 Inflammasome Activation. *Immunity*, *37*, 487–500.

Cossart, R., Dinocourt, C., Hirsch, J. C., Merchan-Perez, A., De Felipe, J., Ben-Ari, Y., Esclapez, M., and Bernard, C. (2001). Dendritic but not somatic GABAergic inhibition is decreased in experimental epilepsy. *Nature Neuroscience*, *4*(1), 52–62.

Cunha, R. A., Correia-De-Sa, T., Sebastiao, A. M., and Ribeiro, T. A. (1996). Preferential activation of excitatory adenosine receptors at rat hippocampal and neuromuscular synapses by adenosine formed from released adenine nucleotides. *British Journal of Pharmacology*, *119*, 253–260.

Czapiga, M., and Colton, C. A. (1999). Function of microglia in organotypic slice cultures. *Journal of Neuroscience Research*, *56*(6), 644–651.

Dam, A. M. (1980). Epilepsy and Neuron Loss in the Hippocampus. *Epilepsia*, *21*(6), 617–629.

de Lanerolle, N. C., Kim, J. H., Robbins, R. J., and Spencer, D. D. (1989). Hippocampal interneuron loss and plasticity in human temporal lobe epilepsy. *Brain Research*, *495*, 387–395.

De Simoni, A., Yu, L. M. Y. (2006). Preparation of organotypic hippocampal slice cultures: interface method. *Nature Protocols*, *1*(3), 1439–1445.

De Simoni, M. G., Perego, C., Ravizza, T., Moneta, D., Conti, M., Marchesi, F., De Luigi, A., Garattini, S., and Vezzani, A. (2000). Inflammatory cytokines and related genes are induced in the rat hippocampus by limbic status epilepticus. *The European Journal of Neuroscience*, *12*(7), 2623–2633.

Debye, B., Schmülling, L., Zhou, L., Rune, G., Beyer, C., and Johann, S. (2018). Neurodegeneration and NLRP3 inflammasome expression in the anterior thalamus of SOD1(G93A) ALS mice. *Brain Pathology*, *28*(1), 14–27.

DeSena, A. D., Do, T., and Schulert, G. S. (2018). Systemic autoinflammation with intractable epilepsy managed with interleukin-1 blockade. *Journal of Neuroinflammation*, *15*(1), 38.

Dorfleutner, A., Chu, L., and Stehlik, C. (2015). Inhibiting the inflammasome: one domain at a time. *Immunological Reviews*, *265*(1), 205–2016.

Dubé, C., Vezzani, A., Behrens, M., Bartfai, T., and Baram, T. Z. (2005). Interleukin-1β Contributes to the Generation of Experimental Febrile Seizures. *Annals of Neurology*, *57*(1), 152–155.

Dyhrfjeld-Johnsen, J., Berdichevsky, Y., Swiercz, W., Sabolek, H., and Staley, K. J. (2010). Interictal spikes precede ictal discharges in an organotypic hippocampal slice culture model of epileptogenesis. *Journal of Clinical Neurophysiology*, *27*(6), 418–424.

Edye, M. E., Walker, L. E., Sills, G. J., Allan, S. M., and Brough, D. (2014). Epilepsy and the inflammasome: Targeting inflammation as a novel therapeutic strategy for seizure disorders. *Inflammasome*, *1*(1), 36–43.

Engel, J. (2001). Mesial Temporal Lobe Epilepsy: What Have We Learned? *The Neuroscientist*, *7*(4), 340–352.

Fekete C, Vastagh C, Dénes Á, Hrabovszky E, Nyiri G, Kalló I, Liposits Z, and Sárvári M. (2018). Chronic Amyloid β Oligomer Infusion Evokes Sustained Inflammation and Microglial Changes in the Rat Hippocampus via NLRP3. *Neuroscience*, *pii: S0306*(18), 30171–30174.

Fernandes-Alnemri, T., Wu, J., Yu, J.-W., Datta, P., Miller, B., Jankowski, W., Rosenberg, S., Zhang, J., and Alnemri, E. (2007). The pyroptosome: a supramolecular assembly of ASC dimers mediating inflammatory cell death via caspase-1 activation. *Cell Death and Differentiation*, *14*, 1590–1604.

Fisher, R. S., Acevedo, C., Arzimanoglou, A., Bogacz, A., Cross, J. H., Elger, C. E., Engel, J., Forsgren, L., French, J. A., Glynn, M., Hesdorffer, D. C., Lee, B. I., Mathern, G. W., Moshé, S. L., Perucca, E., Scheffer, I. E., Tomson, T., … Wiebe, S. (2014). ILAE Official Report: A practical clinical definition of epilepsy. *Epilepsia*, *55*(4), 475–482.

Franchi, L., Eigenbrod, T., and Núñez, G. (2009). TNF-α Mediate Sensitization to ATP and Silica via the NLRP3 Inflammasome in the Absence of Microbial Stimulation 1. *Journal of Immunology*, *183*(2), 792–796.

Freeman, L., Guo, H., David, C. N., Brickey, W. J., Jha, S., and Ting, J. P.-Y. (2017). NLR members NLRC4 and NLRP3 mediate sterile inflammasome activation in microglia and astrocytes. *The Journal of Experimental Medicine*, *214*(5), 1351–1370.

Freeman, L., and Ting, J. P.-Y. (2016). The pathogenic role of the inflammasome in neurodegenerative diseases. *Journal of Neurochemistry*, *136*(Suppl.1), 29–38.

Frotscher, M., and Gähwiler, B. H. (1988). Synaptic organization of intracellularly stained CA3 pyramidal neurons in slice cultures of rat hippocampus. *Neuroscience*, *24*(2), 541–551.

Gähwiler, B. H. (1981). Organotypic monolayer cultures of nervous tissue. *Journal of Neuroscience Methods*, *4*(4), 329–342.

Gähwiler, B. H., Capogna, M., Debanne, D., McKinney, R. A., and Thompson, S. M. (1997). Organotypic slice cultures: a technique has come of age. *Trends in Neurosciences*, *20*(10), 471–477.

Gaidt, M. M., Ebert, T. S., Chauhan, D., Schmidt, T., Schmid-Burgk, J. L., Rapino, F., Robertson, A. A. B., Cooper, M. A., Graf, T., and Hornung, V. (2016). Human Monocytes Engage an Alternative Inflammasome Pathway. *Immunity*, *44*, 833–846.

Gerlach, J., Donkels, C., Münzner, G., and Haas, C. A. (2016). Persistent Gliosis Interferes with Neurogenesis in Organotypic Hippocampal Slice Cultures. *Front. Cell. Neurosci*, *10*, 131.

Ghoumari, A. M., Dusart, I., El-Etr, M., Tronche, F., Sotelo, C., Schumacher, M., and Baulieu, E.-E. (2003). Mifepristone (RU486) protects Purkinje cells from cell death in organotypic slice cultures of postnatal rat and mouse cerebellum. *PNAS*, *100*(13), 7953–7958.

Giulian, D., Baker, T. J., Shih, L.-C. N., and Lachman, L. B. (1986). Interleukin 1 of the central nervous system is produced by ameboid microglia. *The Journal of Experimental Medicine*, *164*, 594–604.

Gogolla, N., Galimberti, I., Depaola, V., and Caroni, P. (2006). Preparation of organotypic hippocampal slice cultures for long-term live imaging. *Nature Protocols*, *1*(3), 1165–1171.

Gómez, C. D., Buijs, R. M., and Sitges, M. (2014). The anti-seizure drugs vinpocetine and carbamazepine, but not valproic acid, reduce inflammatory IL-1β and TNF-α expression in rat hippocampus. *Journal of Neurochemistry*, *130*(6), 770–779.

Gustin, A., Kirchmeyer, M., Koncina, E., Felten, P., and Losciuto, S. (2015). NLRP3 Inflammasome Is Expressed and Functional in Mouse Brain Microglia but Not in Astrocytes. *PLoS ONE*, *10*(6), e0130624.

Hagar, J. A., Powell, D. A., Aachoui, Y., Ernst, R. K., and Miao, E. A. (2013). Cytoplasmic LPS activates caspase-11: implications in TLR4-independent endotoxic shock. *Science* , *341*(6151), 1250–1253.

Haghikia, A., Ladage, K., Hinkerohe, D., Vollmar, P., Heupel, K., Dermietzel, R., and Faustmann, P. M. (2008). Implications of antiinflammatory properties of the anticonvulsant drug levetiracetam in astrocytes. *Journal of Neuroscience Research*, *86*(8), 1781–1788.

Haneklaus, M., O'Neill, L. A. J., and Coll, R. C. (2013). Modulatory mechanisms controlling the NLRP3 inflammasome in inflammation: Recent developments. *Current Opinion in Immunology*, *25*(1), 40–45.

He, J., Zhou, R., Wu, Z., Carrasco, M. A., Kurshan, P. T., Farley, J. E., Simon, D. J., Wang, G., Han, B., Hao, J., Heller, E., Freeman, M. R., Shen, K., Maniatis, T., Tessier-Lavigne, M., Zhuang, X., Huang, B., and Zhang, F. (2016). Prevalent presence of periodic actin–spectrin-based membrane skeleton in a broad range of neuronal cell types and animal species. *PNAS*, *113*(21), 6029–6034.

He, W.-T., Wan, H., Hu, L., Chen, P., Wang, X., Huang, Z., Yang, Z.-H., Zhong, C.-Q., and Han, J. (2015). Gasdermin D is an executor of pyroptosis and required for interleukin-1β secretion. *Cell Research*, *25*, 1285–1298.

He, Y., Franchi, L., and Núñez, G. (2013). Toll-like Receptor Agonists Stimulate Nlrp3-dependent IL-1β Production Independently of the purinergic P2X7 Receptor in Dendritic Cells and in Vivo. *Journal of Immunology*, *190*(1), 334–339.

He, Y., Hara, H., and Núñez, G. (2016). Mechanism and Regulation of NLRP3 Inflammasome Activation. *Trends in Biochemical Sciences*, *41*(12), 1012–1021.

He, Y., Zeng, M. Y., Yang, D., Motro, B., and Núñez, G. (2016). NEK7 is an essential mediator of NLRP3 activation downstream of potassium efflux. *Nature*, *530*, 354–357.

Heida, J. G., Boissé, L., and Pittman, Q. J. (2004). Lipopolysaccharide-induced Febrile Convulsions in the rat: Short-term sequelae. *Epilepsia*, *45*(11), 1317–1329.

Heneka, M. T., Kummer, M. P., Stutz, A., Delekate, A., Saecker, A., Griep, A., Axt, D., Remus, A., Tzeng, T., Gelpi, E., Halle, A., Korte, M., Latz, E., and Golenbock, D. (2013). NLRP3 is activated in Alzheimer´s disease and contributes to pathology in APPPS1 mice. *Nature*, *493*(7434), 674–678.

Henshall, D. C., and Meldrum, B. S. (2012). *Cell death and survival mechanisms after single and repeated brief seizures*. *Jasper's Basic Mechanisms of the Epilepsies* (4th Editio). National Center for Biotechnology Information (US).

Herman, S. T. (2002). Epilepsy after brain insult: targeting epileptogenesis. *Neurology*, *59*(9 Suppl 5), S21-6.

Hoffman, H. M., Mueller, J. L., Broide, D. H., Wanderer, A. A., and Kolodner, R. D. (2001). Mutation of a new gene encoding a putative pyrin-like protein causes familial cold autoinflammatory syndrome and Muckle–Wells syndrome. *Nature Genetics*, *29*(3), 301–305.

Hornung, V., Bauernfeind, F., Halle, A., Samstad, E. O., Kono, H., Rock, K. L., Fitzgerald, K. A., and Latz, E. (2008). Silica crystals and aluminum salts mediate NALP-3 inflammasome

activation via phagosomal destabilization. *Nature Immunology*, *9*(8), 847–856.
Hoss, F., Rodriguez-Alcazar, J. F., and Latz, E. (2017). Assembly and regulation of ASC specks. *Cellular and Molecular Life Sciences*, *74*(7), 1211–1229.
Humpel, C. (2015). Organotypic Brain Slice Culture: a review. *Neuroscience*, *305*, 86–98.
Huuskonen, J., Suuronen, T., Miettinen, R., Groen, T. Van, and Salminen, A. (2005). A refined in vitro model to study inflammatory responses in organotypic membrane culture of postnatal rat hippocampal slices. *Journal of Neuroinflammation*, *2*, 25.
Jeon, K.-I., Xu, X., Aizawa, T., Lim, J. H., Jono, H., Kwon, D.-S., Abe, J.-I., Berk, B. C., Li, J.-D., and Yan, C. (2010). Vinpocetine inhibits NF-kappaB-dependent inflammation via an IKK-dependent but PDE-independent mechanism. *Proceedings of the National Academy of Sciences of the United States of America*, *107*(21), 9795–9800.
Jiang, H., He, H., Chen, Y., Huang, W., Cheng, J., Ye, J., Wang, A., Tao, J., Wang, C., Liu, Q., Jin, T., Jiang, W., Deng, X., and Zhou, R. (2017). Identification of a selective and direct NLRP3 inhibitor to treat inflammatory disorders. *The Journal of Experimental Medicine*, *214*(11), 3219–3238.
Johann, S., Heitzer, M., Kanagaratnam, M., Goswami, A., Rizo, T., Weis, J., Troost, D., and Beyer, C. (2015). NLRP3 inflammasome is expressed by astrocytes in the SOD1 mouse model of ALS and in human sporadic ALS patients. *Glia*, *63*(12), 2260–2273.
Jyonouchi, H., and Geng, L. (2016). Intractable Epilepsy (IE) and Responses to Anakinra, a Human Recombinant IL-1 Receptor Agonist (IL-1ra): Case Reports. *Journal of Clinical & Cellular Immunology*, *7*(5).
Kahlenberg, J. M., and Dubyak, G. R. (2004). Mechanisms of caspase-1 activation by P2X7 receptor-mediated K+ release. *American Journal Cell Physiology*, *286*, C1100–C1108.
Kandratavicius, L., Alves Balista, P., Lopes-Aguiar, C., Ruggiero, R. N., Umeoka, H., Garcia-Cairasco, N., Soares Bueno-Junior, L., and Pereira Leite, J. (2014). Animal models of epilepsy: use and limitations. *Neuropsychiatric Disease and Treatment*, *10*, 1693–1705.
Kawanokuchi, J., Mizuno, T., Takeuchi, H., Kato, H., Wang, J., Mitsuma, N., and Suzumura, A. (2006). Production of interferon-γ by microglia. *Multiple Sclerosis Journal*, *12*(5), 558–564.
Kayagaki, N., Stowe, I. B., Lee, B. L., Rourke, K. O., Anderson, K., Warming, S., Cuellar, T., Haley, B., Roose-girma, M., Phung, Q. T., Liu, P. S., Lill, J. R., Li, H., Wu, J., Kummerfeld, S., Zhang, J., Lee, W. P., … Dixit, V. M. (2015). Caspase-11 cleaves gasdermin D for non-canonical inflammasome signalling. *Nature*, *526*.
Kayagaki, N., Warming, S., Lamkanfi, M., Walle, L. Vande, Louie, S., Dong, J., Newton, K., Qu, Y., Liu, J., Heldens, S., Zhang, J., Lee, W. P., Roose-Girma, M., and Dixit, V. M. (2011). Non-canonical inflammasome activation targets caspase-11. *Nature*, *479*(7371), 117–121.
Kenney-Jung, D. L., Kahoud, R. J., Vezzani, A., Lafrance-Corey, R. G., Ho, M.-L., Muskardin, T. W., Gleich, S. J., Wirrell, E. C., Howe, C. L., and Payne, E. T. (2016). Super-refractory status epilepticus and febrile infection-related epilepsy syndrome treated with anakinra. *Annals of Neurology*, *80*(6), 939–945.
Kettenmann, H., Hanisch, U.-K., Noda, M., and Verkhratsky, A. (2011). Physiology of Microglia. *Physiological Reviews*, *91*, 461–553.
Khare, S., Radian, A. D., Dorfleutner, A., and Stehlik, C. (2016). Methods to measure NLR oligomerization: size exclusion chromatography, co-immunoprecipitation and cross-linking. *Methods in Molecular Biology*, *1417*, 131–143.
Klein, P., Dingledine, R., Aronica, E., Bernard, C., Blümcke, I., Boison, D., Brodie, M. J., Brooks-Kayal, A. R., Engel, J., Forcelli, P. A., Hirsch, L. J., Kaminski, R. M., Klitgaard, H., Kobow, K., Lowenstein, D. H., Pearl, P. L., Pitkänen, A., … Löscher, W. (2018). Commonalities in epileptogenic processes from different acute brain insults: Do they translate? *Epilepsia*, *59*, 37–66.
Krishnan, S. M., Dowling, J. K., Ling, Y. H., Diep, H., Chan, C. T., Ferens, D., Kett, M. M., Pinar, A., Samuel, C. S., Vinh, A., Arumugam, T. V., Hewitson, T. D., Kemp-Harper, B. K., Robertson, A. A. B., Cooper, M. A., Latz, E., Mansell, A., … Drummond, G. R. (2016). Inflammasome activity

is essential for one kidney/deoxycorticosterone acetate/salt-induced hypertension in mice. *British Journal of Pharmacology*, *173*(4), 752–765.

Kwan, P., Arzimanoglou, A., Berg, A. T., Brodie, M. J., Allen Hauser, W., Mathern, G., Moshé, S. L., Perucca, E., Wiebe, S., and French, J. (2009). Definition of drug resistant epilepsy: Consensus proposal by the ad hoc Task Force of the ILAE Commission on Therapeutic Strategies. *Epilepsia*, *51*(6), 1069–1077.

Laake, J. H., Haug, F. M., Wieloch, T., and Ottersen, O. P. (1999). A simple in vitro model of ischemia based on hippocampal slice cultures and propidium iodide fluorescence. *Brain Research Protocols*, *4*(2), 173–184.

Lamkanfi, M., and Dixit, V. M. (2014). Mechanisms and Functions of Inflammasomes. *Cell*, *157*(5), 1013–1022.

Latz, E., Xiao, T. S., and Stutz, A. (2013). Activation and regulation of the inflammasomes. *Nature Reviews Immunology*, *13*(6), 397–411.

Lau, L. T., and Yu, A. C.-H. (2001). Astrocytes Produce and Release Interleukin-1, Interleukin-6, Tumor Necrosis Factor Alpha and Interferon-Gamma Following Traumatic and Metabolic Injury. *Journal of Neurotrauma*, *18*(3), 351–359.

Lawson, L. J., Perry, V. H., Dri, P., and Gordon, S. (1990). Heterogeneity in the distribution and morphology of microglia in the normal adult mouse brain. *Neuroscience*, *39*(1), 151–170.

Lénárt, N., Brough, D., and Dénes, Á. (2016). Inflammasomes link vascular disease with neuroinflammation and brain disorders. *Journal of Cerebral Blood Flow and Metabolism : Official Journal of the International Society of Cerebral Blood Flow and Metabolism*, *36*(10), 1668–1685.

Liddelow, S. A., and Barres, B. A. (2017). Reactive Astrocytes: Production, Function, and Therapeutic Potential. *Cell Press*, *46*, 957–967.

Liu, J., Saponjian, Y., Mahoney, M. M., Staley, K. J., and Berdichevsky, Y. (2017). Epileptogenesis in organotypic hippocampal cultures has limited dependence on culture medium composition. *PLoS ONE*, *12*(2), 1–25.

Lobo-Silva, D., Carriche, G. M., Castro, A. G., Roque, S., and Saraiva, M. (2016). Balancing the immune response in the brain: IL-10 and its regulation. *Journal of Neuroinflammation*, *13*, 297.

Löshcer, W. (2002). Animal models of epilepsy for the development of antiepileptogenic and disease-modifying drugs. A comparison of the pharmacology of kindling and post-status epilepticus models of temporal lobe epilepsy. *Epilepsy Research*, *50*, 105–123.

Lu, A., and Wu, H. (2015). Structural mechanisms of inflammasome assembly. *FEBS Journal*, *282*(3), 435–444.

Magalhães, D. M., Pereira, N., Rombo, D. M., Beltrão-Cavacas, C., Sebastião, A. M., and Valente, C. A. (2018). Ex vivo model of epilepsy in organotypic slices – a new tool for drug screening. *Journal of Neuroinflammation*, under review.

Marchi, N., Fan, Q., Ghosh, C., Fazio, V., Bertolini, F., Betto, G., Batra, A., Carlton, E., Najm, I., Granata, T., and Janigro, D. (2009). Antagonism of peripheral inflammation reduces the severity of status epilepticus. *Neurobiology of Disease*, *33*(2), 171–181.

Maroso, M., Balosso, S., Ravizza, T., Iori, V., Wright, C. I., French, J., and Vezzani, A. (2011). Interleukin-1β Biosynthesis Inhibition Reduces Acute Seizures and Drug Resistant Chronic Epileptic Activity in Mice. *Neurotherapeutics: The Journal of the American Society for Experimental NeuroTherapeutics*, *8*, 304Y315.

Martinon, F., Burns, K., and Tschopp, J. (2002). The Inflammasome : A Molecular Platform Triggering Activation of Inflammatory Caspases and Processing of proIL- 1b. *Molecular Cell*, *10*, 417–426.

Meng, X.-F., Tan, L., Tan, M.-S., Jiang, T., Tan, C.-C., Li, M.-M., Wang, H.-F., and Yu, J.-T. (2014). Inhibition of the NLRP3 inflammasome provides neuroprotection in rats following amygdala kindling-induced status epilepticus. *Journal of Neuroinflammation*, *11*(1), 212.

Miao, E. A., Rajan, J. V, and Aderem, A. (2011). Caspase-1 induced pyroptotic cell death.

Immunological Reviews, *243*(1), 206–214.
Mirrione, M. M., and Tsirka, S. E. (2011). *A Functional Role for Microglia in Epilepsy, Clinical and Genetic Aspects of Epilepsy, Dr. Zaid Afawi (Ed.)*. ISBN: 978-953-307-700-0, InTech.
Misawa, T., Takahama, M., Kozaki, T., Lee, H., Zou, J., Saitoh, T., and Akira, S. (2013). Microtubule-driven spatial arrangement of mitochondria promotes activation of the NLRP3 inflammasome. *Nature Immunology*, *14*(5), 454–460.
Mittelbronn, M., Dietz, K., Schluesener, H. J., and Meyermann, R. (2001). Local distribution of microglia in the normal adult human central nervous system differs by up to one order of magnitude. *Acta Neuropathology*, *101*, 249–255.
Molná, Z. N., and Blakemore, C. (1998). Development of Signals Influencing the Growth and Termination of Thalamocortical Axons in Organotypic Culture. *Experimental Neurology*, *156*, 363–393.
Muller, D., Toni, N., Buchs, P.-A., Nicolas, D., Parisi, L., and Stoppini, L. (2001). Interface Organotypic Hippocampal Slice Cultures. In S. Fedoroff & A. Richardson (Eds.), *Protocols for Neural Cell Culture* (3rd ed., pp. 13–27). Humana Press.
Muñoz-Planillo, R., Kuffa, P., Martínez-Colón, G., Smith, B. L., Rajendiran, T. M., and Núñez, G. (2013). K+ efflux is the Common Trigger of NLRP3 inflammasome Activation by Bacterial Toxins and Particulate Matter. *Immunity*, *38*(6), 1142–1153.
Nakahira, K., Haspel, J. A., Rathinam, V. A., Lee, S.-J., Dolinay, T., Lam, H. C., Englert, J. A., Rabinovitch, M., Cernadas, M., Kim, H. P., Fitzgerald, K. A., Ryter, S. W., and Choi, A. M. (2011). Autophagy proteins regulate innate immune response by inhibiting NALP3 inflammasome-mediated mitochondrial DNA release. *Nature Immunology*, *12*(3), 222–230.
Namba, T., Mochizuki, H., Onodera, M., Namiki, H., and Seki, T. (2007). Postnatal Neurogenesis in Hippocampal Slice Cultures: Early In Vitro Labeling of Neural Precursor Cells Leads to Efficient Neuronal Production. *Journal of Neuroscience Research*, *85*, 1704–1712.
Nedergaard, M., Ransom, B., and Goldman, S. A. (2003). New roles for astrocytes: Redefining the functional architecture of the brain. *Trends in Neurosciences*, *26*(10), 523–530.
Ngugi, Y. K., Bottomley, Y., Kleinschmidt, Y., Sander, W., and Newton, R. (2010). Estimation of the burden of active and life-time epilepsy: A meta-analytic approach. *Epilepsia*, *51*(5), 883–890.
Noraberg, J., Kristensen, B. W., and Zimmer, J. (1999). Markers for neuronal degeneration in organotypic slice cultures. *Brain Research Protocols*, *3*, 278–290.
Oberheim, N. A., Goldman, S. A., and Nedergaard, M. (2012). Heterogeneity of Astrocytic Form and Function. *Methods in Molecular Biology*, *814*, 23–45.
Oprica, M., Eriksson, C., and Schultzberg, M. (2003). Inflammatory mechanisms associated with brain damage induced by kainic acid with special reference to the interleukin-1 system. *Journal of Cellular and Molecular Medicine*, *7*(2), 127–140.
Oroz, J., Barrera-Vilarmau, S., Alfonso, C., Rivas, G. N., and De Alba, E. (2016). ASC Pyrin Domain Self-associates and Binds NLRP3 Protein Using Equivalent Binding Interfaces. *The Journal of Biological Chemistry*, *291*(37), 19487–19501.
Ozaki, E., Campbell, M., and Doyle, S. L. (2015). Targeting the NLRP3 inflammasome in chronic inflammatory diseases : current perspectives. *Journal of Inflammation Research*, *8*, 15–27.
Parent, J. M., Yu, T. W., Leibowitz, R. T., Geschwind, D. H., Sloviter, R. S., and Lowenstein, D. H. (1997). Dentate Granule Cell Neurogenesis Is Increased by Seizures and Contributes to Aberrant Network Reorganization in the Adult Rat Hippocampus. *The Journal of Neuroscience*, *17*(10), 3727–3738.
Pelegrin, P., and Surprenant, A. (2006). Pannexin-1 mediates large pore formation and interleukin-1β release by the ATP-gated P2X7 receptor. *The EMBO Journal*, *25*, 5071–5082.
Perea, G., Navarrete, M., and Araque, A. (2009). Tripartite synapses: astrocytes process and control synaptic information. *Trends in Neurosciences*, *32*(8), 421–431.
Pétrilli, V., Papin, S., Dostert, C., Mayor, A., Martinon, F., and Tschopp, J. (2007). Activation of the NALP3 inflammasome is triggered by low intracellular potassium concentration. *Cell*

Death and Differentiation, *14*, 1583–1589.
Place, D. E., Kanneganti, T.-D., and Thirumala-Devi Kanneganti, T.-D. (2018). Recent advances in inflammasome biology. *Current Opinion in Immunology*, *50*, 32–38.
Raol, Y. H., and Brooks-Kayal, A. R. (2012). *Experimental Models of Seizures and Epilepsies*. *Progress in Molecular Biology and Translational Science* (1st ed., Vol. 105). Elsevier Inc.
Ravizza, T., Gagliardi, B., Noé, F., Boer, K., Aronica, E., and Vezzani, A. (2008). Innate and adaptive immunity during epileptogenesis and spontaneous seizures: Evidence from experimental models and human temporal lobe epilepsy. *Neural Plasticity*, *29*, 142–160.
Ravizza, T., Lucas, S., Balosso, S., Bernardino, L., Ku, G., No, F., Malva, J., Randle, J. C. R., Allan, S., and Vezzani, A. (2006). Inactivation of Caspase-1 in Rodent Brain : A Novel Anticonvulsive Strategy. *Epilepsia*, *47*(7), 1160–1168.
Ravizza, T., and Vezzani, A. (2006). Status epilepticus induces time-dependent neuronal and astrocytic expression of interleukin-1 receptor type I in the rat limbic system. *Neuroscience*, *137*, 301–308.
Ren, H., Kong, Y., Liu, Z., Zang, D., Yang, X., Wood, K., Li, M., and Liu, Q. (2018). Selective NLRP3 (Pyrin Domain-Containing Protein 3) Inflammasome Inhibitor Reduces Brain Injury After Intracerebral Hemorrhage. *Stroke*, *49*, 184–192.
Riederer, B. M., Zagon, I. S., and Goodman, S. R. (1986). Brain Spectrin(240/235) and Brain Spectrin(240/235E): Two Distinct Spectrin Subtypes with Different Locations within Mammalian Neural Cells. *The Journal of Cell Biology*, *102*, 2088–2097.
Rivers-Auty, J., and Brough, D. (2015). Potassium efflux fires the canon : Potassium efflux as a common trigger for canonical and noncanonical NLRP3 pathways. *European Journal of Immunology*, *45*, 2758–2761.
Rutecki, P. A., and Yang, Y. (1998). Ictal Epileptiform Activity in the CA3 Region of Hippocampal Slices Produced by Pilocarpine. *Journal of Neurophysiology*, *79*(6), 3019–3019.
Sarkisian, M. R. (2001). Overview of the Current Animal Models for Human Seizure and Epileptic Disorders. *Epilepsy & Behavior*, *2*, 201–216.
Sayyah, M., Javad-Pour, M., and Ghazi-Khansari, M. (2003). The bacterial endotoxin lipopolysaccharide enhances seizure susceptibility in mice: Involvement of proinflammatory factors: Nitric oxide and prostaglandins. *Neuroscience*, *122*(4), 1073–1080.
Scheffer, I. E., Berkovic, S., Capovilla, G., Connolly, M. B., French, J., Guilhoto, L., Hirsch, E., Jain, S., Mathern, G. W., Moshé, S. L., Nordli, D. R., Perucca, E., Tomson, T., Wiebe, S., Zhang, Y. H., and Zuberi, S. M. (2017). ILAE classification of the epilepsies: Position paper of the ILAE Commission for Classification and Terminology. *Epilepsia*, *58*(4), 512–521.
Schmid-Burgk, J. L., Chauhan, D., Schmidt, T., Ebert, T. S., Reinhardt, J., Endl, E., and Hornung, V. (2016). A Genome-wide CRISPR (Clustered Regularly Interspaced Short Palindromic Repeats) Screen Identifies NEK7 as an Essential Component of NLRP3 Inflammasome Activation. *The Journal of Biological Chemistry*, *291*(1), 103–109.
Schroder, K., and Tschopp, J. (2010). The Inflammasomes. *Cell*, *140*, 821–832.
Shao, B. Z., Xu, Z. Q., Han, B. Z., Su, D. F., and Liu, C. (2015). NLRP3 inflammasome and its inhibitors: A review. *Frontiers in Pharmacology*, *6*, 1–9.
Shi, H., Wang, Y., Li, X., Zhan, X., Tang, M., Fina, M., Su, L., Pratt, D., Hui Bu, C., Hildebrand, S., and et al. (2016). NLRP3 activation and mitosis are mutually exclusive events coordinated by NEK7, a new inflammasome component. *Nature Immunology*, *17*(3), 250–258.
Shi, J., Zhao, Y., Wang, K., Shi, X., Wang, Y., Huang, H., Zhuang, Y., Cai, T., Wang, F., and Shao, F. (2015). Cleavage of GSDMD by inflammatory caspases determines pyroptotic cell death. *Nature*, *526*, 660–665.
Shimada, T., Takemiya, T., Sugiura, H., and Yamagata, K. (2014). Role of Inflammatory Mediators in the Pathogenesis of Epilepsy. *Mediators of Inflammation*, *2014*, 901902.
Sierra, A., Martín-Suárez, S., Valcárcel-Martín, R., Pascual-Brazo, J., Aelvoet, S.-A., Abiega, O., Deudero, J. J., Brewster, A. L., Bernales, I., Anderson, A. E., Baekelandt, V., Maletić-Savatić, M., and Encinas, J. M. (2015). Neuronal Hyperactivity Accelerates Depletion of Neural Stem

Cells and Impairs Hippocampal Neurogenesis. *Cell Stem Cell*, *16*(5), 488–503.
Sinha, S., Patil, S. A., Jayalekshmy, V., and Satishchandra, P. (2008). Do cytokines have any role in epilepsy? *Epilepsy*, *82*, 171–176.
Sofroniew, M. V. (2009). Molecular dissection of reactive astrogliosis and glial scar formation. *Trends in Neurosciences*, *32*(12), 638–647.
Sofroniew, M. V., and Vinters, H. V. (2010). Astrocytes: Biology and pathology. *Acta Neuropathologica*, *119*, 7–35.
Sofroniew, M. V. (2015). Astrocyte barriers to neurotoxic inflammation. *Nature Reviews. Neuroscience*, *16*(5), 249–263.
Song, L., Pei, L., Yao, S., Wu, Y., and Shang, Y. (2017). NLRP3 Inflammasome in Neurological Diseases, from Functions to Therapies. *Frontiers in Cellular Neuroscience*, *11*, 63.
Sousa, C., Biber, K., and Michelucci, A. (2017). Cellular and Molecular Characterization of Microglia: A Unique Immune Cell Population. *Frontiers in Immunology*, *8*, 198.
Stellwagen, D., Beattie, E. C., Seo, J. Y., and Malenka, R. C. (2005). Differential Regulation of AMPA Receptor and GABA Receptor Trafficking by Tumor Necrosis Factor-α. *The Journal of Neuroscience*, *25*(12), 3219–3228.
Stoppini, L., Buchs, P.-A., and Muller, D. (1991). A simple method for organotypic cultures of nervous tissue. *Journal of Neuroscience Methods*, *37*(2), 173–182.
Strauss, K. I., and Elisevich, K. V. (2016). Brain region and epilepsy-associated differences in inflammatory mediator levels in medically refractory mesial temporal lobe epilepsy. *Journal of Neuroinflammation*, *13*, 270.
Subramanian, N., Natarajan, K., Clatworthy, M. R., Wang, Z., and Germain, R. N. (2013). The adapter MAVS promotes NLRP3 mitochondrial localization and inflammasome activation. *Cell*, *153*(2), 348–361.
Sundstrom, L., Iii, B. M., Bradley, M., and Pringle, A. (2005). Organotypic cultures as tools for functional screening in the CNS. *Drug Discovery Today: Targets*, *10*(14), 993–1000.
Takeuchi, O., and Akira, S. (2010). Pattern Recognition Receptors and Inflammation. *Cell*, *140*, 805–820.
Tang, Y., and Le, W. (2016). Differential Roles of M1 and M2 Microglia in Neurodegenerative Diseases. *Molecular Neurobiology*, *53*, 1181–1194.
Thöne, J., Ellrichmann, G., Faustmann, P. M., Gold, R., and Haghikia, A. (2012). Anti-inflammatory effects of levetiracetam in experimental autoimmune encephalomyelitis. *International Immunopharmacology*, *14*(1), 9–12.
Ting, J. P. Y., Lovering, R. C., Alnemri, E. S. P. D., Bertin, J., Boss, J. M., Davis, B., Flavell, R. A., Girardin, S. E., Godzik, A., Harton, J. A., Hoffman, H. M., Hugot, J.-P., Inohara, N., MacKenzie, A., Maltais, L. J., Nunez, G., Ogura, Y., … Ward, P. A. (2008). The NLR gene family: An official nomenclature. *Immunity.*, *28*(3), 285–287.
Turrin, N. P., and Rivest, S. (2004). Innate immune reaction in response to seizures: implications for the neuropathology associated with epilepsy. *Neurobiology of Disease*, *16*, 321–334.
Uludag, I. F., Duksal, T., Tiftikcioglu, B. I., Zorlu, Y., Ozkaya, F., and Kirkali, G. (2015). IL-1β, IL-6 and IL1Ra levels in temporal lobe epilepsy. *Seizure*, *26*, 22–25.
Van Hout, G. P. J., Bosch, L., Ellenbroek, G. H. J. M., De Haan, J. J., Van Solinge, W. W., Cooper, M. A., Arslan, F., De Jager, S. C. A., Robertson, A. A. B., Pasterkamp, G., and Hoefer, I. E. (2017). The selective NLRP3-inflammasome inhibitor MCC950 reduces infarct size and preserves cardiac function in a pig model of myocardial infarction. *European Heart Journal*, *38*(11), 828–836.
Vezzani, A., Balosso, S., and Ravizza, T. (2008). The role of cytokines in the pathophysiology of epilepsy. *Brain, Behavior, and Immunity*, *22*(6), 797–803.
Vezzani, A., and Baram, T. Z. (2007). New Roles for Interleukin-1 Beta in the Mechanisms of Epilepsy. *Epilepsy Currents*, *7*(2), 45–50.
Vezzani, A., Conti, M., De Luigi, A., Ravizza, T., Moneta, D., Marchesi, F., and De Simoni, M. G.

(1999). Interleukin-1β Immunoreactivity and Microglia Are Enhanced in the Rat Hippocampus by Focal Kainate Application: Functional Evidence for Enhancement of Electrographic Seizures. *The Journal of Neuroscience*, *19*(12), 5054–5065.

Vezzani, A., Friedman, A., and Dingledine, R. J. (2013). The role of inflammation in epileptogenesis. *Neuropharmacology*, *69*, 16–24.

Vezzani, A., and Granata, T. (2005). Brain Inflammation in Epilepsy: Experimental and Clinical Evidence. *Epilepsia*, *46*(11), 1724–1743.

Vezzani, A., Maroso, M., Balosso, S., Sanchez, M.-A., and Bartfai, T. (2011). IL-1 receptor/Toll-like receptor signaling in infection, inflammation, stress and neurodegeneration couples hyperexcitability and seizures. *Brain Behavior and Immunity*, *25*, 1281–1289.

Vezzani, A., Moneta, D., Conti, M., Richichi, C., Ravizza, T., De Luigi, A., De Simoni, M. G., Sperk, G., Andell-Jonsson, S., Lundkvist, J., Iverfeldt, K., Bartfai, T., Dorris, H. L., and Stevens, C. F. (2000). Powerful anticonvulsant action of IL-1 receptor antagonist on intracerebral injection and astrocytic overexpression in mice. *Proceedings of the National Academy of Sciences*, *97*, 11534–11539.

Vornov, J. J., Tasker, R. C., and Coyle, J. T. (1991). Direct observation of the agonist-specific regional vulnerability to glutamate, NMDA, and kainate neurotoxicity in organotypic hippocampal cultures. *Experimental Neurology*, *114*(1), 11–22.

Walsh, J. G., Muruve, D. A., and Power, C. (2014). Inflammasomes in the CNS. *Nature Reviews Neurology*, *15*, 84–97.

Walther, H., Lambert, J. D. C., Jones, R. S. G., Heinemann, U., and Hamon, B. (1986). Epileptiform activity in combined slices of the hippocampus, subiculum and entorhinal cortex during perfusion with low magnesium medium. *Neuroscience Letters*, *69*, 156–161.

Wang, C., Yang, L., Zhang, J., Lin, Z., Qi, J., and Duan, S. (2016). Higher expression of monocyte chemoattractant protein 1 and its receptor in brain tissue of intractable epilepsy patients. *Journal of Clinical Neuroscience*, *28*, 134–140.

Wang, Q., and Andreasson, K. (2010). The organotypic hippocampal slice culture model for examining neuronal injury. *Journal of Visualized Experiments*, *JoVE. 44*.

Wang, S., Cheng, Q., Malik, S., and Yang, J. (2000). Interleukin-1β Inhibits γ-Aminobutyric Acid Type A (GABAA) Receptor Current in Cultured Hippocampal Neurons. *The Journal of Pharmacology and Experimental Therapeutics*, *292*(2), 497–504.

Wang, Y., Yang, C., Mao, K., Chen, S., Meng, G., and Sun, B. (2013). Cellular localization of NLRP3 inflammasome. *Protein & Cell*, *4*(6), 425–431.

Welser-Alves, J. V, and Milner, R. (2013). Microglia are the major source of TNF-α and TGF-β in postnatal glial cultures; regulation by cytokines, lipopolysaccharide, and vitronectin. *Neurochemistry International*, *63*(1).

Wong, M. (2011). Epilepsy in a Dish: An in Vitro Model of Epileptogenesis. *Epilepsy Currents*, *11*(5), 153–154.

Xu, D., Miller, S. D., and Koh, S. (2013). Immune mechanisms in epileptogenesis. *Frontiers in Cellular Neuroscience*, *7*, 1–8.

Yang, D., He, Y., Muñ Oz-Planillo, R., Liu, Q., and Nú, G. (2015). Caspase-11 Requires the Pannexin-1 Channel and the Purinergic P2X7 Pore to Mediate Pyroptosis and Endotoxic Shock. *Immunity*, *43*, 923–932.

Youm, Y.-H., Nguyen, K. Y., Grant, R. W., Goldberg, E. L., Bodogai, M., Kim, D., D 'agostino, D., Planavsky, N., Lupfer, C., Kanneganti, T. D., Kang, S., Horvath, T. L., Fahmy, T. M., Crawford, P. A., Biragyn, A., Alnemri, E., and Dixit, V. D. (2015). Ketone body β-hydroxybutyrate blocks the NLRP3 inflammasome-mediated inflammatory disease. *Nature Medicine*, *21*(3), 263–269.

Zendedel, A., Johann, S., Mehrabi, S., Joghataei, M.-T., Hassanzadeh, G., Kipp, M., and Beyer, C. (2016). Activation and Regulation of NLRP3 Inflammasome by Intrathecal Application of SDF-1a in a Spinal Cord Injury Model. *Molecular Cell*, *53*, 3063–3075.

Zhai, Y., Meng, X., Ye, T., Xie, W., Sun, G., and Sun, X. (2018). Inhibiting the NLRP3

Inflammasome Activation with MCC950 Ameliorates Diabetic Encephalopathy in db/db Mice. *Molecules*, *23*(3), 522.

Zhang, F., Jin, H., Wu, L., Shao, J., Wu, X., Lu, Y., and Zheng, S. (2016). Ligustrazine disrupts lipopolysaccharide-activated NLRP3 inflammasome pathway associated with inhibition of Toll-like receptor 4 in hepatocytes. *Biomedicine & Pharmacotherapy*, *78*, 204–209.

Zhang, H. (2011). Anti-IL-1β therapies. *Recent Patents on DNA & Gene Sequences*, *5*(2), 126–135.

Zhang, W., Smith, C., Howlett, C., and Stanimirovic, D. (2000). Inflammatory Activation of Human Brain Endothelial Cells by Hypoxic Astrocytes In Vitro Is Mediated by IL-lβ. *Journal of Cerebral Blood Flow and Metabolism*, *20*, 967–978.

Zhang, W., Xu, X., Kao, R., Mele, T., Kvietys, P., Martin, C. M., and Rui, T. (2014). Cardiac Fibroblasts Contribute to Myocardial Dysfunction in Mice with Sepsis: The role of NLRP3 inflammasome activation. *PLoS ONE*, *9*(9).

Zhang, Z.-T., Du, X.-M., Ma, X.-J., Zong, Y., Chen, J.-K., Yu, C.-L., Liu, Y.-G., Chen, Y.-C., Zhao, L.-J., and Lu, G.-C. (2016). Activation of the NLRP3 inflammasome in lipopolysaccharide-induced mouse fatigue and its relevance to chronic fatigue syndrome. *Journal of Neuroinflammation*, *13*(1), 71.

Zhang, Z., Larner, S. F., Liu, M. C., Zheng, W., Hayes, R. L., and Wang, K. K. W. (2009). Multiple alphaII-spectrin breakdown products distinguish calpain and caspase dominated necrotic and apoptotic cell death pathways. *Apoptosis*, *14*, 1289–1298.

Zhou, R., Yazdi, A. S., Menu, P., and Tschopp, J. (2011). A role for mitochondria in NLRP3 inflammasome activation. *Nature*, *469*(7329), 221–225.